



**Final Report: NIOSH Grant 5 R01 OH02858- (04- 06)**

---

# **Computational Methods in Industrial Ventilation**

**Principal Investigator: Dr. Michael R. Flynn**

**University of North Carolina @ Chapel Hill**

# TABLE OF CONTENTS

<b>Abstract</b>	<b>3</b>
<b>List of Publications and Reports</b>	<b>4</b>
<b>Significant Findings</b>	<b>5</b>
<b>Utility of Findings</b>	<b>7</b>
<b>Specific Aims and Relationship to Publications</b>	<b>9</b>
<b>Appendix</b>	<b>13</b>

---

## Abstract

This is the Final Performance Report for NIOSH Grant 5 R01 OH02858-(03-06), entitled “Computational Methods in Industrial Ventilation.” It is presented as a list of publications with reprints, and a discussion of how these papers relate to the Specific Aims. At the time this report was submitted, three of the eight publications were in various stages of completion - one is in press, another in review, and a final paper under preparation for submission (see List of Publications and Reports). A brief summary of the results of these papers are found in this report in the section on Specific Aims and their Relationship to the Publications.

This research demonstrates that computational fluid dynamics (CFD) and dimensional analysis are powerful tools for simulating human exposure to aerosols generated in spray painting applications. The process, outlined in the publications, of creating a conceptual model using dimensional analysis and principles of similarity and then implementing this within the CFD framework, provides a powerful tool for any exposure control problem. The examination of this process with field data shows the utility and limitations of such an approach.

---

## List of Publications and Reports

Fourteen publications and reports were generated as a result of this project. The numbers #1- #14 which identify each document below are used subsequently in this report for identification.

#1. Carlton, G. and Flynn, M.R. "A model to Estimate Worker Exposure to Spray Paint Mists" Appl. Occup and Env. Hyg. 12(5):375-382, (1997).

#2. Carlton, G. and Flynn, M.R. "Field Evaluation of an Empirical-Conceptual Exposure Model" Appl. Occup and Env. Hyg. 12(8):555-561, (1997).

#3. Carlton, G. and Flynn, M.R. "The Influence of Spray Painting Parameters on Breathing Zone Particle Size Distributions" Appl. Occup and Env. Hyg. 12(11):744-750, (1997).

#4. Flynn, M.R., Gatano, B., McKernan, J., Dunn, K. Balzicko, B., and Carlton G.N. "Modeling worker exposure to airborne contaminants generated during compressed air spray painting. Ann. Occup. hyg. 43(1):67-76, (1999).

#5. Flynn, M.R., and Carlton, G. "Exposure Models for Contaminant Control Decisions Involving Ventilation" in *Ventilation '97: Global Developments in Industrial Ventilation Proceedings of the 5<sup>th</sup> International Symposium on Ventilation for Contaminant Control*, eds. H. Goodfellow and E. Tahti; Ottawa Sept 14-17 1997, CEIA-ACIE.

#6. Flynn, M.R., and Sills, E.D. "On the use of computational fluid dynamics in the prediction and control of exposure to airborne contaminants – an illustration using spray painting" Ann. Occup. hyg. In Press.

#7. Tan, Y, and Flynn, M.R. "Experimental Evaluation of a Mathematical Model for Predicting Transfer Efficiency of a High Volume – Low Pressure Air Spray Gun" submitted to Appl. Occup. and Env. Hyg.

#8. Flynn, M.R. and Sills, E.D. "Numerical Simulation of Human Exposure to Aerosols Generated during Spray Painting" Under Preparation for submission to Journal of Fluids Engineering.

#9 Flynn, M.R. "Evaluating Uncertainties in computational fluid dynamic simulations of human exposure to paint-spray aerosols" submitted to *Ventilation 2000 6<sup>th</sup> International Symposium on Ventilation for Contaminant Control*, to be held in Helsinki, Finland; June 4-7 2000.

In addition to the publications listed above 4 Masters Technical Reports and 1 Ph.D. dissertation resulted from this project. They are listed below:

#10. Gary Carlton (1997) Ph.D. " A Model to Estimate a Worker's Exposure to Spray Paint Mists"

#11. John McKernan (1997) MSPH "Effect of Position and Motion on Personal Exposure in a HVLP Spray Painting Operation"

#12. Kevin Dunn (1997) MSEE "An Investigation of Factors Affecting the Development of an Empirical-Conceptual Model for Estimating Spray Paint Exposure in a Cross Draft Spray Booth"

#13. Betty Gatano (1997) MSEE "Determining Transfer Efficiency from an HVLP Spray Gun"

#14. Brian Blazicko (1998) MSEE "The Evaluation of Momentum Flux to Estimate Exposure from Spray Painting Operations"

---

## Significant Findings

The primary hypothesis of this research is that “the lowest exposure results when the worker is to the side of the object being painted ( $90^\circ$  -orientation), with the spray gun in the downstream hand; rather than standing in front of the workpiece as is typically the case ( $180^\circ$  - orientation).” The results of this research clearly illustrate that for the situation examined, (i.e., a flat plate in a cross draft booth), and for most compressed air-spray painting guns; this is not true, and that exactly the opposite is the case. The lower exposure will be in the  $180^\circ$  orientation. It is only when the source momentum is extremely low that the  $90^\circ$  orientation is superior. This is illustrated in several of the publications (#1, #4 and #10) and, is supported by the field study (#2) and numerical work (#5, #6, #8, and #9).

The effects of motion (#11) and in which hand the spray gun is held (#12) were examined in wind-tunnel studies. The results suggest that motion seems to produce results midway between the two stationary positions (i.e.,  $90^\circ$  and  $180^\circ$ ) and that in the  $90^\circ$  position when the spray gun is held in the upstream hand lower breathing zone concentrations result than when the gun is in the downstream hand. However the results of the motion study are not reported with confidence. The spraying motion that the robot-mannequin produced was not a reasonable representation of a real spray painter, as it was quite exaggerated. In addition the robot-mannequin was too large for the small wind tunnel and the data that resulted would not be directly scalable to a real person. In contrast the smaller mannequin which provided good scaling data. The effect associated with which hand the gun is in was supported by 2-d numerical work (#5); but also needs further evaluation.

A surprisingly accurate model for estimating transfer efficiency is developed based on a simple impactor theory and size distribution data predicted using the Kim and Marshall reference. This model is confirmed with numerical simulations and is important in estimating overspray generation rates. This model essentially completes the exposure model (described in publications #4 and #7) allowing a dimensionless breathing zone concentration to be predicted as a function of the momentum flux ratio, and geometry.

The major positive results may be summarized as follows: (1) Through the use of dimensional analysis and scale model wind-tunnel studies a simple mathematical model was developed to predict human exposure to total mass generated during spray painting operations in cross-draft booths. This model was evaluated very favorably with field studies. (2) Commercially available Computational Fluid Dynamics (CFD) software in conjunction with algorithms developed in-house, were used to generate estimates of human exposure to aerosols generated during spraying operations. These simulations produced breathing zone concentrations that were in good agreement with the field-validated model. (3) Use of a dimensionless breathing-zone concentration as a function of a momentum flux ratio is a powerful tool to assess control intervention alternatives for human exposures to airborne contaminants.

There are two important limitations in the study. First is the inability of the commercial CFD package (FIDAP v 8.0) to provide the aerosol concentrations directly. This is because the residence time of the aerosol trajectories within the breathing zone cannot be calculated directly in commercial software (FIDAP v8.01). The information for each trajectory must be written to disk, the resulting file reformatted (using a perl script we developed in-house specifically for the FIDAP output files) and then run through our aerosol algorithm to generate estimates of concentration, transfer efficiency, overspray generation rate, and dermal deposition rates. The fact that these data files approach 1 gigabyte each and over 50 such files may be processed per simulation results in a great inefficiency. Discussions with the FIDAP (FLUENT) software group indicated that access to the source code was not an option, and that developing the capability to do such calculations was not a high priority in upcoming versions of the code.

Second, the work here uses, with the exception of the field study, a non-volatile oil. The effects of evaporation on the model are only indirectly dealt with. While the assumption that vapor will be transported similarly to the aerosol seems a reasonable first approximation, there is clearly room for improvement. The use of total mass (i.e., both vapor and solid) as the dependent variable in the model obscures some of the details that would be useful to hygienists.

---

## Utility of Findings

The results of this research are useful in several ways. The mathematical model of exposure to contaminants generated in spray painting operations allows the industrial hygiene engineer to estimate the effects of changing various parameters on the worker's exposure. The model addresses not only the effects of ventilation, but work practices (specifically orientation and distance of spray gun to work piece surface), and transfer efficiency (and hence contaminant generation rate). The computational fluid dynamics approach provides a framework for examining much more complex (and realistic) problems than the simple dimensional analysis model. More complex shapes, downdraft configurations, and even motion are possible with this tool. Useful "numerical flow visualizations" can be produced on rather coarse meshes that provide helpful information on the design of ventilation systems, and for EPA Pre-Manufacture Notification exposure estimations (see examples on the following page). It should be noted that the general approach of using CFD for the spray painting problem that is outlined here can serve as a blueprint for other processes as well. On a very practical level the work done here shows the importance of work-practices in conjunction with ventilation as an exposure control. The orientation of the spraying with respect to the airflow direction is a critical variable in achieving lower exposure.

In addition, this research provides a methodology for developing further, the use of computational fluid dynamics as a tool for occupational hygienists. This is accomplished by a controlled analysis of the uncertainties involved. The creation of a simple conceptual model based on dimensional analysis provides the data necessary to examine both the CFD results and reality. This allows assessment of the major sources of error and to identify how further improvements can be made efficiently.

Below are some numerical flow visualizations from the FIDAP and AVS computer codes.

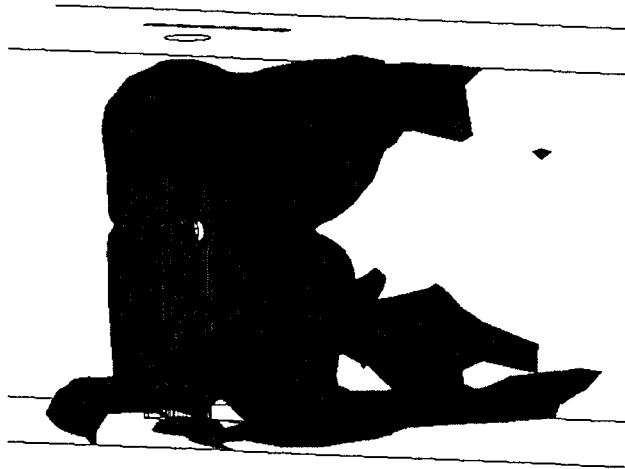


Figure 1: Visualization of FIDAP output for 3-d turbulent flow simulation of spray painting. Painter is represented by circular cylinder, the flat plate being sprayed is obscured by the concentration iso-contour that is displayed. Booth air flow is from left to right. Simulation indicates significant concentration in breathing zone area compared with results below, in Figure 2.

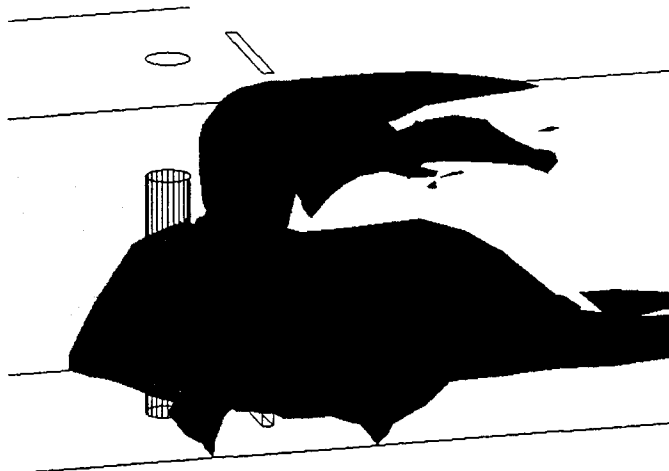


Figure 2: Same situation depicted above only now air flow is from the back of the worker (still left to right). The breathing zone is clear of contaminant.



---

## Specific Aims and Relationship to Publications

The original proposal stated – “The primary hypothesis is that the lowest exposure results when the worker is to the side of the object being painted, with the spray gun in the downstream hand; rather than standing in front of the workpiece as is typically the case. The following specific aims are proposed: (1) Improve existing numerical algorithms and use commercially available CFD packages to generate predictions of breathing zone concentration for specific work practices described in the primary hypothesis above, and incorporating factors listed in specific aim (3) below. (2) Construct a working laboratory model of a spray operation using a moveable mannequin and actual compressed air spray gun. The model will be placed within our wind tunnel to simulate a spray paint booth, and used to determine aerosol cut-sizes for estimating mass generation rates in the overspray. (3) Conduct experiments using this laboratory model to calibrate numerical predictions of exposure and validate the primary hypothesis; the following parameters will be examined: (a) wind tunnel air velocity, (b) mannequin mobility, (c) orientation of mannequin to air flow direction, (d) contaminant generation rate, and (e) whether the spray gun is in the upstream or downstream hand. Concentration measurements of tracer gas and aerosols will be made from the mannequin's breathing zone. (4) Use flow visualization to confirm numerically predicted flow patterns, and to demonstrate the effects of boundary layer separation. Smoke wires will be used to produce video recordings of the flow patterns, and provide insights into the mechanisms of exposure. (5) Conduct a field validation of the model in actual spray paint booths. Personal samples will be taken to confirm the primary hypothesis, and evaluate the numerical predictions of worker exposure.”

**Specific Aim (1)** is addressed in four of the publications:

Flynn, M.R., and Carlton, G. “Exposure Models for Contaminant Control Decisions Involving Ventilation” in *Ventilation '97: Global Development in Industrial Ventilation Proceedings of the 5<sup>th</sup> International Symposium on Ventilation for Contaminant Control*, eds. H. Goodfellow and E. Tahti; Ottawa Sept 14-17 1997, CEIA-ACIE.

Flynn, M.R., and Sills, E.D. “On the use of computational fluid dynamics in the prediction and control of exposure to airborne contaminants – an illustration using spray painting” *Ann. Occup. Hyg.* In Press;

Flynn, M.R. and Sills, E.D. “Numerical Simulation of Human Exposure to Aerosols Generated during Spray Painting” Under Preparation for submission to *Journal of Fluids Engineering*.

Flynn, M.R. “Evaluating Uncertainties in computational fluid dynamic simulations of human exposure to paint-spray aerosols” submitted to *Ventilation 2000 6<sup>th</sup> International Symposium on Ventilation for Contaminant Control*, to be held in Helsinki, Finland; June 4-7 2000.

**Specific Aims (2) and (3)** are addressed in the four publications that follow. Studies dealing with motion and which hand the spray gun is in are in the Masters Technical Reports by McKernan and Dunn which are included in the Appendix. Because numerical algorithms for aerosol transport were developed all measurements were made with aerosols not tracer gas.

Carlton, G. and Flynn, M.R. "A model to Estimate Worker Exposure to Spray Paint Mists" Appl. Occup and Env. Hyg. 12(5):375-382, (1997).

Carlton, G. and Flynn, M.R. "The Influence of Spray Painting Parameters on Breathing Zone Particle Size Distributions" Appl. Occup and Env. Hyg. 12(11):744-750, (1997).

Flynn, M.R., Gatano, B., McKernan, J., Dunn, K. Balzicko, B., and Carlton G.N. "Modeling worker exposure to airborne contaminants generated during compressed air spray painting. Ann. Occup. hyg. 43(1):67-76, (1999).

Tan, Y, and Flynn, M.R. "Experimental Evaluation of a Mathematical Model for Predicting Transfer Efficiency of a High Volume – Low Pressure Air Spray Gun" submitted to Appl. Occup. And Env. Hyg.

**Specific Aim (4)** No publications specifically address this aim - the basic flow patterns predicted were observed in the wind tunnel but were difficult to document with photos due to the high momentum flux of the jet. The smoke wire technique did not provide good visualization for this complex flow.

**Specific Aim (5)** is addressed in: Carlton, G. and Flynn, M.R. "Field Evaluation of an Empirical-Conceptual Exposure Model" Appl. Occup and Env. Hyg. 12(8):555-561, (1997).

Because 3 of the publications are in various stages of completion a summary of each with respect to the specific aims is given below:

(A) Flynn, M.R., and Sills, E.D. "On the use of computational fluid dynamics in the prediction and control of exposure to airborne contaminants – an illustration using spray painting" Ann. Occup. Hyg. In Press;

Reprints for this paper will be forwarded as soon as they are available. We have returned the galley to the journal, and anticipate publication shortly. The major significance of this work is to demonstrate that our CFD based model correctly ranks the 90° orientation as the high exposure case relative to the 180° case. The paper identifies guidelines for selecting the appropriate number of trajectories, the timestep size, and the duration of the simulation in order to achieve convergent results. The finite element meshes used in this work were coarse level meshes, and the jet size was rather large ( 1 inch square), in addition the momentum flux from the jet was not matched to experiment (only the momentum flux ratio was matched). These issues are addressed in the manuscript currently under preparation, see (B) below.

(B) Flynn, M.R. and Sills, E.D. “Numerical Simulation of Human Exposure to Aerosols Generated during Spray Painting” Under Preparation for submission to Journal of Fluids Engineering.

This paper is currently under preparation – the numerical simulations were conducted using a ½ inch square jet, the momentum flux exiting the jet was matched to experiment as was the momentum flux ratio. Mesh refinement studies were conducted with improved meshes and excellent results were obtained between numerically predicted dimensionless breathing-zone concentrations and those measured in wind tunnel studies, which in turn were field validated (see Table I below). The paper presents a detailed analysis of uncertainties involved – especially those related to aspiration efficiency of filter cassettes. The paper also presents results on numerical predictions of transfer efficiency which are in good agreement with measurements.

Table I -- Results of the most recent simulations using a 0.5 inch square jet. These results will be incorporated into publication #8.

	# of Nodes	Transfer Efficiency	CHUD/mo Unadjusted	CHUD/mo Adjusted for aspiration efficiency of filter cassette	MMD	GSD
Mesh 5	581,000	0.81	0.37	0.13±0.1	11	2.0
Mesh 4	338,000	0.81	0.23	-	-	-
Mesh 3	228,000	0.81	0.035	-	-	-
Experiment						
¼ J nozzle	N/A	0.94	Unknown	0.135 ±0.02	24	1.6
HVLP gun	N/A	0.8	N/A	N/A	N/A	N/A

(C) Tan, Y, and Flynn, M.R. “Experimental Evaluation of a Mathematical Model for Predicting Transfer Efficiency of a High Volume – Low Pressure Air Spray Gun” submitted to Appl. Occup. And Env. Hyg.

This paper further examines the transfer efficiency model proposed in Flynn, M.R., Gatano, B., McKernan, J., Dunn, K. Balzicko, B., and Carlton G.N. “Modeling worker exposure to airborne contaminants generated during compressed air spray painting. Ann. Occup. hyg. 43(1):67-76, (1999). It specifically confirms the model over distances representative of real spray processes and provides a valuable tool in estimating contaminant generation rates. This paper was submitted in Dec of 1999.

---

## Appendix

Attached are two Masters Technical Reports addressing the issues of spray motion; in which hand the spray gun is held; and sampler location effects.

Technical Report 1: John McKernan (1997) MSPH “*Effect of Position and Motion on Personal Exposure in a HVLP Spray Painting Operation*”

Technical Report 2: Kevin Dunn (1997) MSEE “*An Investigation of Factors Affecting the Development of an Empirical-Conceptual Model for Estimating Spray Paint Exposure in a Cross Draft Spray Booth*”

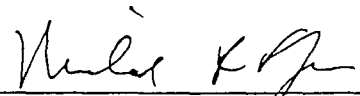
# **An Investigation of Factors Affecting the Development of an Empirical-Conceptual Model for Estimating Spray Paint Exposure in a Cross Draft Spray Booth**

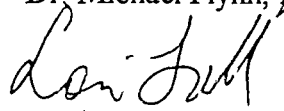
by  
Kevin H. Dunn

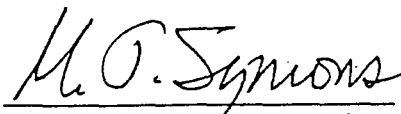
A report submitted to the faculty of The University of North Carolina at Chapel Hill in  
partial fulfillment of the requirements for the degree of Master of Science in  
Environmental Engineering in the Department of Environmental Sciences and  
Engineering, School of Public Health

Chapel Hill, 1997

Approved by:

  
\_\_\_\_\_  
Dr. Michael Flynn, Advisor

  
\_\_\_\_\_  
Dr. Lori Todd, Reader

  
\_\_\_\_\_  
Dr. Michael Symons, Reader

## **ABSTRACT**

### **Kevin H. Dunn. An Investigation of Factors Affecting the Development of an Empirical-Conceptual Model for Estimating Spray Paint Exposure in a Cross Draft Spray Booth (Under the direction of Dr. Michael Flynn)**

An empirical-conceptual modeling approach was developed by Carlton for estimating worker exposure to air contaminants during high pressure conventional air atomization spray painting. McKernan and Gatano sought to extend this model to the case of high volume, low pressure (HVLP) spray application technology. Significant differences between the Carlton and Gatano/McKernan model were established.

This research used a similar experimental methodology as Carlton and Gatano/McKernan to investigate the nature of these differences and to evaluate the sensitivity of the HVLP model to variations in test setup and sampling methodologies. A series of experiments using a mannequin, flat plate, and an HVLP spray application system were performed in a 25 ft<sup>2</sup> simulated cross draft spray booth. Spray gun hand orientation and lapel sampling location resulted in significant differences in measured breathing zone concentrations at similar test conditions. Minimal effects however were attributed to excessive wind tunnel blockage.

## ACKNOWLEDGMENTS

I would like to thank my advisor, Dr. Michael Flynn for his guidance and support throughout this project. I would also like to thank my committee members Dr. Lori Todd and Dr. Michael Symons for their help in answering my questions and for helping to develop my skills under their instruction.

I would also like to thank my research partners John McKernan and Betty Gatano for working out the kinks in the system and providing me with a good base from which to start my studies. I would also like to acknowledge the efforts of Randall Goodman in setting up the paint booth for my use and providing materials and help in the second phase of testing. Finally, I would like to acknowledge the National Institute for Occupational Safety and Health (NIOSH) for providing funding for this research and financial support of my education. This work was supported by NIOSH grant #5 R01 OH02858, “Computational Methods in Industrial Ventilation.”

## TABLE OF CONTENTS

LIST OF TABLES	v
LIST OF FIGURES	vi
1.0 Introduction	1
1.1 Background and Objectives	3
2.0 Conceptual Model Development Theory	7
3.0 Experimental Methodology	11
Determination of Overspray and Transfer Efficiency	14
Determination of Breathing Zone Concentration	15
4.0 Results	17
4.1 Differences between Upstream and Downstream Hands	17
4.2 Sample Location Effects	18
4.3 Tunnel Blockage Ratios and Scaling Effects	18
5.0 Discussion	19
5.1 Differences between Upstream and Downstream Handedness	19
5.2 Sample Location Effects	21
5.3 Tunnel Blockage Ratios and Scaling Effects	22
6.0 Conclusions	23
REFERENCES	25
Appendix A: Wind Tunnel Experimental Methods and Data	41
Appendix B: Paint Booth Experimental Methods and Data	66
Appendix C: Statistical Analysis and Results	77



## **LIST OF TABLES**

Table 1: Wilcoxon Statistical Test Results for the Effects of Lapel Sample Locations.....40

Table 2: Comparison of Blockage Ratios between the Wind Tunnel and Paint Booth.....40

## LIST OF FIGURES

Figure 1: Spray Painting Worker/Workpiece Orientation .....	29
Figure 2: Functional Relationship between the Dimensionless Groups for Carlton and McKernan/Gatano data sets.....	30
Figure 3: Spray Gun Hand Orientation.....	31
Figure 4: Experimental Setup.....	32
Figure 5: Schematic of Compressor and Spray Pot Systems.....	33
Figure 6: The Effects of Upstream versus Downstream Handedness on the Dimensionless Groups.....	34
Figure 7: Transfer Efficiency as a Function of $m_a/m_i$ .....	35
Figure 8: Effects of Wind Tunnel Blockage on Dimensionless Groups.....	36
Figure 9: Diagram of Overspray Pattern.....	37
Figure 10: Comparison of the Effects of Motion on Downstream Hand Concentrations..	38
Figure 11: Functional Relationships between Dimensionless Groups for All Data Sets....	39

## 1.0 Introduction

Spray finishing is a widely used process throughout industry for the coating of metallic parts, wood furniture, and even for the fabrication of fiberglass boats. A spray gun operates by atomizing liquid coatings with high pressure air (conventional spray guns) or through a high volume of low pressure air (HVLP spray guns). The droplets formed from this process are propelled towards the workpiece with some impacting on the part. A significant portion of the liquid however does not coat the part and is carried away by the air stream, sometimes reaching the breathing zone of the worker. The inhalation of these small droplets, called overspray, may result in adverse health effects for the worker.

<sup>(1)</sup> Paints consist of several chemical components including inorganic pigments diluted in a mixture of solvent carrier, binder, and other additives to enhance coating properties. Common pigments used in paints contain compounds of toxic metals including lead, cadmium, and chromium. Another hazardous component used primarily in automotive clear coats is isocyanates which have resulted in skin and eye irritation as well as respiratory effects.<sup>(1,2)</sup>

The primary exposure control method used in the spray painting of large parts is a ventilated booth. The conventional spray booth is constructed of sheet metal with an open entrance for conveying parts into and out of the paint area. An exhaust fan in the rear of the booth typically delivers air velocities of around 100 feet per minute (fpm) to control

solvent buildup (flammability), to prevent contamination of the part coating and to minimize worker exposure to toxic chemicals.<sup>(3)</sup> Recently, a new generation of high transfer efficiency application devices have been studied to evaluate their impact on reducing air emissions of process contaminants and subsequently worker exposure to these chemicals. The transfer efficiency is the ratio of the amount of material sprayed to the amount of material deposited on the workpiece. A high transfer efficiency means that more material is transferred to the part and less material is exhausted from the process.

The effect of higher transfer efficiency may translate into reduced worker exposure to overspray contaminants. A comparison of conventional and HVLP spray guns conducted by the National Institute of Occupational Safety and Health (NIOSH) showed that the HVLP system tested was about 30% more efficient than the conventional spray gun based on measured film thickness. The corresponding particulate overspray concentration was reduced by a factor of 2. A theoretical derivation of the relationship between transfer efficiency and air contaminant concentration shows that increased transfer efficiencies result in a greater than proportional decrease in solvent and particulate overspray concentration.<sup>(4)</sup> Recent recommendations by NIOSH based on these results have placed emphasis on the use of HVLP as a mechanism to minimize overspray generation. NIOSH released a Hazard Controls Bulletin in January 1996 which recommended the use of HVLP, downdraft ventilation and respiratory protection to control worker exposure to toxic contaminants.<sup>(5)</sup>

Most companies are slowly replacing their conventional spray guns with the newer HVLP systems. The reasons for these conversions are two-fold: changing environmental regulations and reducing operating costs. In 1989, the South Coast Air Quality Management District (SCAQMD) became the first region of the country to mandate the use of HVLP or other high transfer efficiency coating technologies (transfer efficiency greater than 65%).<sup>(6)</sup> The SCAQMD has gone on to mandate the use of high transfer efficiency application technologies in several other sectors including automotive body shops (Rule 1151), fiberglass fabrication (Rule 1162) and wood furniture manufacturing (Rule 1136).<sup>(7,8,9)</sup> The Environmental Protection Agency (EPA) has followed suit in its development of the National Emissions Standards for Hazardous Air Pollutants (NESHAP). The recently promulgated Wood Furniture Maximum Achievable Control Technology (MACT) standard restricts the use of conventional spray guns in most application processes used in furniture manufacturing.<sup>(10)</sup>

### ***1.1 Background and Objectives***

One of the primary goals of local exhaust ventilation and the use of the new high transfer efficiency spraying equipment is to limit worker exposure to air contaminants to an acceptable level. Although the American Conference of Governmental Industrial Hygienists (ACGIH) ventilation design manual provides recommendations on paint booth design and operational parameters (like air flow rate)<sup>(3)</sup>, the ability of these engineering controls to meet the recommended limits is not known until personal sampling is

performed. Carlton developed an empirical-conceptual model to relate worker exposure to spray painting process parameters. <sup>(11)</sup> This conceptual model attempted to account for the main processes which lead to worker exposure. The resulting model defined worker exposure in terms of seven major factors including: overspray mass generation rate ( $m_0$ ); spray nozzle pressure ( $p_n$ ); paint viscosity ( $\mu_l$ ); freestream velocity ( $U$ ); dimensions of the worker (height,  $H$  and breadth,  $D$ ); and worker orientation to the freestream (see Figure 1). Based on each of the primary processes, the relevant parameters were chosen and grouped into two dimensionless ratios which incorporated aspects of each important exposure mechanism. The following are the non-dimensional groupings:

Carlton number (non-dimensional nozzle pressure):  $\frac{p_n H}{\mu_l U}$

Non-dimensional Concentration:  $\frac{CHUD}{m_0}$

A mannequin, flat plate, and conventional pneumatic spray atomization nozzle were used in a small scale wind tunnel to evaluate the functional relationship between these two groups. Carlton performed a series of tests with the mannequin and workpiece oriented in both the  $180^\circ$  (airflow is to the worker's back) and  $90^\circ$  (airflow is to the worker's side) to develop the model for each of these commonly used configurations (Figure 1). A regression of the data set gathered by Carlton resulted in the following relationships. <sup>(11)</sup>

90° orientation:

$$\frac{CHUD}{m_0} = \frac{1}{\left\{ 7.44 + 1.08 \times 10^3 \exp \left[ -5.64 \times 10^{-7} \frac{p_n H}{\mu_l U} \right] \right\}}, \quad r^2 = 0.98$$

180° orientation:

$$\frac{CHUD}{m_0} = 3.23 \times 10^{-2} \exp \left[ -1.94 \times 10^{-7} \left( \frac{p_n H}{\mu_l U} \right) \right], \quad \text{for } \frac{p_n H}{\mu_l U} < 10^7, \quad r^2 = 0.95$$

$$\frac{CHUD}{m_0} = 0.006, \quad \text{for } \frac{p_n H}{\mu_l U} > 10^7$$

Further research performed by Gatano and McKernan sought to extend this model to a High-Volume, Low-Pressure spray gun.<sup>(12)</sup> A similar experimental methodology was employed including: a full scale automated mannequin, a larger flat plate and a commercial HVLP spray gun system installed in the small experimental wind tunnel. The results of their research showed a significant difference in the 90° orientation from the Carlton model. A plot of the results of both the Gatano/McKernan and Carlton data set is shown in Figure 2.<sup>(11,12)</sup>

This study sought to evaluate the nature of the differences between the Carlton model and the Gatano/McKernan HVLP results. The sensitivity of the HVLP model to various operational and sampling alternatives was investigated to determine if differences in the experimental methodologies used by McKernan and Gatano could account for the variation between their results and the Carlton model. The effects of three setup configurations on the model were evaluated in this study including: spray gun hand orientation (see Figure 3); concentration sample location (upstream versus downstream lapel); and wind tunnel blockage ratios. These effects were evaluated only in the 90° orientation as the McKernan/Gatano data set fit the Carlton model well in the 180° orientation.

The difference between handedness was investigated for the 90° worker orientation. The mannequin throughout this experimental study had the spray gun placed in the upstream hand (see Figure 3). A series of tests were performed by Gatano and McKernan with the gun in the downstream hand of the mannequin. A comparison of the differences between the non-dimensional concentration across a range of Carlton numbers was examined to determine the impact of handedness on the model development for the HVLP system. The effect of sample location was also investigated during this study. The mannequin was outfitted simultaneously with a sampler on both the upstream and downstream lapel. The resulting concentrations were analyzed to determine if a sampling location choice resulted in a significant difference in measured breathing zone concentrations. The final research question which was investigated during this study was



the effect of scaling or tunnel blockage ratios. The blockage ratio is the ratio of the area of the test object (mannequin and plate) to the cross-sectional area of the overall test section (wind tunnel). To investigate the magnitude of these effects, the mannequin and spray system were moved from the small scale experimental wind tunnel into a full size paint booth and a series of test conditions were run.

## **2.0 Conceptual Model Development Theory**

The benefit of the empirical-conceptual modeling approach is that once a limited number of process parameters are known, an estimate of worker exposure can be calculated. Also, the benefits of altering some of these parameters, such as increasing spray booth exhaust flow rates, can be semi-quantitatively evaluated. This modeling approach was employed by Carlton for the conventional spray system and focused on evaluating the parameters of the three main processes which lead to worker exposure to hazardous contaminants.<sup>(11)</sup>

The main processes which dominate exposure in spray painting tasks include paint droplet formation, transfer, and overspray transport.<sup>(11)</sup> The spray gun produces droplets by the shear forces generated by the action of the high velocity gas acting on the liquid jet. The atomization air is delivered in a parallel flow pattern around the liquid. The HVLP spray gun has a pair of air atomization orifices which surround the liquid orifice and delivers a high volume of low pressure air to cause the liquid stream to disintegrate into a

fine spray mist. This process is called pneumatic atomization and is used in spray painting to produce droplets typically less than 50  $\mu\text{m}$  in size which are in turn deposited on the workpiece by impaction.<sup>(13)</sup>

Droplet formation is the first stage of the process which leads to paint deposition and the generation of overspray. The droplet size distribution generated by pneumatic aspiration has been shown to be a function of the mass flow rates of air and liquid, the physical properties of the fluid, and the relative velocity of the liquid to the gas stream. Kim and Marshall developed an empirical relationship for determining the mass median diameter of droplets produced by atomization and reported these findings<sup>(13)</sup>:

- 1) The mass median diameter of a spray decreased to a limiting mass median diameter as the ratio of the mass flow rates of air to liquid ( $m_a/m_l$ ) increases;
- 2) An increase in liquid viscosity ( $\mu_l$ ) results in an increase in the mass median diameter of the droplets produced by atomization; and
- 3) The mass median diameter of a spray at a constant  $m_a/m_l$  was larger for lower air velocities for a given atomizer.

A conventional spray gun atomizes at a higher nozzle pressure than an HVLP system (65 psi vs. 10 psi). This higher pressure results in a relative velocity between the

spray droplets and the atomization air stream being much higher for the conventional system than the HVLP spray gun. The conventional spray system however operates at a lower  $m_a/m_l$  than the HVLP gun since the volumetric flow rate of atomization air for a conventional gun is significantly lower than that of the HVLP. These operational differences result in the spray distribution (MMD) generated by the HVLP being larger than that produced by a conventional spray gun. The larger droplets produced result in differences in both droplet transfer characteristics and solvent evaporation rates because of the lower total surface area of the HVLP distribution than the finer droplet distribution produced by the conventional spray gun.

The spray droplet transfer process is another major component in the determination of worker exposure. After the droplets leave the gun, they are propelled by the momentum imparted to them by the jet and the surrounding envelope of atomization air. As the jet meets the workpiece, the flow is diverted along the boundary of the flat plate. Some of the larger particles with sufficient inertia will impact on the plate while the smaller particles will be carried along the stream lines away from the workpiece. Simple impaction theory indicates that the cut size (size at which 50% of the particles of a given size will impact the plate) of the impaction process is proportional to the particle size. Therefore, larger particles will most likely be transferred to the workpiece while the smaller particles will be conveyed away from the workpiece by the freestream. As was previously shown, the HVLP produces a coarser spray droplet distribution and therefore more droplets are likely to impact resulting in a higher transfer efficiency and a lower

contaminant overspray generation rate than the conventional spray system. This result has been shown in practice with conventional spray transfer efficiencies typically ranging from 30–40% while HVLP transfer efficiencies have been reported above 65%.<sup>(4)</sup> Another difference in the droplet transport mechanisms of the HVLP and the conventional atomizer used by Carlton is the substantially higher momentum flux of the HVLP spray gun due to its higher volumetric air flow rate. The parameter used in the model to account for droplet transfer mechanisms is the nozzle pressure ( $p_n$ ).

The final process considered in the model development is overspray transport. The overspray is the collection of particles which do not have the inertia required to deviate from the air stream and impact on the part. Researchers have shown that these particles are generally 2.9–9.7  $\mu\text{m}$  in size.<sup>(14)</sup> These droplets are diverted along the workpiece boundary and dispersed by the action of the jet and the booth freestream. The spray booth ventilation system is designed to transport these droplets away from the part and collect them by dry filtration or by wet scrubbers.

The research performed by Carlton showed a significant difference in overspray exposure based on the worker/workpiece orientation.<sup>(11)</sup> The traditional recommended orientation is to place the contaminant generation source (spray gun) between the worker and the exhaust. George et al. showed that a reverse flow region formed downstream of the worker due to vortex shedding.<sup>(15)</sup> This reverse flow region caused contaminants to be transported back into the workers breathing zone. The breathing zone concentration

(BZC) was shown to be a function of the freestream velocity ( $U$ ), the worker's height ( $H$ ) and the worker's breadth ( $D$ ) by George et al. and other researchers.<sup>(15,16,17)</sup> The George et al. study, however, was performed with a source of negligible momentum and did not simulate a realistic spray painting operation. Kim and Flynn subsequently showed that the addition of a strong contaminant injection rate, similar to the case for spray painting, eventually prevents the formation of this vortex street and resulted in a dramatic reduction in the BZC of contaminants when compared to the case with a quiescent source.<sup>(18)</sup>

### **3.0 Experimental Methodology**

The experimental setup shown in Figure 4 was used to determine the relationship between the non-dimensional groupings of interest. A mannequin was placed in a wind tunnel which simulated a cross draft spray paint booth. The mannequin was outfitted with an electronically controlled trigger device which allowed for remote activation/deactivation of the spray painting gun. A 3 x 3 foot flat plate was used to simulate a workpiece. The use of a flat plate was chosen to enhance reproducibility among runs due to uniform air jet rebound characteristics. The mannequin was also outfitted with an air sampling cassette to measure breathing zone concentrations. The runs were performed with the mannequin oriented  $90^\circ$  to the freestream (see Figure 1). The spray gun was held in the upstream hand for comparison with additional data to evaluate the impact of handedness on breathing zone concentration. Breathing zone

samples were taken on both the upstream and downstream lapel to determine the effect of sampling location on measured concentration.

The wind tunnel has a cross sectional area of 25 ft<sup>2</sup> (5 ft by 5 ft) and is eight feet in depth. A bell-shaped inlet flange was constructed on the entry to reduce the effects of flow separation and to provide a more uniform flow. A pegboard and filter bank were also installed in the rear of the tunnel to assist in maintaining uniform flow throughout the depth of the tunnel. A pitot tube was installed to provide an indication of the tunnel static pressure and an air flow calibration curve was generated by performing a 16 point hot wire anemometer traverse across the tunnel cross sectional area. Tunnel freestream velocities of 45-325 feet per minute (fpm) were measured at tunnel static pressures ranging from 0.02 to 0.7 inches of water. Average freestream velocities from 75-350 fpm with longitudinal component of freestream turbulence intensities of 6-11% are possible in the tunnel.<sup>(11)</sup>

Following the completion of the experimental runs in the wind tunnel, the test setup including the mannequin and HVLP spray system was relocated to a full size paint booth located on the campus of the University of North Carolina at Chapel Hill. The paint booth cross sectional measurements were 7.25 ft x 6.25 ft and was 13.5 ft in depth. The room housing the paint spray booth was in the machine shop of the School of Public Health with several benches and cabinets located near the inlet to the booth which caused fairly high turbulence in the paint booth. A sheet metal flange was also installed on the

entrance to the booth to minimize the effects of flow separation at the booth entrance. The flowrate through the tunnel is adjustable by varying a pulley on the fan belts which in turn controls the fan speed. The fan was set initially to provide approximately 100 fpm and was not varied during the experiment due to difficulty in precise adjustment of fan speed. The air velocity was measured by the thermo-anemometer on a 12 point grid across a the paint booth cross section. A series of experiments were run in the paint booth to evaluate the effects of wind tunnel blockage on the exposure model.

The test system used was a pressure fed HVLP spray painting system (see Figure 5). A compressor was set to 100 psi to provide a constant source of air to the feed tank. The compressor also had a filter on the outlet to remove any moisture, dusts, or oils from the feed air. The air pressure was regulated at the feed tank to maintain approximately 10 psi on the liquid feed while the pressure to the gun was regulated separately to attain the desired air cap pressure for testing.

A DeVilbiss MSV-533-4-FF model HVLP spray gun was used throughout the test. The spray gun is constructed out of 400 grade stainless steel and fitted with a #33A air cap which is recommended for most common coating materials with required flow rates up to 12 oz/min. The spray gun is designed to operate at a nominal air cap pressure of 10 psi. The gun will produce 10 psi at the cap when the gun inlet pressure is set to a nominal pressure of 50 psi. An air cap test kit was used to measure the pressure at the cap while varying the gun inlet pressure at the feed tank regulator. The gun is also outfitted with 2

knobs to allow the operator to easily adjust the flow of air or liquid. The operator typically will make adjustments to the liquid flowrate based on the required coating thickness. Adjustment of the air knob allows the operator to control the fan pattern produced by the gun. This control knob would be adjusted based on the shape and size of the workpiece.<sup>(19)</sup> The air knob was set to produce an elliptical pattern used frequently in manufacturing. The liquid and air knobs were not adjusted throughout testing so that good reproduction of test conditions could be achieved from run to run.

Inland #99 neutral paraffinic vacuum pump oil was used instead of actual paint during this experiment. This was done mostly due to safety concerns with using paint. The vacuum pump oil was selected based on nonvolatility and because its viscosity is similar to enamel paints. The oil is also compatible with the materials in the wetted sections of the spray gun. The variation of the viscosity with temperature was measured using a Haake falling ball viscometer and corrections were applied to the data to account for actual environmental conditions.

### **Determination of Overspray and Transfer Efficiency**

The calculation of overspray generation rate and transfer efficiency was performed based on mass balance methodology. The amount of liquid sprayed was calculated by weighing the feed pot before and after each experimental run. The liquid mass flowrate was calculated by dividing the mass of the liquid sprayed by the run time. A trough was



placed under the flat plate to collect all the spray droplets that had impacted on the part. This trough was weighed before and after each run to measure the amount of liquid transferred to the workpiece. A simple ratio of the amount of the liquid transferred to the workpiece to the total amount of liquid used during the run provided the transfer efficiency. The mass overspray generation rate ( $m_0$ ) was also calculated by subtracting the mass flow rate of liquid transferred to the workpiece from the total mass flow rate of liquid used during each run.

#### **Determination of Breathing Zone Concentration**

NIOSH Method 0500 for total aerosol mass was used to perform the sampling and analysis of all breathing zone concentrations (C). A 37 mm polyvinyl chloride filter with a 5  $\mu\text{m}$  pore size was used at a sampling rate of 2.0 lpm.<sup>(20)</sup> An Aircheck personal sampling pump Model No.224-PCXR8 was used throughout the test. Run time was adjusted to collect an adequate sample mass (0.1-2 mg) for weighing and typically ranged from 5-10 minutes. Filter weights were measured by a Cahn 27 electrobalance which has a sensitivity of 0.0001 mg and a stated accuracy of  $\pm 0.005\%$ .

Previous research has shown that open and closed faced cassettes tend to significantly under-represent the aerosol when sampling from a moving airstream with the sampler oriented normal to the airstream (as in this research).<sup>(21)</sup> A sampler developed by the Institute of Occupational Medicine (IOM) was used in this study to minimize the

effects of under-sampling associated with the open and closed face cassettes. Mark and Vincent developed the British personal inhalable aerosol sampler (PIAS) which is comprised of a 37 mm cassette with a circular 15 mm diameter entry.<sup>(22)</sup> A test performed by the IOM evaluated many different international personal samplers by placing the sampler on a mannequin and rotating the mannequin through 360° during each run to achieve a non-orientation specific sample. The IOM testing was performed over a range of freestream velocities from 0.5-3.0 m/s and a range of particle sizes up to about 75 µm. The PIAS showed sampling efficiencies which were consistent with the ACGIH Inspirable Particulate Mass (IPM) curve which represents what a worker breathes in through the nose and mouth during normal respiration. The gravimetric analysis method recommended by the IOM was to weigh the complete cassette before and after each run to minimize particle losses to the internal surfaces of the sampler.<sup>(23)</sup> These losses have been shown to be a significant portion of the overall mass aspirated by the sampler (up to 40%).<sup>(24)</sup> In accordance with NIOSH method 0500, only the filter was weighed before and after the runs therefore, the results of the samples in this study are therefore likely to be less than the actual concentration of contaminant in the breathing zone.

## 4.0 Results

### *4.1 Differences between Upstream and Downstream Hands*

During this research, runs were performed with the spray gun in the upstream hand for comparison with the Gatano/McKernan downstream hand data set. Breathing zone concentrations were taken on the downstream lapel for all of the Gatano/McKernan data set. Only the downstream lapel samples from the upstream hand data set are therefore used for comparison to the Gatano/McKernan data set to minimize any bias introduced by the choice of sample location. A linear plot of the Carlton number versus the non-dimensional concentration is shown for both upstream and downstream hand orientations (see Figure 6). This plot shows that the upstream hand non-dimensional concentrations are much lower than the downstream hand concentration at Carlton numbers greater than  $1.0 \times 10^6$ . Also, a difference in transfer efficiency between the two data sets (upstream and downstream hand) was observed. The plot of transfer efficiency versus the ratio of mass flow rate of air to liquid is shown in Figure 7. The transfer efficiency measured during the upstream hand runs was noticeably higher than the downstream runs from the Gatano and McKernan data set.

#### ***4.2 Sample Location Effects***

The mannequin was outfitted with air sampling cassettes on both the upstream and downstream lapel during the experimental wind tunnel test runs. The effects of sample location on the measured breathing zone concentration (BZC) are shown in Table 1. As can be seen, for all cases in the 90<sup>0</sup> orientation with the gun in the upstream hand, the contaminant concentration measured on the downstream lapel was consistently higher than that of the upstream lapel. The downstream concentration was were primarily between 5-30% (7 of 11) percent higher than the corresponding upstream lapel measured concentrations.

#### ***4.3 Tunnel Blockage Ratios and Scaling Effects***

To investigate the effects of wind tunnel blockage on the model, the mannequin and flat plate were moved from the small experimental wind tunnel into a larger full size spray booth. The paint booth freestream velocity was set to a nominal value of approximately 100 fpm and the HVLP nozzle pressure was varied to map out a region of Carlton numbers. The results of the runs performed in the paint booth are shown along with the results of the wind tunnel data in Figure 8. The least squares regression line for the wind tunnel data is plotted to illustrate the distribution of the paint booth data with respect to the wind tunnel data. As seen in the figure, the paint booth non-dimensional concentrations seem to be consistent with the wind tunnel data at high Carlton numbers but are slightly lower than the wind tunnel data at lower Carlton numbers.

## 5.0 Discussion

### *5.1 Differences between Upstream and Downstream Handedness*

The differences in handedness are believed to be due to the impact of the differences in the flow patterns of the overspray mist. As can be seen in Figure 9, if the spray gun is moved from the upstream to the downstream hand, the cloud generated by the overspray mist (jet 1) would be translated towards the breathing zone of the worker. As the spray gun is moved to the downstream hand, the contaminant cloud recirculation zone is moved towards the breathing zone (and the downstream lapel) of the worker. As the overspray mist is formed from the spraying operation (when the gun is in the upstream hand), the droplets have a longer length to travel to reach the breathing zone of the worker. This allows the droplets to be dispersed by the fresh air entering the booth and results in lower breathing zone concentrations. The BZCs measured during the downstream hand spraying were approximately 2-7 times greater than those measured during upstream hand spraying. The mannequin arm was stationary during both the upstream and downstream testing, however, an additional study incorporating side to side motion was performed with the gun in the downstream hand (see Figure 10). The results showed that contaminant concentrations were significantly reduced possibly indicating an averaging of the upstream and downstream hand effects.

The handedness differences seen also hint at a difference in contaminant concentration regimes. As can be seen from Figure 6, there is a linear relationship

between non-dimensional nozzle pressure and BZC for the upstream hand orientation. This implies that as the Carlton number increases (indicating an increase in nozzle pressure and/or a decrease in the wind tunnel freestream velocity) the contaminant concentration linearly increases. This outcome makes intuitive sense with the factors discussed thus far. If the paint booth velocity is increased, we'd expect to see a decrease in the BZC. Also, as discussed previously, as the nozzle pressure is increased, the transfer efficiency decreases and the BZC also increases. There is a practical limit however where an increase in nozzle pressure will no longer result in an increase in worker BZC. This is due to the fact that at some limiting nozzle pressure, the region around the worker begins to resemble a well mixed volume. In this operational regime, the rate of overspray entering the worker's breathing zone equals the rate of overspray removed by the exhaust flow. This operational condition was reached during the downstream hand spray tests at a non-dimensional nozzle pressure of approximately greater than  $1.0\text{E}+06$ . The upstream hand testing showed that this point was not reached even at Carlton numbers of approximately  $2.3\text{E}+06$ . This may be indicative of the differences in the overspray plume between each of these orientations.

The differences in the transfer efficiency seen in Figure 7 are puzzling. The wind tunnel and paint booth results of the upstream hand transfer efficiencies were consistently higher than those of the downstream hand. The paint booth data, however, was closer to the downstream hand data set. The most logical reason for a difference would seem to be a difference in test set up or conduct. The lower transfer efficiencies seen in the

McKernan/Gatano data set might be due to the placement of the workpiece with respect to the spray gun. The flat plate position may affect the transfer efficiency by altering the amount of overspray which is diverted behind the workpiece. The plate was centered on the spray gun from side to side for the upstream hand data sets. The spray gun distance was set and checked prior to each run and was held at a eight inches from the plate and is not suspected to have caused the discrepancies.

### *5.2 Sample Location Effects*

A Wilcoxon signed rank test was performed to validate the observed differences seen in Table 1. The test showed a difference at a level of significance of  $p < 0.01$ . The greatest differences were observed at low nozzle pressures corresponding to the lowest sample masses which would have inherent variance. The reason for the differences may be due to the effects of the wake of the gun discharge. As the spray gun propels the paint towards the workpiece, one jet of material flows toward the tunnel exhaust while a second jet is directed towards the booth inlet (see Figure 9). NIOSH showed that the second jet is dispersed into the oncoming air stream and flows back into the worker's breathing zone.<sup>(1)</sup> Both lapel samples will therefore receive the majority of the sampled mass from the second jet stream. However, the downstream lapel may also receive a dose from the first jet due to the reverse flow region formed downstream of the body whereas the upstream lapel is unlikely to receive a significant dose from the first jet. This phenomenon may be unique to the upstream hand configuration as the effect should be

diluted as the downstream jet is moved closer to the exhaust filters (i.e. to the downstream hand).

### ***5.3 Tunnel Blockage Ratios and Scaling Effects***

Previous researchers have shown that the flow characteristics change depending on the overall blockage of the test section. Taylor and Whitelaw observed that as the blockage ratio increased, there was an increase in the length and a decrease in the width of the recirculation region downstream of the test object.<sup>(25)</sup> The consequences of these effects with respect to the test situation of placing a near full size mannequin and plate in a small experimental wind tunnel were unknown. The blockage ratio of the paint booth and wind tunnel are shown in Table 2 for comparison. The regression line for the analogous wind tunnel data is plotted along with the results of the paint booth data are shown in Figure 8. As one can see, the effects of blockage seem to create minimal effects. At higher non-dimensional nozzle pressures, the data points lie distributed about the wind tunnel regression line. However, at low nozzle pressures, the concentrations were slightly lower than those measured in the wind tunnel. A partial F test was performed to determine if the slopes and intercepts of the regressions were equal.<sup>(26)</sup> The result of the F test indicated that the lines were coincident at a level of significance of 0.05. Therefore in the nominal operational region of the HVLP system, the wind tunnel blockage did not seem to have caused a significant bias in the data set. This effect however, may be



important in the  $180^\circ$  orientation as the blockage ratio is substantially higher than that of the  $90^\circ$  orientation.

## 6.0 Conclusions

A significant difference exists between the model developed by Carlton for the conventional spray gun and the HVLP system for the  $90^\circ$  orientation. These differences can be seen in Figure 11. The results of the Carlton model showed that the relationship between the non-dimensional groups is fairly constant within the region of operation for conventional spray guns (Carlton numbers of  $1.2 \times 10^7$  to  $2.0 \times 10^7$ ) with  $CHUD/m_0$  values for the  $90^\circ$  orientation greater than an order of magnitude higher than the  $180^\circ$  orientation. However, these curves show a crossover at lower values of the Carlton number (less than  $5.0 \times 10^6$ ) suggesting that the  $90^\circ$  orientation might be preferable when operating in this region, as with the HVLP system.<sup>(11)</sup> The results of the research performed by McKernan and Gatano as well as the tests performed by the author of this paper suggest that this is not the case. Although the McKernan/Gatano  $180^\circ$  orientation HVLP data seems to match up with the Carlton model, the  $90^\circ$  orientation results suggest that a mechanism not considered in the Carlton model may be resulting in significantly higher non-dimensional concentrations than predicted.<sup>(12)</sup>

There is also a significant difference between the exposures measured associated with the hand position of the spray gun. The downstream hand resulted in a measured

breathing zone concentration that was a factor of 2-7 times higher than that of the upstream hand. This effect is diluted however when a side to side motion was tested. This result suggests that testing of actual spray painting operations needs to be completed before a thorough evaluation of this model can be completed. In many cases, work practices will result in significant variability between this model and actual measured concentrations. Therefore, this model may be useful in that it may provide an order of magnitude estimate of exposure and may help in evaluating optimizing process parameters to reduce worker exposure.

The effects of sampling location and tunnel blockage ratios were also studied. The comparison of lapel sampling locations showed higher breathing zone concentrations measured consistently on the downstream lapel. This result suggests that the conservative approach to evaluating worker exposure to contaminants, in the  $90^0$  orientation with the spray gun in the upstream hand performed in a cross draft booth, would be to place the sampler on the downstream lapel of the worker. The lapel samples should tend to give a higher concentration than the actual breathing zone because of the effects of the reverse flow region which occur downstream of the body. Finally, the wind tunnel blockage ratio did not seem to significantly affect the results of the experiments. The results of the full scale paint booth test runs showed that at moderate Carlton numbers, there were negligible differences in the non-dimensional concentration number while at low pressures the non-dimensional concentrations were slightly lower than those measured in the wind tunnel.

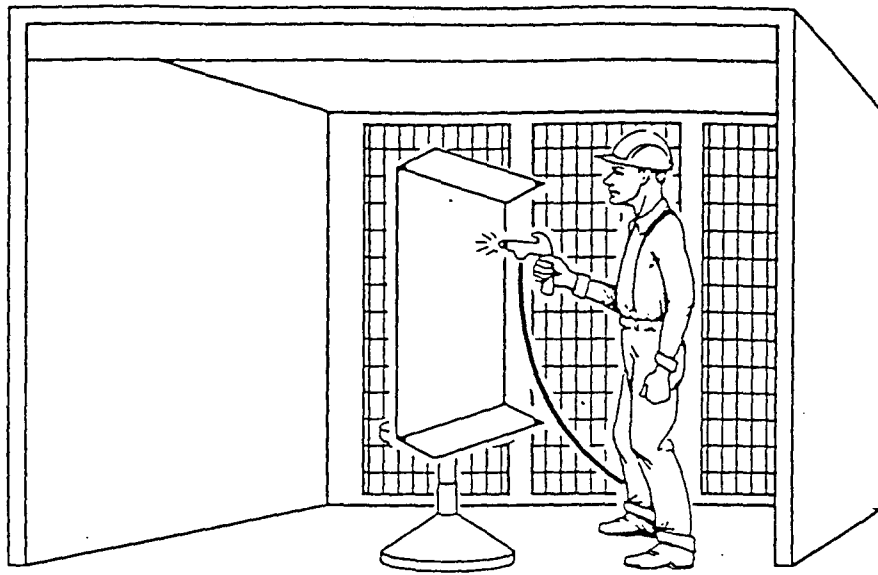
## REFERENCES

1. Heitbrink, W.A.; Wallace, M.E.; Bryant, C.J.; Ruch, W.E.: Control of Paint Overspray in Autobody Repair Shops. **Am. Ind. Hyg. Assoc. J.** 56:1023-1032 (1995).
2. Burgess, W. A.: Recognition of Health Hazards in Industry. A Review of Materials and Processes, pp. 247-275. John Wiley and Sons, Inc., New York, NY (1995).
3. American Conference of Governmental Industrial Hygienists: Industrial Ventilation, A Manual of Recommended Practice. ACGIH, Cincinnati, OH (1995).
4. Heitbrink, W.A.; Verb, R.H.; Fischbach, T.J.; Wallace, M.E.: A Comparison of Conventional and High Volume-Low Pressure Spray-Painting Guns. **Am. Ind. Hyg. Assoc. J.** 57:304-310 (1996).
5. National Institute for Occupational Safety and Health: Control of Paint Overspray in Autobody Repair Shops. DHHS (NIOSH) Publication No. 96-106. NIOSH, Cincinnati, OH (1996).
6. Cedoz, R.; Treuschel, J.: HVLP, the 'Wonder' Gun. **Industrial Finishing**. (1993).
7. South Coast Air Quality Management District: "Regulation XI source specific standards, Rule 1151, Motor Vehicle and Mobile Equipment Non-Assembly Line Coating Operations" (amended March 8, 1996), South Coast Air Quality Management District, Diamond Bar, CA (local air pollution control regulation).

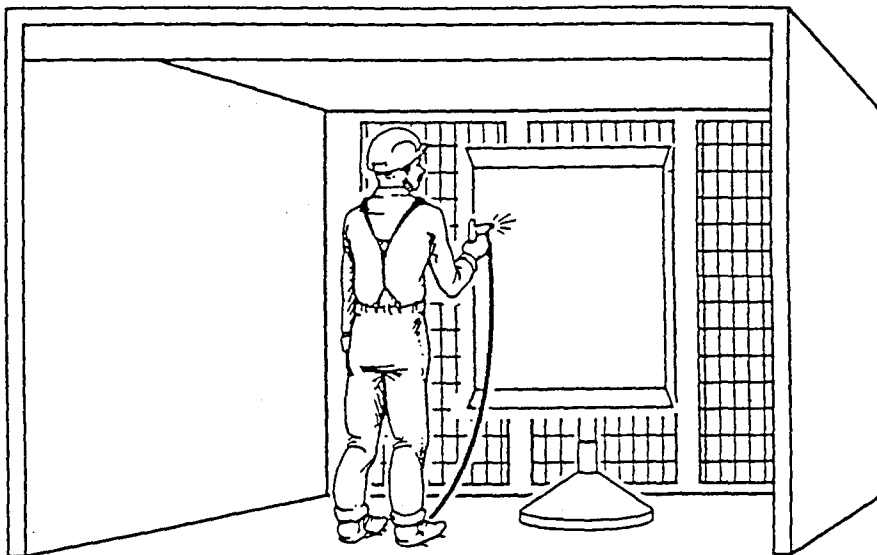
8. South Coast Air Quality Management District: "Regulation XI source specific standards, Rule 1162, Polyester Resin Operations" (amended May 13, 1994), South Coast Air Quality Management District, Diamond Bar, CA (local air pollution control regulation).
9. South Coast Air Quality Management District: "Regulation XI source specific standards, Rule 1136, Wood Products Coatings" (amended June 14, 1996), South Coast Air Quality Management District, Diamond Bar, CA (local air pollution control regulation).
10. U.S. Environmental Protection Agency: "Final Standards for Hazardous Air Pollutant Emissions from Wood Furniture Manufacturing Operations; Final Rule", 40 CFR Parts 9 and 63 (1995).
11. Carlton, G.N.: A Model to Estimate Worker Exposure to Spray Paint Mists. Ph.D. Thesis, University of North Carolina at Chapel Hill, NC (1996).
12. McKernan, J.: Effect of position and Motion on Personal Exposure in a HVLP Spray Painting Operation. Masters Technical Report, University of North Carolina at Chapel Hill, NC. (1997).
13. Kim, K.Y.; Marshall, W.R.: Drop-Size Distributions from Pneumatic Atomizers. **AIChE J.** 17(3):575-584 (1971).
14. D'Arcy, J.B.; Chan, T.L.: Chemical Distribution in High Solids Paint Overspray Aerosols. **Am Ind. Hyg. Assoc. J.** 51(3):132-138 (1990).

15. George, D.K.; Flynn, M.R.; Goodman, R.: The Impact of Boundary Layer Separation on Local Exhaust Design and Worker Exposure. **Appl. Occup. Environ. Hyg.** 5(8): 501-509 (1990).
16. Kim, T.; Flynn, M.R.: Modeling a Worker's Exposure From a Hand-Held Source in a Uniform Freestream. **Am. Ind. Hyg. Assoc. J.** 52(11):456-463 (1991).
17. Kim, T.; Flynn, M.R.: Airflow Pattern Around a Worker in a Uniform Freestream. **Am. Ind. Hyg. Assoc. J.** 52(7):287-296 (1991).
18. Kim, T.; Flynn, M.R.: The Effect of Contaminant Source Momentum on a Worker's Breathing Zone Concentration in a Uniform Freestream. **Am. Ind. Hyg. Assoc. J.** 53(12): 757-766 (1992).
19. DeVilbiss: The ABC's of Spray Finishing, A Working Guide to the Selection and Use of Spray Finishing Equipment. ITT DeVilbiss Maumee, OH (1995).
20. National Institute for Occupational Safety and Health: Particulates Not Otherwise Regulated, Total: Method 0500. In: NIOSH Manual of Analytical Methods, 4th Edition. P.M. Eller, Ed. NIOSH, Cincinnati, OH (1994).
21. Buchan, R.M.; Soderholm, S.C.; Tillery, M.I.: Aerosol Sampling Efficiency of 37 mm Filter Cassettes. **Am. Ind. Hyg. Assoc. J.** 47(12):825-831 (1986).
22. Mark, D.; Vincent, J.H.: A New Personal Sampler for Airborne Total Dust in Workplaces. **Ann. Occup. Hyg.** 30(1):89-102 (1986).
23. Vincent, J.H.; Mark, D.: Entry Characteristics of Practical Workplace Aerosol Samplers in Relation to the ISO Recommendations. **Ann. Occup. Hyg.** 34(3): 249-262 (1990).

24. Demange, J.; Gendre, J.C.; Herve-Bazin, B.; Carton, B.; Peltier A.: Aerosol Evaluation Difficulties Due to Particle Deposition on Filter Holder Inner Walls. **Ann. Occup. Hyg.** 34(4): 399-403 (1990).
25. Taylor, A.M.K.P.; Whitelaw, J.H.: Velocity Characteristics in the Turbulent Near Wakes of Confined Axisymmetric Bluff Bodies. **J. Fluid Mech.** 139:391-416 (1984).
26. Kleinbaum, D.G.; Kupper, L.L.; Muller, K.E.: Applied Regression Analysis and Other Multivariate Methods, pp. 271-274. 2nd ed. Duxbury Press, Belmont, CA (1988).



**90° Orientation**



**180° Orientation**

Figure 1: Spray Painting Worker/Workpiece Orientation

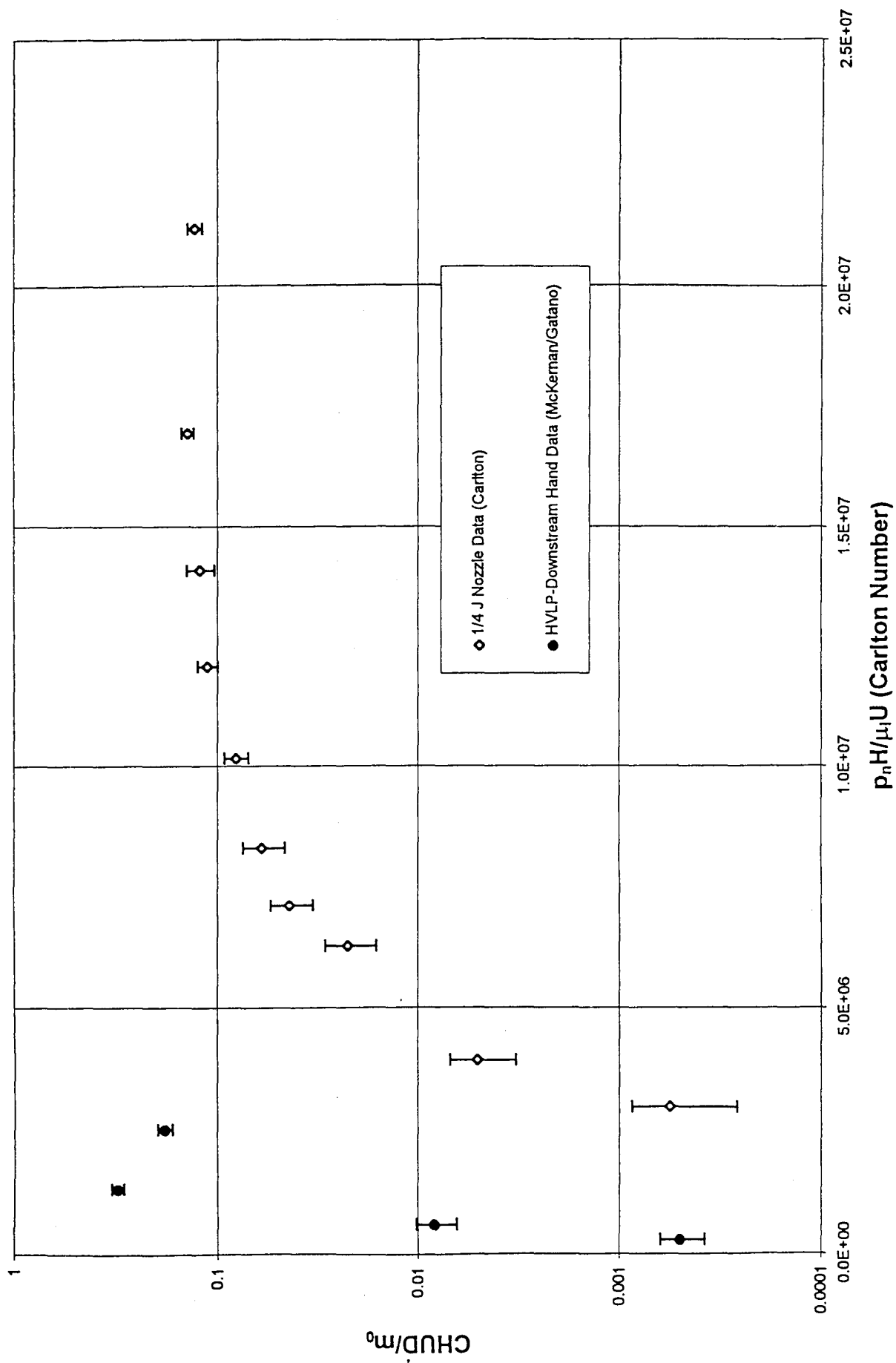
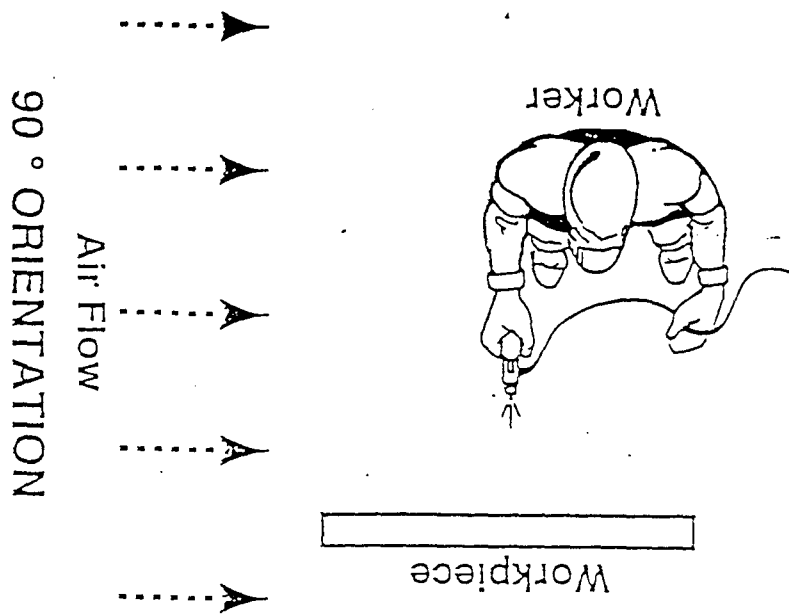
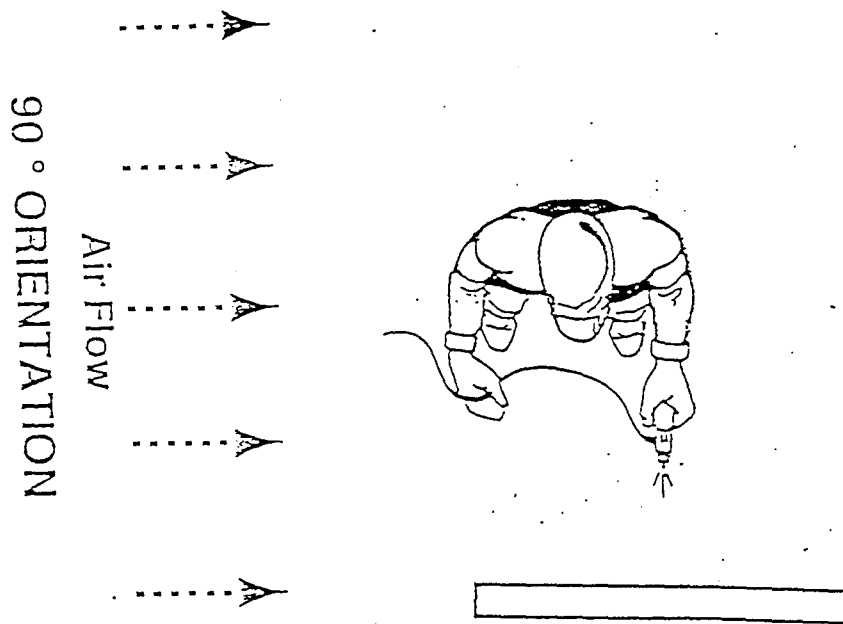


Figure 2: Functional relationship between the dimensionless groups for Carlton and McKernan/Gatano datasets





### Upstream Spray Hand



### Downstream Spray Hand

Figure 3: Spray Gun Hand Orientation

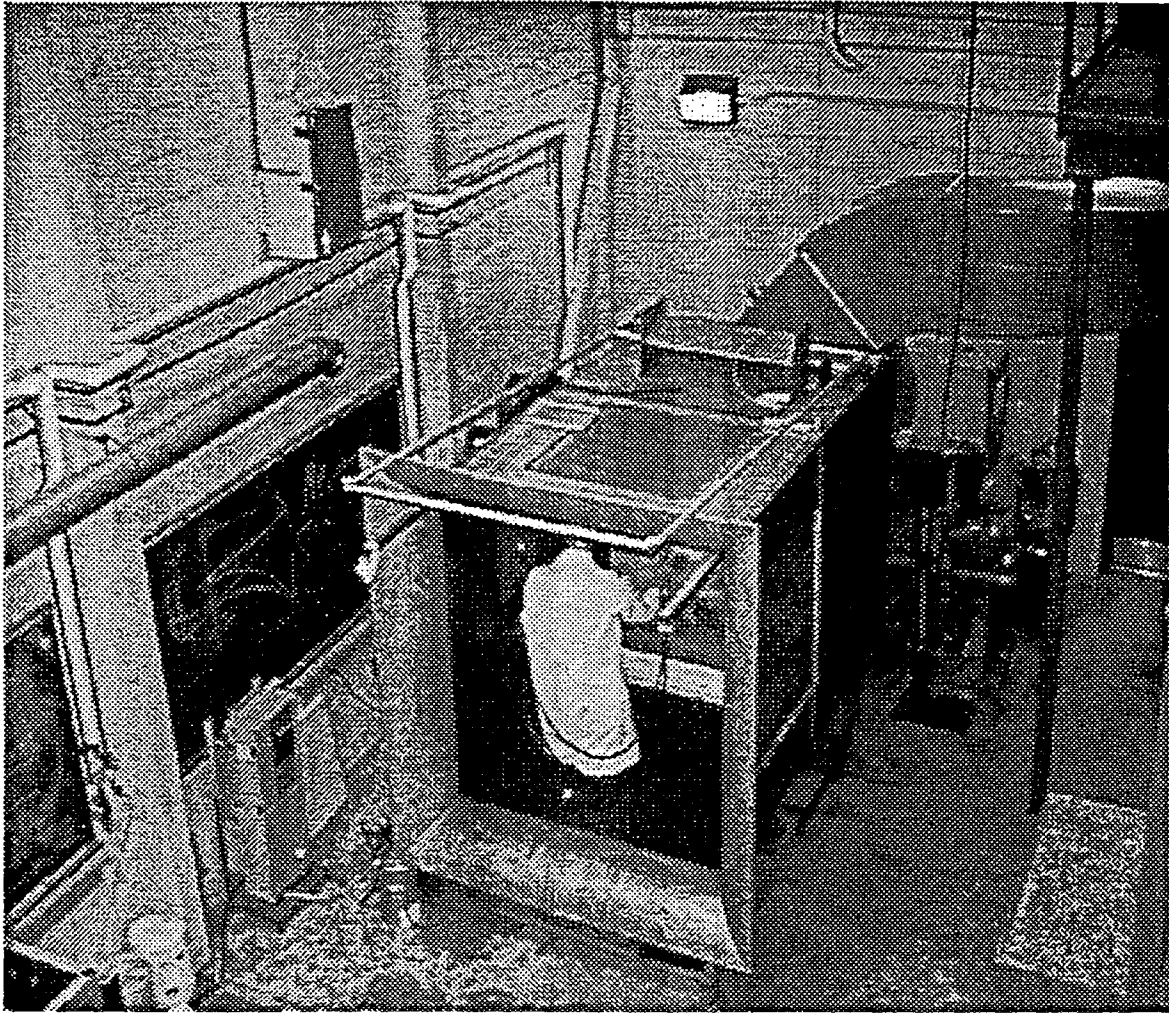
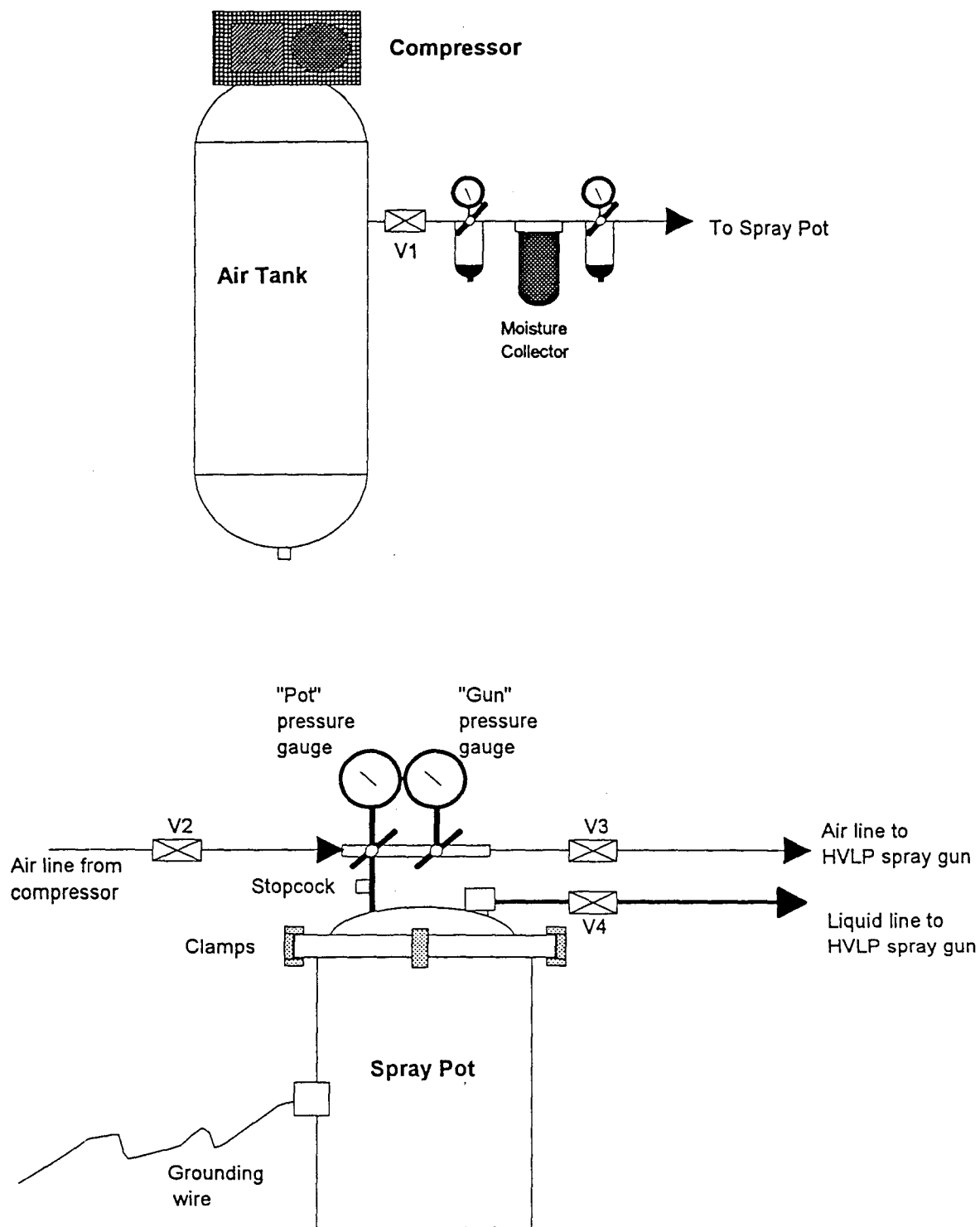


Figure 4: Experimental Setup



**Figure 5: Schematic of Compressor and Spray Pot Systems**

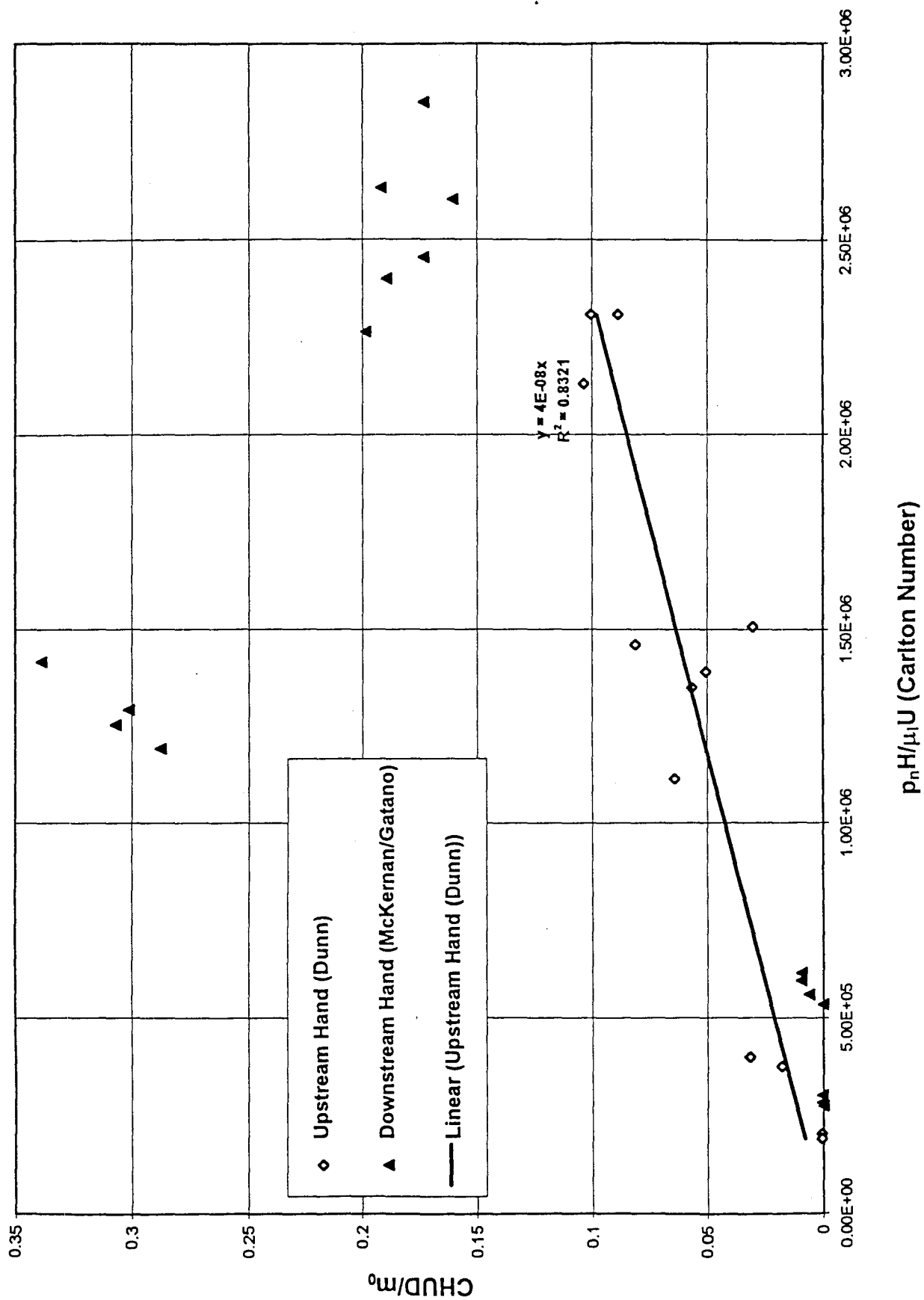


Figure 6: The Effects of Upstream versus Downstream Handedness

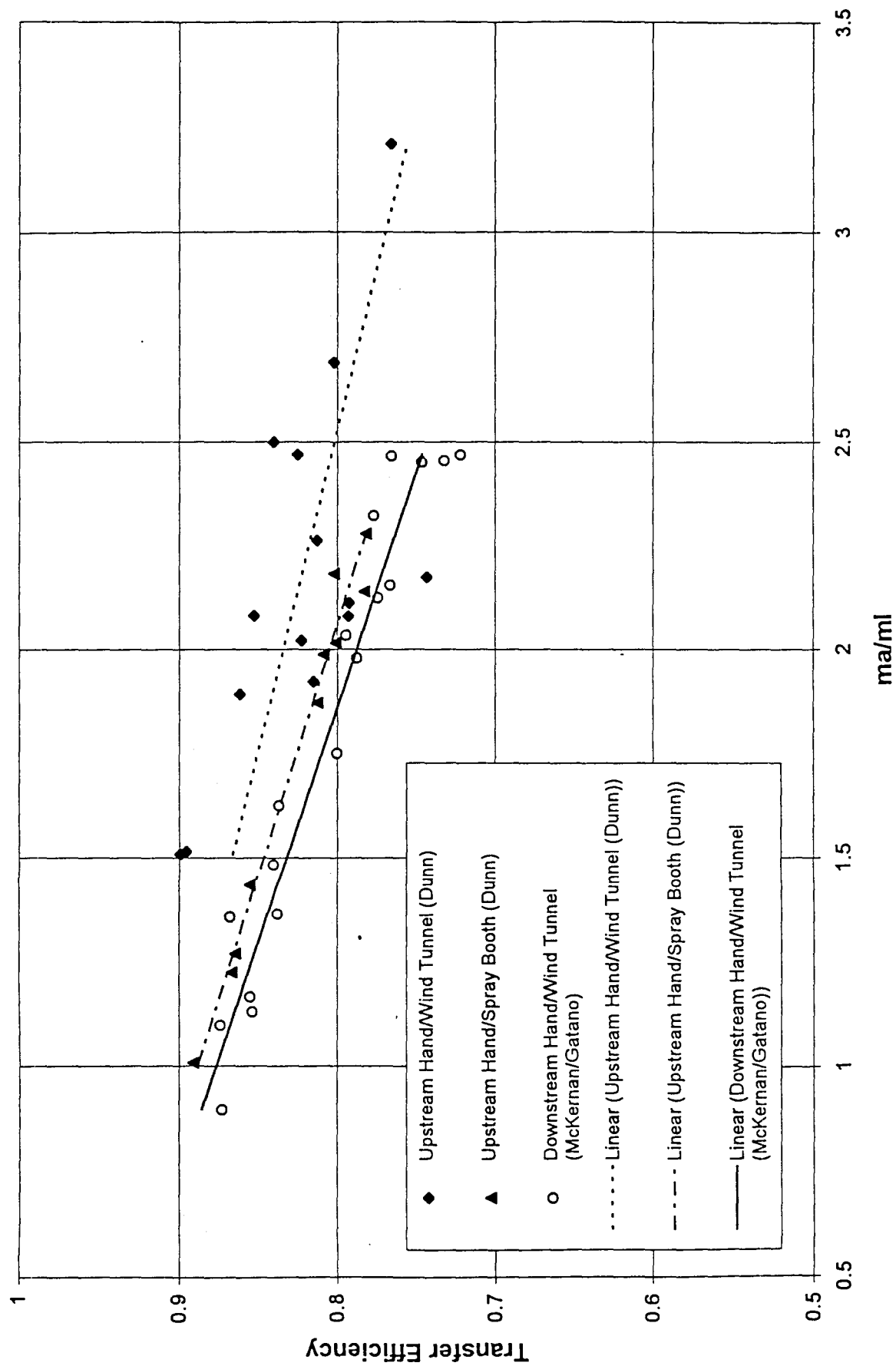


Figure 7: Transfer Efficiency as a Function of the Ratio of Mass Flowrates of Air to Liquid ( $m_a/m_l$ )

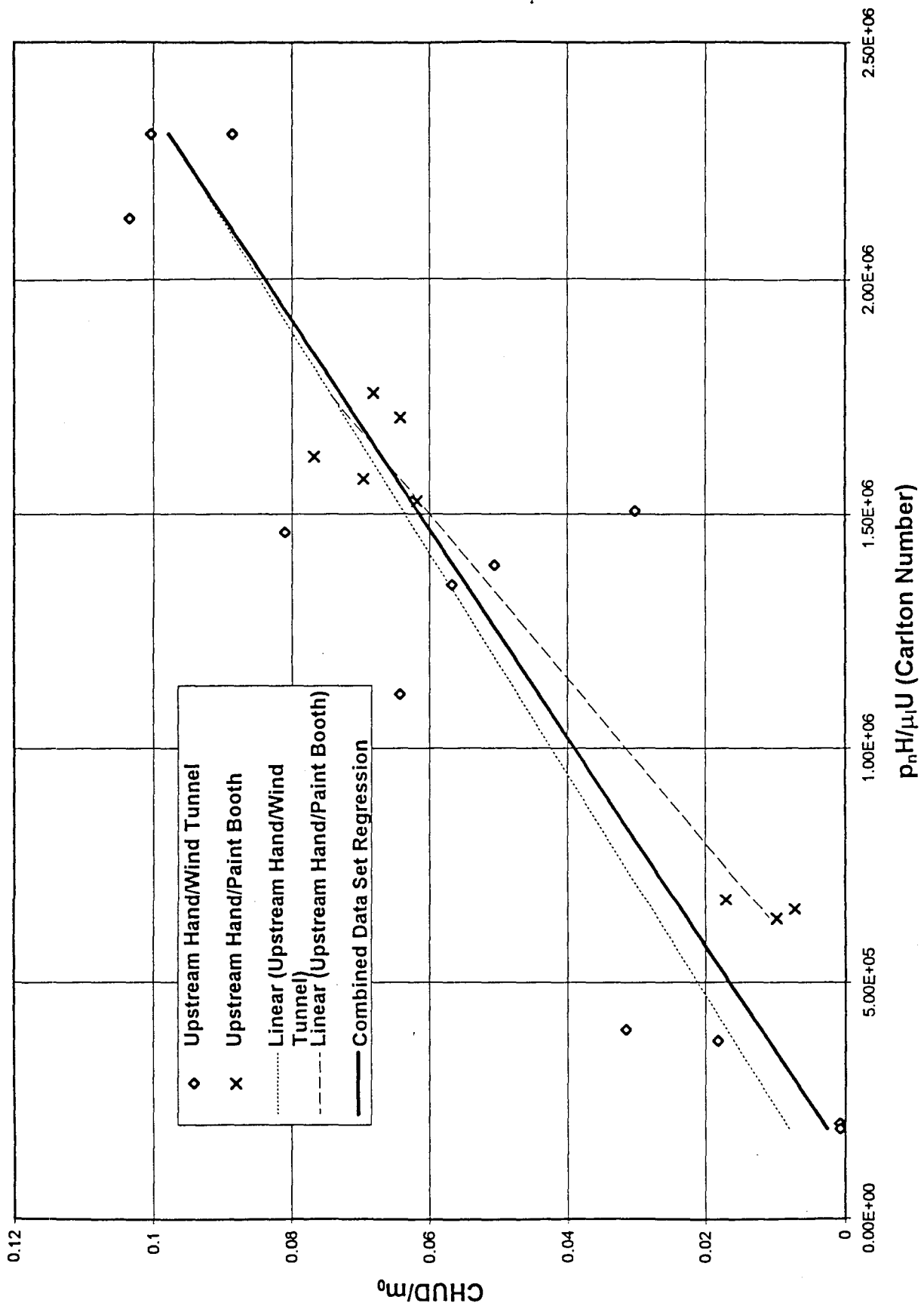


Figure 8 - Effects of wind tunnel blockage on test results

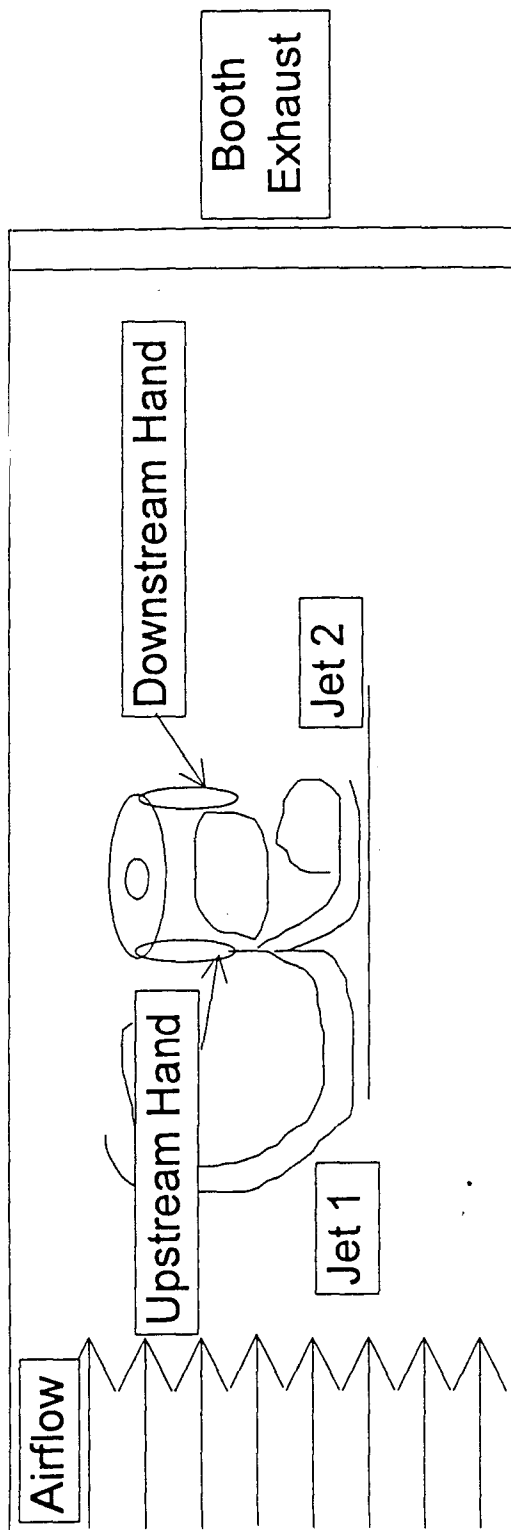


Figure 9: Diagram of Overspray Pattern

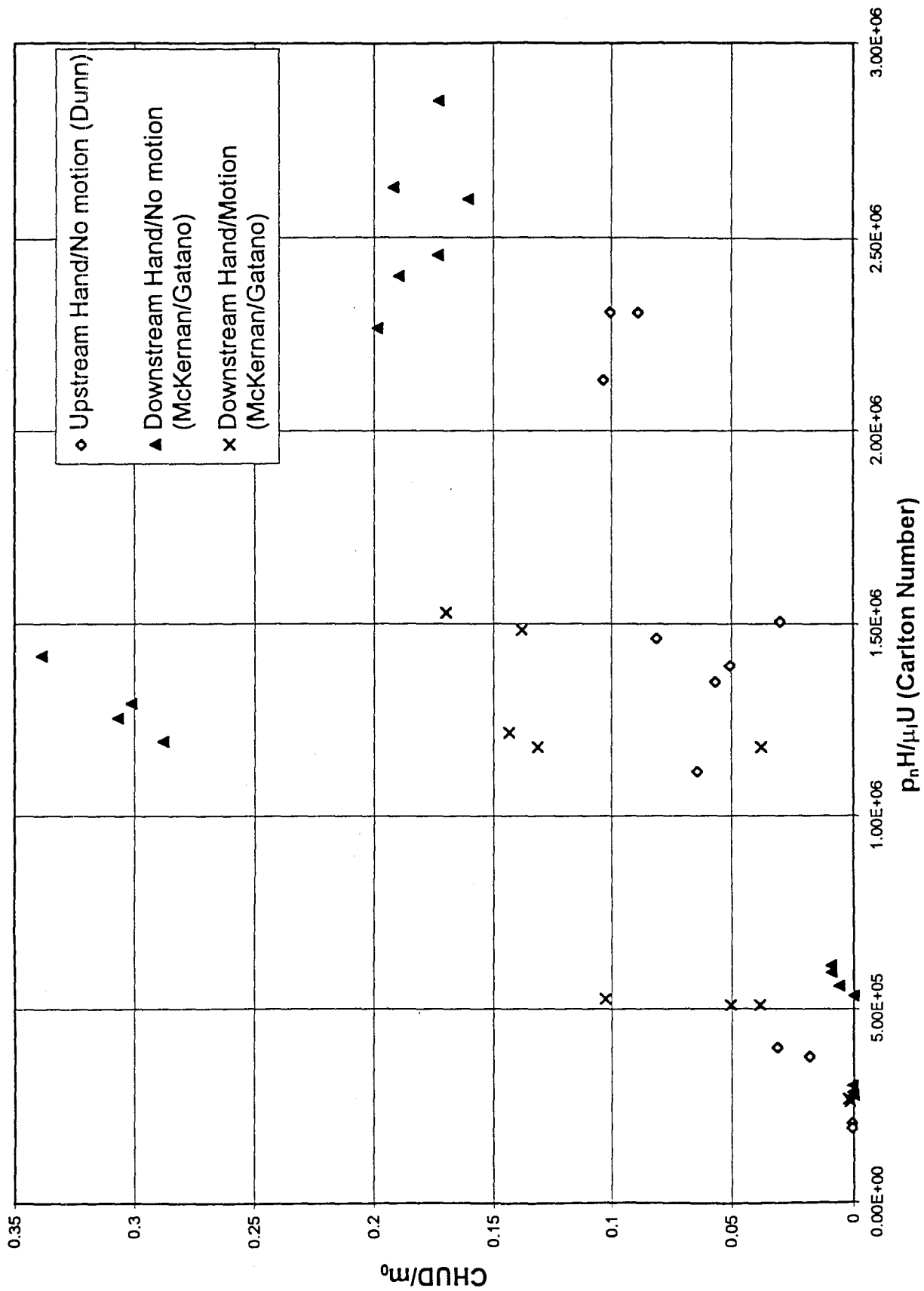


Figure 10: Comparison of the Effects of Motion on Downstream Hand Concentrations





Run #	Carlton #	Concentration		Difference	Rank	"+" Ranks	"- " Ranks	%Diff
		Upstream	Downstream					
1	2.31E+06	232.88	273.68	40.80	10	10	0	14.9
4	2.13E+06	169.01	258.56	89.56	11	11	0	34.6
5	1.51E+06	68.92	73.02	4.10	3	3	0	5.6
6	1.39E+06	63.90	80.47	16.58	7	7	0	20.6
7	1.46E+06	94.54	117.27	22.73	9	9	0	19.4
8	1.35E+06	61.28	69.57	8.30	6	6	0	11.9
9	2.03E+05	0.17	0.35	0.17	2	2	0	49.7
10	4.00E+05	14.28	21.23	6.95	5	5	0	32.8
12	1.91E+05	0.24	0.32	0.07	1	1	0	22.7
13	3.77E+05	5.05	11.88	6.84	4	4	0	57.5
14	1.11E+06	69.56	86.88	17.32	8	8	0	19.9
						66	0	

Table 2: Blockage Ratio Comparison between Paint Booth and Wind Tunnel

	Experimental Wind Tunnel	Paint Booth
Cross sectional area of test section (ft <sup>2</sup> )	25	45
Projected area of test article (ft <sup>2</sup> )	5.44	5.44
Blockage ratio	0.22	0.12

## **Appendix A: Wind Tunnel Experimental Methods and Data**

### **A.1. ThermoAnemometer Calibration**

An Alnor Compuflow<sup>®</sup> model 8565 ThermoAnemometer was used throughout this project to measure air velocity. The unit is a portable hand-held instrument capable of measuring velocities from 20-3000 fpm. The thermal anemometer uses both a velocity sensor and temperature sensor. The velocity sensor is a fine nickel wire located in the probe tip heated with a constant current. As air passes over the velocity sensor, the sensor is cooled and a change in resistance occurs. The air speed has been shown to be proportional to the change in resistance of the velocity sensor. The anemometer was calibrated in a small wind tunnel with a cross sectional area of 2.56 ft<sup>2</sup>. The calibration setup is shown in Figure A.1. A bell shaped streamline entry was used to provide uniform flow into the test section. A screen was also placed in the back of the test section to assist in maintaining uniform flow across the calibration wind tunnel. An electronically controlled butterfly damper valve provided flow regulation across the range of required airstream velocities.

Volumetric airflow was measured by a calibrated orifice connected to an inclined manometer. Atmospheric conditions were also recorded including wet and dry bulb

temperature (sling psychrometer) and barometric pressure (Fischer-Scientific barometer). The calibration was performed in accordance with ACGIH recommended practice for the calibration of air measuring instruments.<sup>(3)</sup> The results of this calibration are shown in Table A.1. A least squares linear regression was performed to fit the data. The calibration curve is shown in Figure A.2. The applicable regression equation is:

$$\text{Actual velocity (fpm)} = 1.0848 (\text{Reading}_{\text{instrument}}) - 9.5625, r^2 = 0.999 \quad (1)$$

## **A.2. Orifice Flowmeter Calibration**

A sharp-edged orifice was used to measure volumetric airflow through the calibration wind tunnel. The orifice meter was calibrated using the test setup as described in the previous paragraph (see Figure A.1.). The orifice was mounted between flanged ducting sections and gaskets were used to seal the installation. A pressure tap on either side of the orifice was connected to a Dwyer No. 400 Air Velocity Meter (inclined manometer) for measurement of differential pressure during calibration. The Dwyer manometer has a range of 0-10 in w.g. with a resolution of 0.01 in w.g. from 0-1 in. w.g. The orifice flowmeter causes an increase in airspeed by using a sharp edged flow obstruction, typically a flat plate with a beveled edge on the downstream side. The airflow can then be determined by the measurement of the resultant change in static pressure across the orifice and using the conservation of momentum equation to relate this differential pressure with the volumetric flowrate. A six point pitot tube traverse was

performed in accordance with ACGIH guidelines to provide actual airflow measurement.<sup>(3)</sup> Two traverses across the duct diameter made at right angles were performed to carefully map out the velocity distribution and agreements between the traverses were easily within the standard of 10%. The traverses were taken at a distance greater than the recommended standard of 7.5 duct diameters downstream of any major flow disturbance. These measurements were taken at eight distinct orifice differential pressures corresponding to airflows within the range of interest (100-900 cfm). The results of this calibration are shown in Table A.1.

### **A.3. Calibration of the Experimental Wind Tunnel**

Airstream velocity through the experimental (large) wind tunnel is one of the primary variables of interest in this project. A sixteen point traverse was performed across the tunnel cross section. A bank of filters were installed on a pegboard in the rear of the tunnel to assist in maintaining uniform airstream velocity throughout the tunnel. A bell shaped entry was also installed on the tunnel to minimize the effects of flow separation cause by a vena contracta on the tunnel entrance. The flowrate through the tunnel is adjustable by varying the speed of the fan via a Toshiba Tosvert model 130H1 variable torque transistor inverter. See Figure A.4. for the experimental wind tunnel setup.

The air velocity was measured by the thermo-anemometer on a 16 point grid across a range of tunnel static pressures. The tunnel static pressure was measured by a

pitot tube installed in the exhaust duct downstream of the tunnel exit prior to the fan. A Dwyer Model No. 424 Air Velocity Meter (inclined manometer) was used to measure the tunnel static pressure throughout the experiment. The freestream velocity ( $U$ ) was determined from the average of the sixteen readings and was regressed on the square root of the tunnel static pressure as shown in Figure A.4. A linear regression of the dataset yielded a best fit equation:

$$\text{Freestream Velocity (U)} = 403.75 (\text{SP}_{\text{tunnel}})^{1/2}, \quad r^2 = 0.9995 \quad (2)$$

#### A.4. Vacuum Pump Oil Viscosity

The vacuum pump oil viscosity was measured using a Haake falling ball viscometer with a constant temperature bath. Viscosity measurements were taken at nine temperatures ranging from 20<sup>0</sup> C to 36<sup>0</sup>C. A graph of the results of these measurements is shown in Figure A.5. A best fit regression equation for viscosity is:

$$\text{Viscosity (cp)} = 678.95 \exp[(-0.0306)\text{Temperature}(^{\circ}\text{F})], \quad r^2 = 0.9988 \quad (3)$$

#### A.5. Experimental Setup

The HVLP spray painting setup is shown in Figure A.6. A photograph of the compressor and spray paint system is shown in Figure A.7. The pressure at the

compressor /accumulator exit was set to 100 psi and the regulator downstream of the desiccator was set to 90 psi. The compressor was set to start if the pressure in the accumulator dropped to 140 psi or lower so that a constant delivery pressure was maintained. The “gun” pressure regulator was fixed and not altered throughout the testing, rather the “pot” pressure regulator was adjusted to vary the nozzle pressure and thus the air flowrate from the gun. A calibration of the “pot” pressure versus gun air cap pressure was performed using an air cap test kit. This test kit allows the user to check the air pressure at the center and fan air ports to verify that the required pressure exists to provide adequate atomization. The results of this test are shown in Table A.2.

The HVLP gun has two adjustment screws on the spray gun body to allow the user to adjust the air or liquid flowrates (see Figure A.8). Typically, the air adjustment screw is used to vary the fan pattern of the gun. The operator adjusts the fan pattern based on the shape of the part being coated to minimize overspray and reduce material usage. The liquid adjustment screw is sometimes also changed to impart the desired coating thickness to the part. In this project, the fan pattern was set to emulate that of an ellipse, which is used frequently throughout industry. A calibration was also performed to measure the spray gun airflow at each “pot” regulator setting. The airflow was measured using a Collins P-1700-120 chain-compensated 120 liter spirometer. The time required to displace a known volume of air from the gasometer was measured. Measurements were made across a range of “pot” gauge pressures and subsequent air cap pressures between 2.5 - 11.5 psi. The measurements were also repeated for a series of three air adjustment

screw settings (1-3 complete rotations). The results of these tests are listed in Table A.3. and shown graphically in Figure A.9. The linear regression equation relating spray gun airflow to air cap pressure is :

$$\text{Volumetric Flowrate (cfm)} = 1.0076(\text{air cap pressure, psi}) + 5.1589, \quad r^2 = 0.9863 \quad (4)$$

#### **A.6. Calibration of the Sample Pump**

The mannequin breathing zone concentration was determined by sampling for the aerosol via NIOSH Method 0500. An IOM sampler was utilized to minimize the effects of particle size on inlet efficiency. The sampling pump used was an SKC Universal Flow Sample Pump Catalog No. 224-PCXR8. This pump is equipped with a rotameter mounted on the case to allow the user to monitor the flow throughout sampling. The electrical control system also has a constant flow system which increases motor voltage as the back pressure increases. This provides for constant flow even as the back pressure of the filter increases due to loading.

The pump and sampler was calibrated before and after each run. This assured that significant drift could not affect the volume of air sampled and therefore the measured concentration. An open faced sampler calibration setup was used to perform the pump/sampler calibrations. The combined pump and sampler (with filter & backing pad) was calibrated together to account for the effect of sampler pressure drop on the sample



flowrate. A Gilian Gillibrator (bubble flowmeter) with a 0-2 lpm cell was the primary standard used to perform the pump calibration.

#### **A.7. Filter and Vacuum Oil Weights**

The PVC 37 mm sampling filters were placed in a desiccator for a period of at least 2 hours prior to and following sampling. The filters were weighed on a Cahn 27 Electrobalance on the 20 Loop A setting which has a range of 0-20 mg with a resolution of 1 $\mu$ g. The sensitivity of the balance is reported to be 0.0001 mg with an accuracy of  $\pm 0.005\%$ . The balance was zeroed and calibrated with a 200 mg Class M calibrating weight in accordance with manufacturer's specifications before each series of experimental runs. A radioactive ionizing unit was passed over the filters before weighing to discharge any static electricity buildup on the filter which may cause erroneous readings.

The mass of liquid used during the experimental runs and the mass transferred to the plate was measured by a mass balance method. The liquid feed pot was weighed prior to each run and following the completion of each run. The amount of liquid transferred was measured by the weighing of the drip trough placed underneath the plate before and after each run. A Mettler PM34-K Deltarange digital scale was used to measure the quantities of liquid used and transferred. The Mettler scale was calibrated at the factory and was in calibration during the entire period of testing. The scale was zeroed, as necessary, before each measurement.

## **A.8. Experimental Data**

The experimental identification table is shown in Table A.4. This table shows the conditions under which the test run was performed including data such as environmental conditions, freestream velocity ( $U$ ), mannequin orientation, nozzle pressure ( $p_n$ ) breathing zone concentration (BZC) sample location, and dimensionless nozzle pressure (Carlton number). Two concentration samples were collected for each run and are given the designation A or B. The calculated overspray data is shown in Table A.5. This table includes information such as mass flow rates of air and liquid, mass of liquid transferred, and overspray generation rate ( $m_0$ ), and transfer efficiency. The breathing zone concentration data is shown in Table A.6. This table includes information such as sample filter weights, blank filter weights, and calculated dimensionless concentration. Samples # 2A and 3A were taken from the mannequin mouth and problems with the test setup prevented the collection of adequate sample mass for analysis. These samples were therefore excluded from analysis. Run #11 was not included in the analysis as the sample mass was much greater than the limits specified in NIOSH Method 0500. Sample calculations are shown in section A.11 below.

## **A.9. Sample Calculations (for Run Number 1)**

### **A.9.1 $m_a/m_l$**

The measured value of  $m_a$ , at total nozzle pressure = 11.5 psi was 285 g/min.

$$m_l = \frac{\text{mass container(before)} - \text{mass container(after)}}{\text{sampling time}}$$

$$= \frac{(3400.9 - 2986.8)g}{183.97 \text{ sec}} \times \left( \frac{60 \text{ sec}}{\text{min}} \right) = 135.1 \text{ g/min}$$

$$\frac{m_a}{m_l} = \frac{285 \text{ g/min}}{135.1 \text{ g/min}} = 2.1$$

#### A.9.2 Transfer Efficiency

$$m_{\text{transferred}} = \frac{\text{mass trough(before)} - \text{mass trough(after)}}{\text{sampling time}}$$

$$\frac{(551.9 - 223.8)g}{183.97 \text{ sec}} \times \left( \frac{60 \text{ sec}}{\text{min}} \right) = 107.0 \text{ g/min}$$

$$\text{T.E.} = \frac{\text{liquid transfer rate } (m_{\text{transferred}})}{\text{total liquid mass flowrate } (m_l)} = \frac{107.0 \text{ g/min}}{135.1 \text{ g/min}}$$

$$= 0.792$$

#### A.9.3 $p_n H/\mu_l U$

From equation (A-2),

$$\text{Freestream Velocity } (U) = 403.75 (0.05)^{1/2} = 73.0 \text{ ft/min}$$

From equation (A-3)

$$\mu_1 (\text{cp}) = 678.95 \exp[(-0.0306)(75^{\circ}\text{F})] = 68.41 \text{ cp}$$

$$\begin{aligned} \frac{p_n H}{m_1 U} &= \frac{(6.5 \text{ psi})(51 \text{ in})}{(68.41 \text{ cp})(73.0 \text{ fpm})} \times \left( \frac{\text{atm}}{14.7 \text{ psi}} \right) \times \left( \frac{1.01325 \times 10^6 \text{ dynes / cm}^2}{\text{atm}} \right) \times \\ &\quad \left( \frac{\text{ft}}{12 \text{ in}} \right) \times \left( \frac{\text{cp}}{0.01 \text{ dyne-s / cm}^2} \right) \times \left( \frac{60 \text{ sec}}{\text{min}} \right) \\ &= 2.29 \times 10^6 \end{aligned}$$

#### A.9.4 CHUD/ $m_0$

From sample # 1A

$$\begin{aligned} \frac{\text{CHUD}}{m_0} &= \frac{(280.30 \text{ mg / m}^3)(51 \text{ in})(73.0 \text{ ft / min})(14 \text{ in})}{28.05 \text{ g / min}} \times \left( \frac{1 \text{ ft}^2}{144 \text{ in}^2} \right) \times \\ &\quad \left( \frac{0.02832 \text{ ft}^3}{1 \text{ m}^3} \right) \times \left( \frac{1 \text{ g}}{1000 \text{ mg}} \right) \\ &= 0.1028 \end{aligned}$$

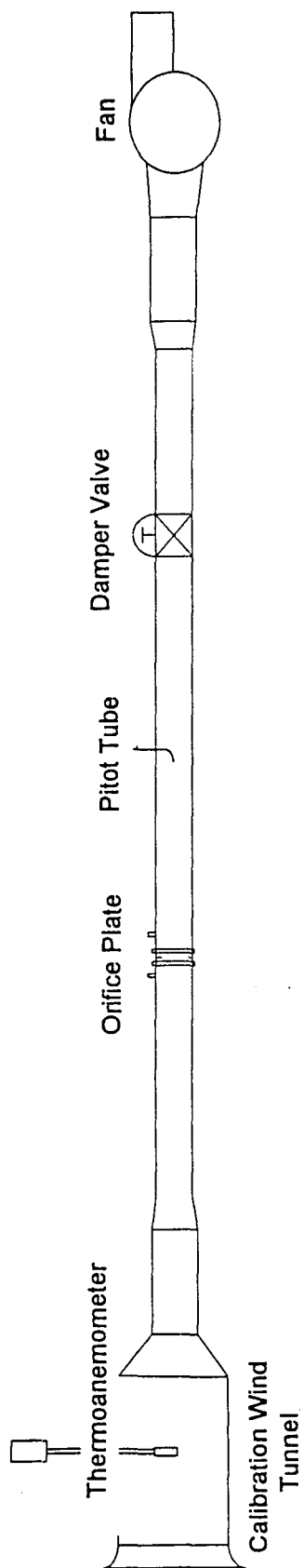


Figure A.1: Thermoanemometer Calibration Set up

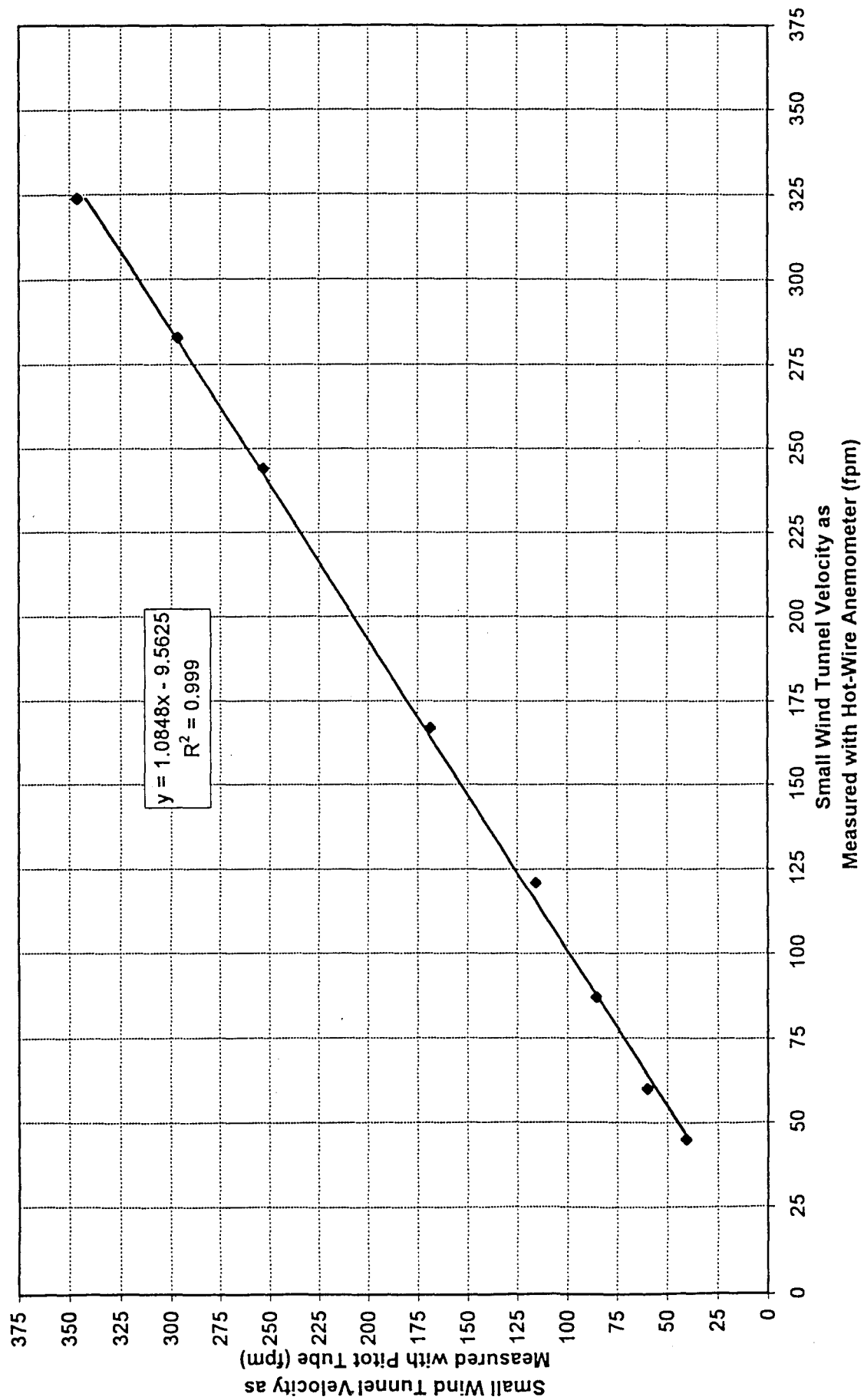


Figure A.2.: Calibration Curve for Thermo-anemometer

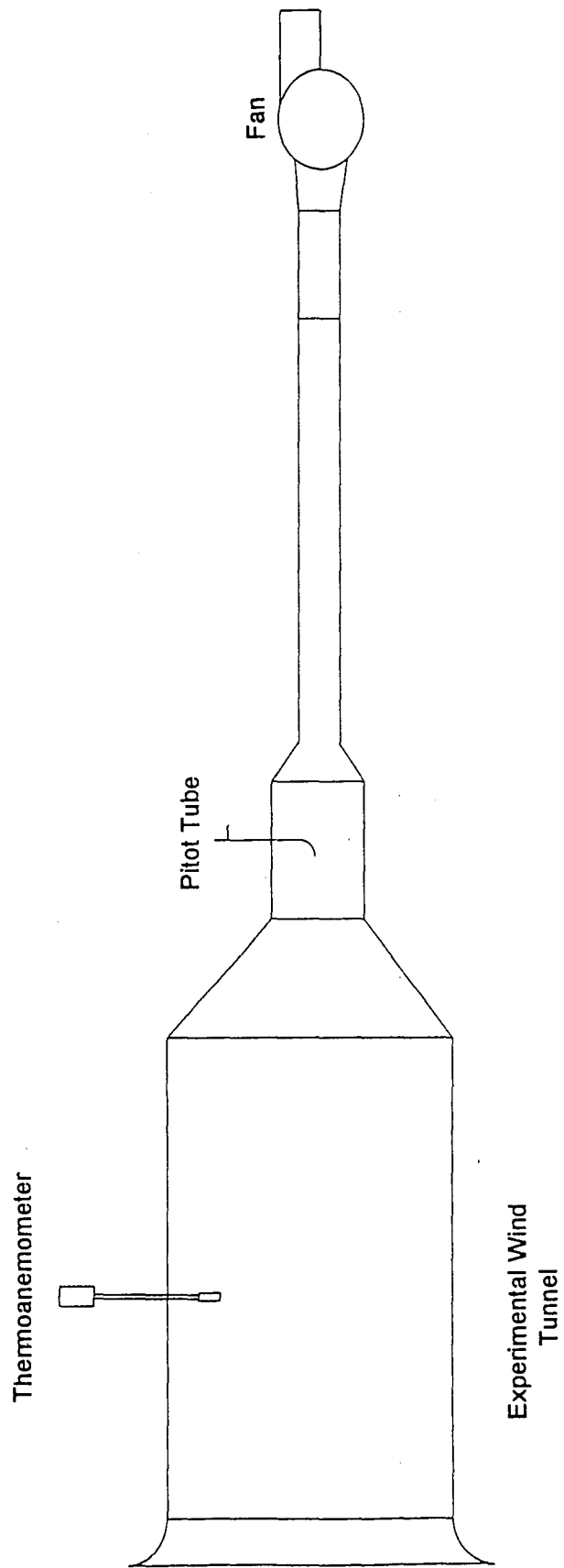


Figure A.3: Experimental wind tunnel calibration set up

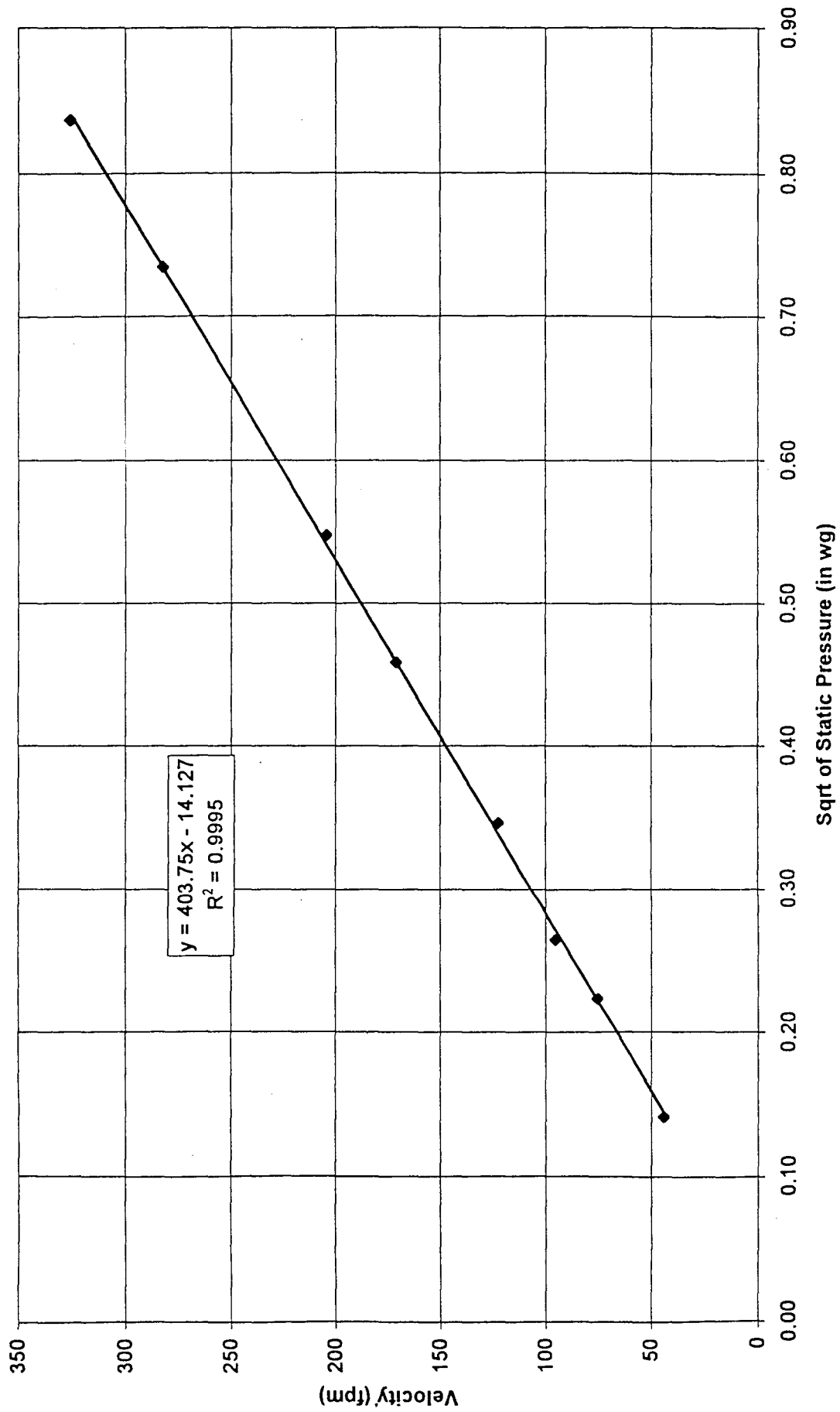


Figure A. 4: Experimental Wind Tunnel Air flow Calibration Curve



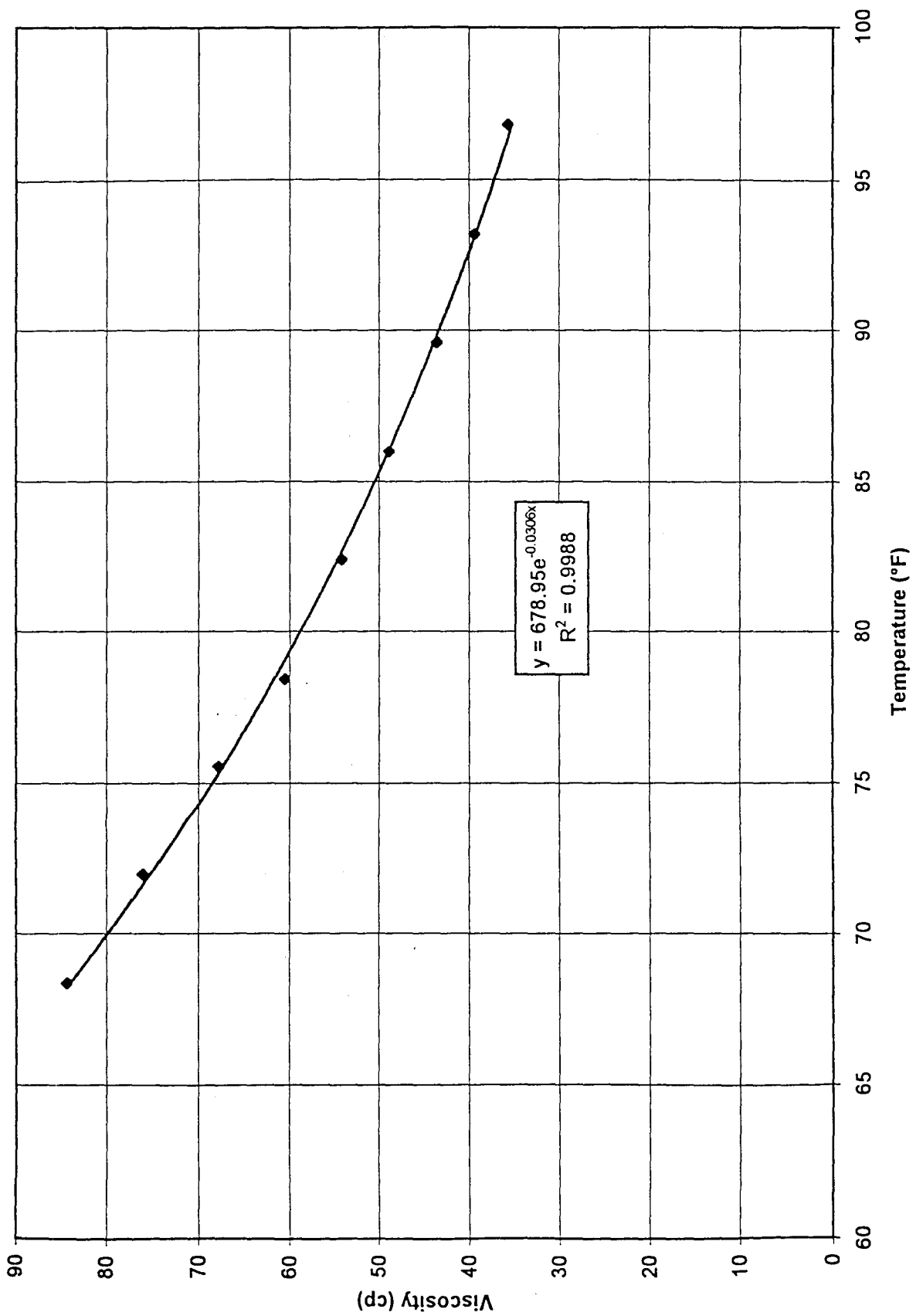


Figure A.5: Viscosity of Oil as a function of temperature

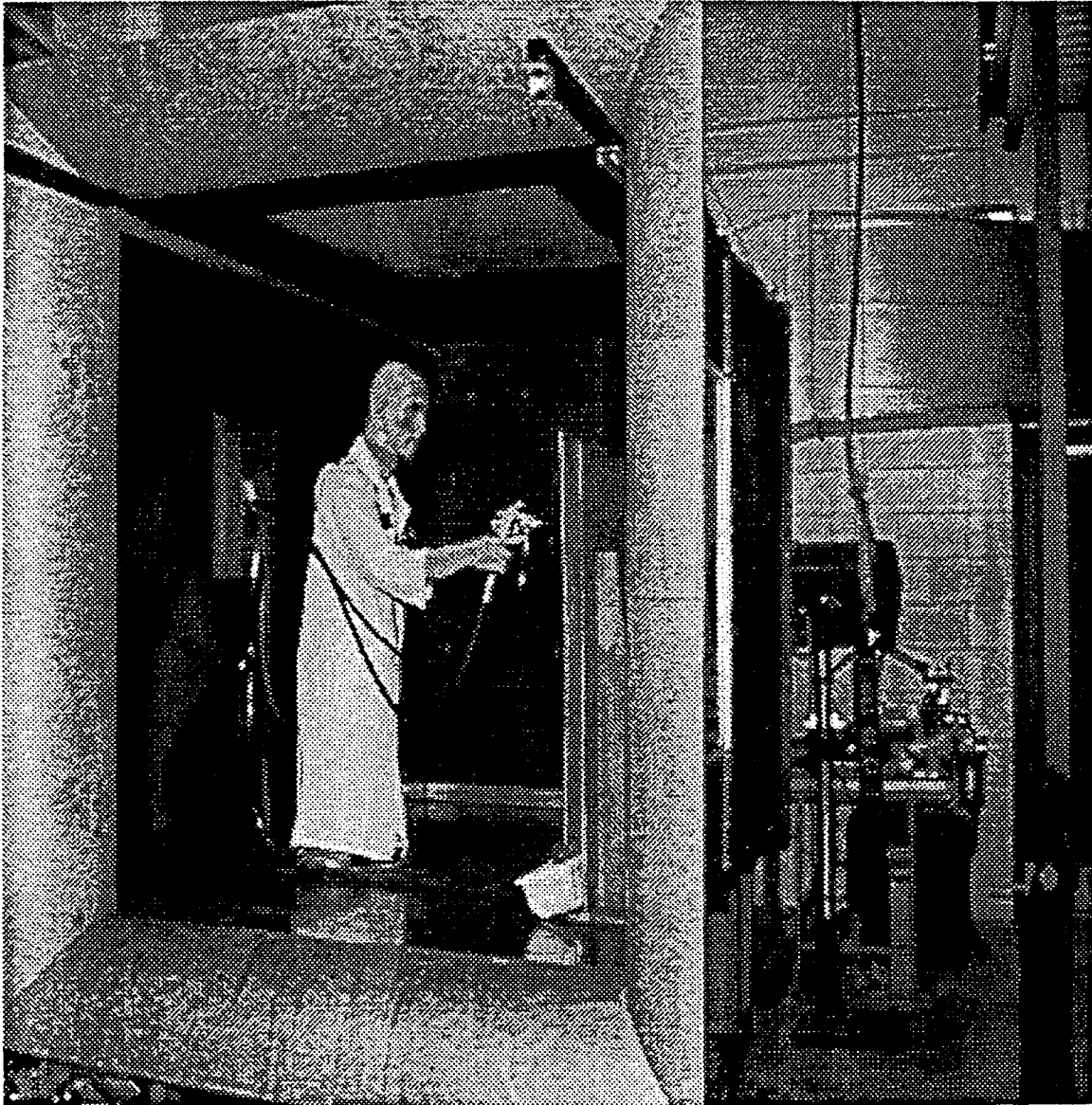


Figure A.6: Test Setup

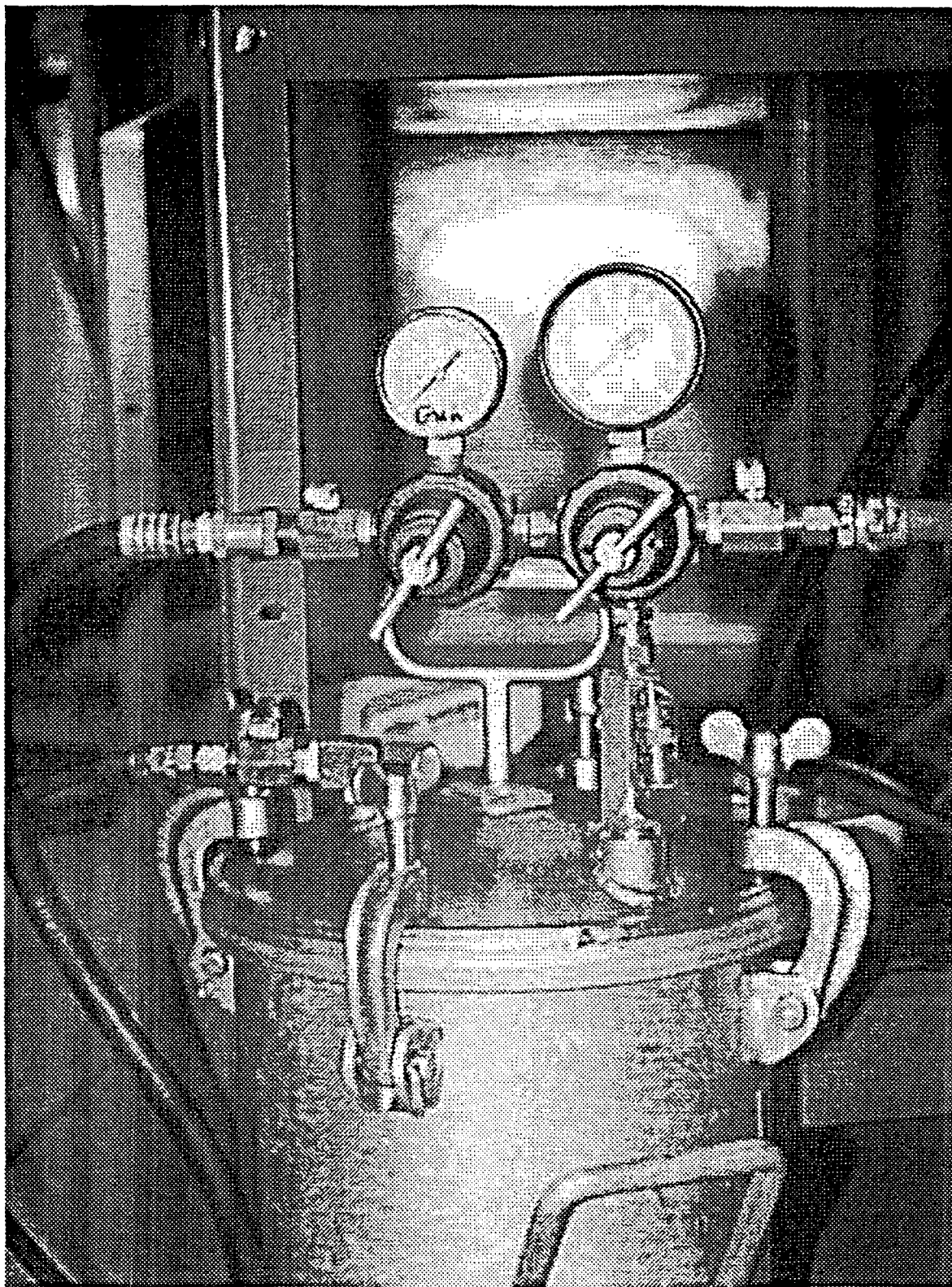


Figure A.7: Spray Pot Set Up



Figure A.8: High Volume, Low Pressure Spray Gun

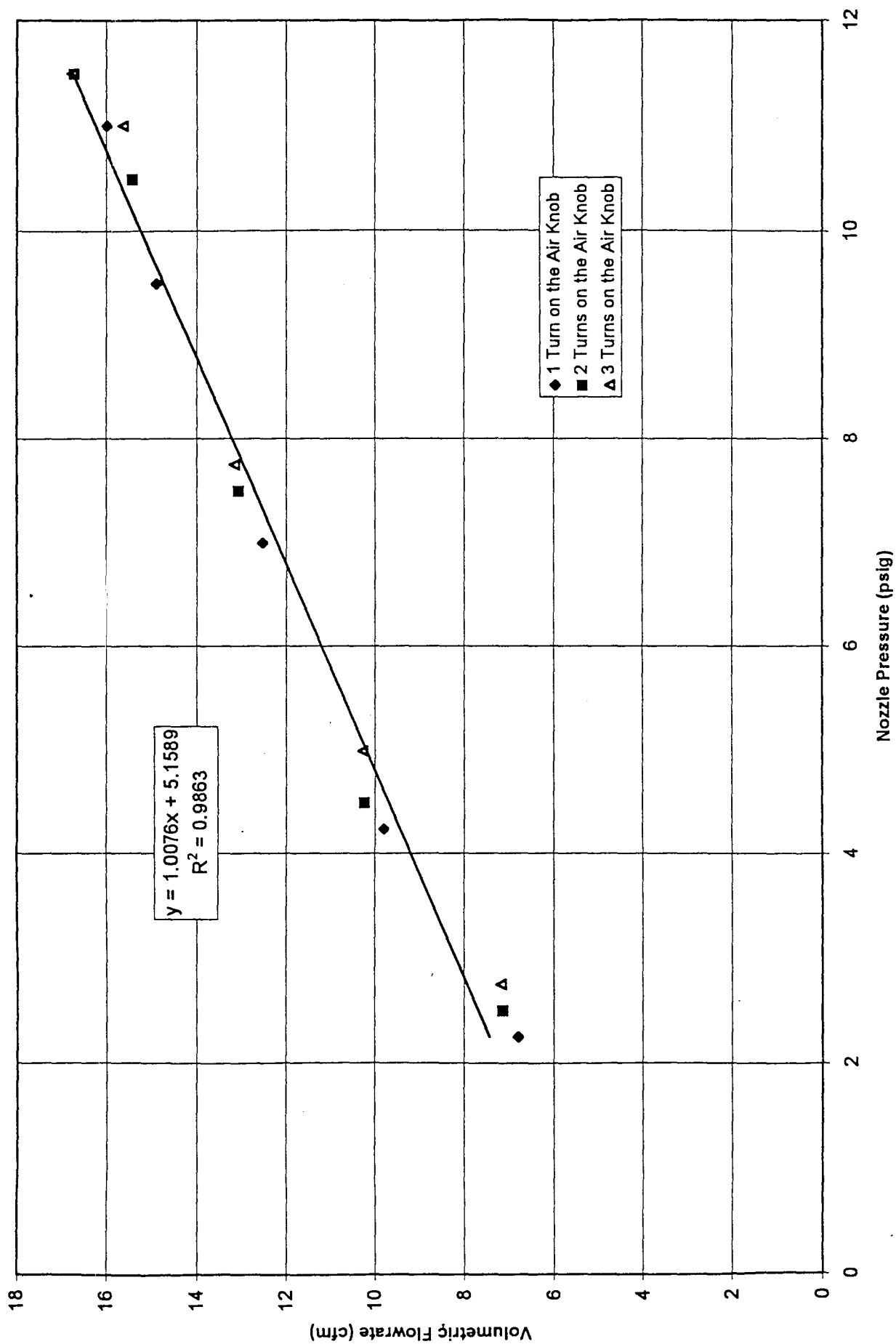


Figure A.9: Volumetric Air Flowrate from the HVLP Gun as a Function of Nozzle Pressure and Fan Pattern

Table A.1.: Thermo-anemometer and Orifice Calibration Data

Orifice Pressure (in wg)	SQRT (Orifice Pressure (in wg)	Velocity in Duct (fpm)	Air Volume (Q), CFM	Velocity in Small Wind Tunnel (fpm)	Direct Reading Thermal Anemometer (fpm)
0.10	0.32	1184	103	41	45
0.20	0.45	1750	153	60	60
0.50	0.71	2495	218	86	87
1.00	1.00	3367	294	116	121
2.00	1.41	4909	428	169	167
5.00	2.24	7379	644	254	244
7.00	2.65	8637	754	297	283
9.80	3.13	10076	879	346	324

Table A.2 Determination of Air Pressure at the Cap and the Horns

Gauge Pressure (psig)	Number of Turns on Air Knob	Pressure in Cap (psig)	Pressure in Horns (psig)
53	0	10	0
53	1	7	4
53	2	6.5	5
53	3	6.5	5
46	0	8	0
46	1	6	3.5
46	2	6	4.5
46	3	6	5
38	0	6	0
38	1	4.25	2.25
38	2	4.25	3.25
38	3	4.5	3.5
27	0	4	0
27	1	2.75	1.5
27	2	2.5	2.0
27	3	3.0	2.0
16	0	2	0
16	1	1.75	0.75
16	2	1.5	1.0
16	3	1.75	1.0

Table A.3 - Spray Gun Volumetric Airflow versus Air Cap Pressure

Nozzle Pressure (psig) Tot=Cap + Horn	Average Volumetric Flowrate (cfm)		
	1 turn	2 turn	3 turn
11	15.99		
11.5		16.71	
11.5			16.76
9.5	14.89		
10.5		15.42	
11			15.63
7	12.54		
7.5		13.07	
7.75			13.17
4.25	9.8		
4.5		10.24	
5			10.28
2.25	6.79		
2.5		7.13	
2.75			7.17



Table A.4: Experimental Identifier Sheet

Run Number	Static Pressure (in wg)	Freestream Velocity (fpm)	Liquid Temperature (F)	Viscosity (cp)	Air Temperature (F)	Gauge Pressure (psig)	Nozzle Pressure Cap (psig)	Nozzle Pressure Cap&Horn (psig)	Sample Location
1A	0.05	73.0	75	68.41	81	53	6.5	11.5	Upstream
1B	0.05	73.0	75	68.41	81	53	6.5	11.5	Downstream
2A	0.05	73.0	75	68.41	81	53	6.5	11.5	Mouth
2B	0.05	73.0	75	68.41	81	53	6.5	11.5	Downstream
3A	0.05	73.0	75	68.41	81	46	6	10.5	Mouth
3B	0.05	73.0	75	68.41	81	46	6	10.5	Downstream
4A	0.05	73.0	75	68.41	81	46	6	10.5	Upstream
4B	0.05	73.0	75	68.41	81	46	6	10.5	Downstream
Blank									
5A	0.08	99.0	71	77.32	74	53	6.5	11.5	Upstream
5B	0.08	99.0	71	77.32	74	53	6.5	11.5	Downstream
6A	0.08	99.0	71	77.32	74	46	6	10.5	Upstream
6B	0.08	99.0	71	77.32	74	46	6	10.5	Downstream
Blank									
7A	0.08	99.0	70	79.72	70	53	6.5	11.5	Upstream
7B	0.08	99.0	70	79.72	70	53	6.5	11.5	Downstream
8A	0.08	99.0	70	79.72	70	46	6	10.5	Upstream
8B	0.08	99.0	70	79.72	70	46	6	10.5	Downstream
Blank									
9A	0.16	150.3	67	87.39	66	16	1.5	2.5	Upstream
9B	0.16	150.3	67	87.39	66	16	1.5	2.5	Downstream
10A	0.12	126.8	67	87.39	66	27	2.5	4.5	Upstream
10B	0.12	126.8	67	87.39	66	27	2.5	4.5	Downstream
11A	0.08	99.0	67	87.39	66	46	6	10.5	Upstream
11B	0.08	99.0	67	87.39	66	46	6	10.5	Downstream
Blank									
12A	0.16	150.3	65	92.90	64	16	1.5	2.5	Upstream
12B	0.16	150.3	65	92.90	64	16	1.5	2.5	Downstream
13A	0.12	126.8	65	92.90	64	27	2.5	4.5	Upstream
13B	0.12	126.8	65	92.90	64	27	2.5	4.5	Downstream
14A	0.085	102.8	65	92.90	64	46	6	10.5	Upstream
14B	0.085	102.8	65	92.90	64	46	6	10.5	Downstream
Blank									

Table A.5: Transfer Efficiency/Overspray Worksheet

Run Number	Run Time (s)	Bucket Weight (g)		Trough Weight (g)		Mass of Liquid Sprayed (g/min)	Mass of Liquid Transferred (g/min)	Mass of Liquid Overspray (m <sub>o</sub> ) (g/min)	Mass of Air (g/min)**	m <sub>a</sub> /m <sub>l</sub>	Transfer Efficiency	Carifton Number
		Before	After	Before	After							
1	183.97	3400.9	2986.8	223.8	551.9	135.1	107.0	28.0	285	2.1	0.792	2.3E+6
2	183.17	3302.8	2884.3	235.8	587.7	137.1	108.7	28.4	285	2.1	0.793	2.3E+6
3	182.21	3210.2	2807.8	241.2	572.4	132.5	109.1	23.4	268	2.0	0.823	2.1E+6
4	187.85	3470.9	3035	241.1	596.5	139.2	113.5	25.7	268	1.9	0.815	2.1E+6
5	241.71	3234.4	2705.9	239.7	632.4	131.2	97.5	33.7	285	2.2	0.743	1.5E+6
6	244.5	3090.2	2607.3	245.3	637.9	118.5	96.3	22.2	268	2.3	0.813	1.4E+6
7	240.74	3262.2	2798.8	235.8	618.3	115.5	95.3	20.2	285	2.5	0.825	1.5E+6
8	242.48	3170.3	2737.1	245.5	609.7	107.2	90.1	17.1	268	2.5	0.841	1.3E+6
9	723.75	3340.8	2300.4	228.4	1160.6	86.3	77.3	9.0	131	1.5	0.896	2.0E+5
10	433.06	3208.7	2579.7	251.8	794	87.1	75.1	12.0	165	1.9	0.862	4.0E+5
11	605.92	3116.4	2110.4	257.3	1064.2	99.6	79.9	19.7	268	2.7	0.802	1.2E+6
12	900.51	3142.6	1843.3	244	1412.7	86.6	77.9	8.7	131	1.5	0.899	1.9E+5
13	528.52	2988.4	2289.7	267.3	863.4	79.3	67.7	11.6	165	2.1	0.853	3.8E+5
14	302.24	2880.2	2459.8	272.9	594.8	83.5	63.9	19.6	268	3.2	0.766	1.1E+6

TABLE A.6. DIMENSIONLESS CONCENTRATION TOLERANCE

Run Number	Date	Mass of Liquid Overspray (m <sub>o</sub> ) (g/min)	Time (s)	Filter Weight (m)		Sample Mass (mg)	Sampling Flowrate (lpm)	Concentration (mg/m <sup>3</sup> )	Carlton Number	CUHD/m <sub>o</sub>
				Before	After					
1A	10/30/96	28.05	183.97	13.133	14.741	1.608	1.87	280.30	2.3E+6	0.1028
1B	10/30/96	28.05	183.97	13.405	14.719	1.314	1.89	226.75	2.3E+6	0.0832
2A	10/30/96	28.37	183.17	13.800	13.869	0.069	1.87	12.08	2.3E+6	0.0044
2B	10/30/96	28.37	183.17	14.010	15.420	1.410	1.89	244.37	2.3E+6	0.0886
3A	10/30/96	23.45	182.21	13.180	13.175	-0.005	1.87	-0.88	2.1E+6	-0.0004
3B	10/30/96	23.45	182.21	13.300	15.471	2.171	1.89	378.25	2.1E+6	0.1659
4A	10/30/96	25.71	187.85	13.740	14.730	0.990	1.87	169.01	2.1E+6	0.0676
4B	10/30/96	25.71	187.85	13.110	14.640	1.530	1.89	258.56	2.1E+6	0.1034
Blank	10/30/96			13.401	13.404	0.003				
5A	11/6/96	33.71	240.74	13.784	14.313	0.529	1.91	68.92	1.5E+6	0.0285
5B	11/6/96	33.71	240.74	13.757	14.311	0.554	1.89	73.02	1.5E+6	0.0302
6A	11/6/96	22.16	242.48	13.964	14.458	0.494	1.91	63.90	1.4E+6	0.0402
6B	11/6/96	22.16	242.48	14.050	14.665	0.615	1.89	80.47	1.4E+6	0.0506
Blank	11/6/96			13.416	13.415	-0.001				
7A	11/7/96	20.16	240.74	13.897	14.620	0.723	1.91	94.54	1.5E+6	0.0654
7B	11/7/96	20.16	240.74	13.980	14.882	0.902	1.92	117.27	1.5E+6	0.0811
8A	11/7/96	17.07	242.48	13.820	14.292	0.472	1.91	61.28	1.3E+6	0.0500
8B	11/7/96	17.07	242.48	13.650	14.189	0.539	1.92	69.57	1.3E+6	0.0568
Blank	11/7/96			13.882	13.855	-0.027				
9A	11/19/96	8.97	723.75	13.559	13.563	0.004	1.90	0.17	2.0E+5	0.0004
9B	11/19/96	8.97	723.75	12.343	12.351	0.008	1.91	0.35	2.0E+5	0.0008
10A	11/19/96	12.03	433.06	12.580	12.776	0.196	1.90	14.28	4.0E+5	0.0212
10B	11/19/96	12.03	433.06	12.816	13.109	0.293	1.91	21.23	4.0E+5	0.0315
11A	11/19/96	19.72	605.92	12.872	18.454	5.582	1.90	290.61	1.2E+6	0.2055
11B	11/19/96	19.72	605.92	12.901	16.062	3.161	1.91	163.71	1.2E+6	0.1157
Blank	11/19/96			13.596	13.592	-0.004				
12A	11/20/96	8.70	900.51	12.906	12.913	0.007	1.91	0.24	1.9E+5	0.0006
12B	11/20/96	8.70	900.51	12.990	12.999	0.009	1.90	0.32	1.9E+5	0.0008
13A	11/20/96	11.65	528.52	12.795	12.880	0.085	1.91	5.05	3.8E+5	0.0077
13B	11/20/96	11.65	528.52	12.710	12.909	0.199	1.90	11.88	3.8E+5	0.0182
14A	11/20/96	19.55	302.24	14.330	15.000	0.670	1.91	69.56	1.1E+6	0.0515
14B	11/20/96	19.55	302.24	12.894	13.726	0.832	1.90	86.88	1.1E+6	0.0643
Blank	11/20/96			12.283	12.283	0.000				

## **Appendix B: Paint Booth Experimental Methods and Data**

### **B.1. ThermoAnemometer Calibration**

An Alnor Compuflow<sup>®</sup> model 8565 ThermoAnemometer was used to perform the paint booth traverse in this phase of testing. The unit is a portable hand-held instrument capable of measuring velocities from 20-3000 fpm. The anemometer was calibrated in a small wind tunnel with a cross sectional area of 2.56 ft<sup>2</sup> according to the procedure described in appendix section A.1. The results of this calibration are shown in Table B.1 and in Figure B.1. A least squares linear regression was performed to fit the data. The applicable regression equation is:

$$\text{Actual velocity (fpm)} = 0.973 (\text{Reading}_{\text{instrument}}) - 8.6843, \quad r^2 = 0.998 \quad (1)$$

### **B.2. Paint Booth Freestream Velocity Profile**

The paint booth is located in the basement of the Rosenau Hall on the campus of the Univeristy of North Carolina at Chapel Hill. A twelve point traverse was performed at across the paint booth cross section. The room housing the paint spray booth was in the machine shop of the School of Public Health with several benches and cabinets located

near the inlet to the booth which caused fairly high turbulence in the paint booth. A layout of the paint booth and machine shop is shown in Figure B.2. A bank of filters were installed in the rear of the booth to collect the overspray and assist in maintaining uniform airstream velocity throughout the booth. A sheet metal flange was also installed on the entrance to the booth to minimize the effects of flow separation at the booth entrance. The flowrate through the tunnel is adjustable by varying a pulley on the fan belts which in turn causes the fan blades to spin at higher/lower revolutions per minute (rpm). The fan was set initially to approximately 100 fpm and was not varied during the experiment due to difficulty in precise adjustment of fan speed. The air velocity was measured by the thermo-anemometer on a 12 point grid across a the paint booth cross section and the results are shown in Table B.2.

### **B.3. Experimental Setup**

The setup of the HVLP spraygun and pot was identical to that described in appendix A section A.6. A schematic of the HVLP spray painting setup is shown in Figure A.6. The liquid and air adjustment screws were set to the same positions as used in the wind tunnel tests. A compressor provided the air for the spray gun and the operation was identical to that described previously for the experimental wind tunnel operation.

#### **B.4. Filter and Vacuum Oil Weights**

The PVC 37 mm sampling filters were placed in a desiccator for a period of at least 2 hours prior to and following sampling. The filters were weighed on a Cahn 27 Electrobalance on the 20 Loop A setting which has a range of 0-20 mg with a resolution of 1 $\mu$ g. The sensitivity of the balance is reported to be 0.0001 mg with an accuracy of  $\pm 0.005\%$ . The balance was zeroed and calibrated with a 200 mg Class M calibrating weight in accordance with manufacturer's specifications before each series of experimental runs. A radioactive ionizing unit was passed over the filters before weighing to discharge any static electricity buildup on the filter which may cause erroneous readings.

The mass of liquid used during the experimental runs and the mass transferred to the plate was measured by a mass balance method. The liquid feed pot was weighed prior to each run and following the completion of each run. The amount of liquid transferred was measured by the weighing of the drip trough placed underneath the plate before and after each run. An Ohaus Model 1900 Industrial Lab Balance was used to measure the quantities of liquid used and transferred.

#### **B.5. Experimental Data**

The experimental identification table is shown in Table B.2. This table shows the conditions under which the test run was performed including data such as environmental conditions, freestream velocity ( $U$ ), mannequin orientation, nozzle pressure ( $p_n$ ) breathing

zone concentration (BZC) sample location, and dimensionless nozzle pressure (Carlton number). Breathing zone concentration samples were collected only on the downstream lapel for each run during the paint booth runs. The calculated overspray data is shown in Table B.3. This table includes information such as mass flow rates of air and liquid, mass of liquid transferred, and overspray generation rate ( $m_0$ ), and transfer efficiency. The breathing zone concentration data is shown in Table B.4. This table includes information such as sample filter weights, blank filter weights, and calculated dimensionless concentration. Sample calculations are shown in section A.11.

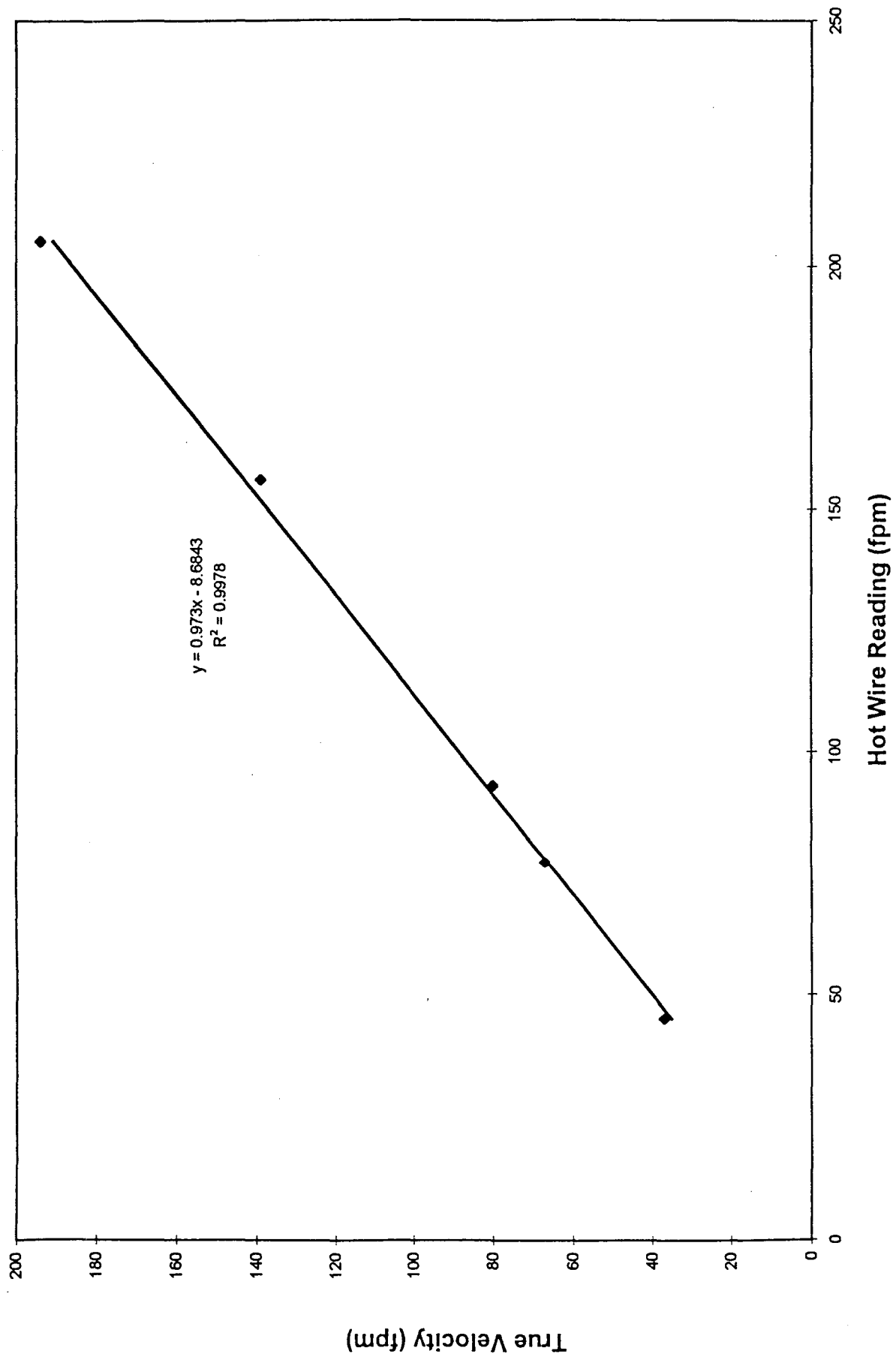


Figure B.1: Thermo-Anemometer Calibration Curve



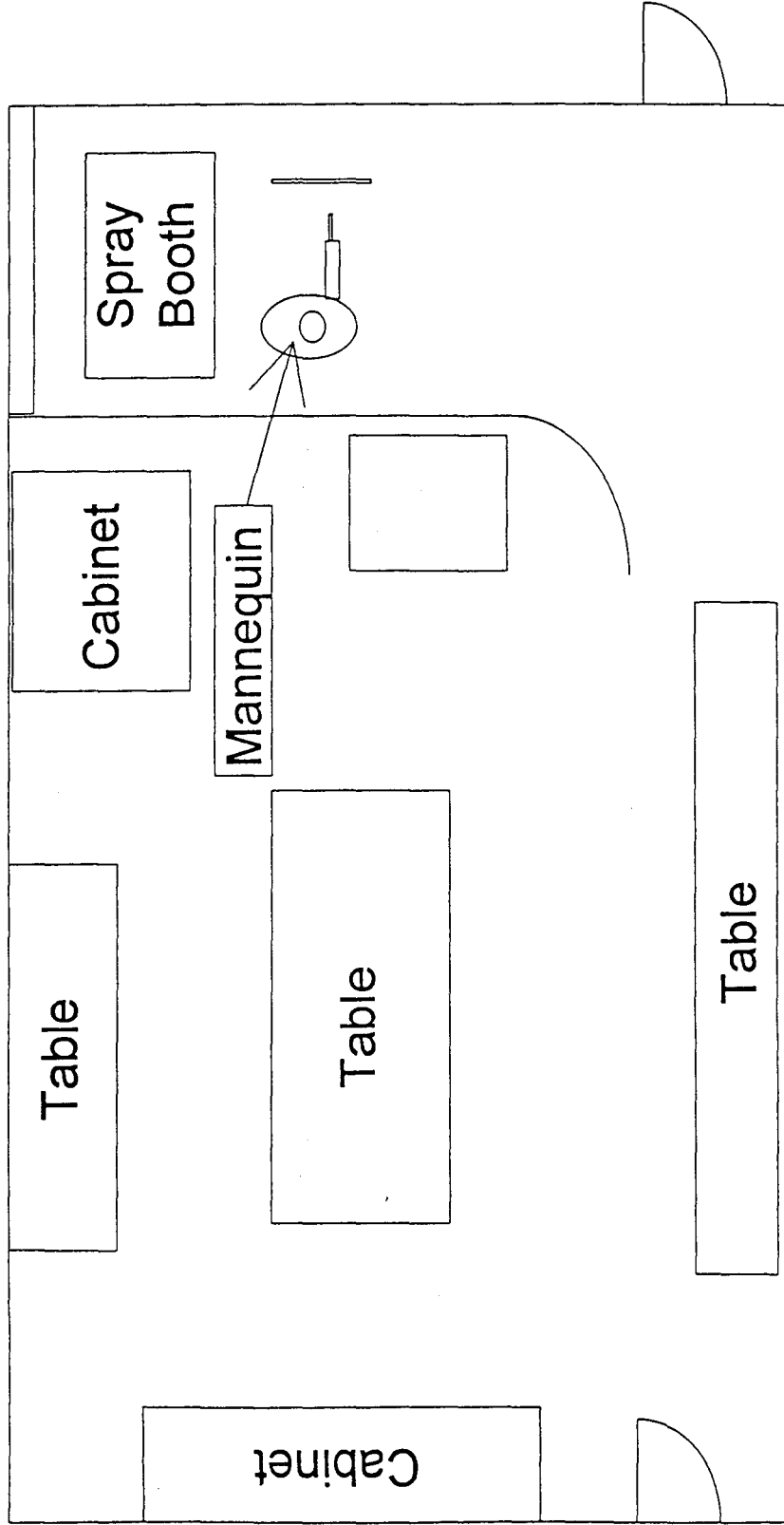


Figure B.2: Paint Booth Area Layout

Table B.1.: Thermo-Anemometer Calibration Data

Orifice Pressure (in wg)	SQRT (Orifice Pressure (in wg))	Velocity in Duct (fpm)	Air Volume (Q), CFM	Velocity in Small Wind Tunnel (fpm)	Direct Reading Thermal Anemometer (fpm)
0.08	0.28	1080	94	37	45
0.30	0.55	1951	170	67	77
0.41	0.64	2326	203	80	93
1.30	1.14	4047	353	139	156
2.30	1.52	5657	494	194	205

Table B.2: Paint Booth Velocity Profile

44.5	91.4	120.5
52.3	99.3	129.4
102.1	96.4	145.7
119.3	115.4	138.8

Note: All Velocities are in feet per minute (fpm).

Table B.3: Experimental Identifier Sheet

Run Number	Static Pressure (in wg)	Freestream Velocity (fpm)	Liquid Temperature (F)	Viscosity (cp)	Air Temperature (F)	Gauge Pressure (psig)	Nozzle Pressure Cap (psig)	Nozzle Pressure Cap & Horn (psig)	Orientation	Sample Location
1	n/a	93.0	74	70.54	74	53	6.5	11.5	90°	Upstream
2	n/a	93.0	74	70.54	74	46	6	10.5	90°	Downstream
3	n/a	93.0	74	70.54	74	27	2.5	4.5	90°	Upstream
4	n/a	93.0	74	70.54	74	16	1.5	2.5	90°	Downstream
Blank	n/a	n/a	n/a	n/a	n/a	n/a	n/a	n/a	n/a	n/a
5	n/a	93.0	73	72.73	75	53	6.5	11.5	90°	Upstream
6	n/a	93.0	73	72.73	75	46	6	10.5	90°	Downstream
7	n/a	93.0	73	72.73	75	27	2.5	4.5	90°	Upstream
Blank	n/a	n/a	n/a	n/a	n/a	n/a	n/a	n/a	n/a	n/a
8	n/a	93.0	72	74.99	75	27	2.5	4.5	90°	Upstream
9	n/a	93.0	72	74.99	75	46	6	10.5	90°	Downstream
10	n/a	93.0	72	74.99	75	53	6.5	11.5	90°	Upstream
Blank	n/a	n/a	n/a	n/a	n/a	n/a	n/a	n/a	n/a	n/a

Table B.4: Transfer Efficiency/Overspray Worksheet

Run Number	Run Time (s)	Bucket Weight (g)		Trough Weight (g)		Mass of Liquid Sprayed (g/min)	Mass of Liquid Transferred (g/min)	Mass of Liquid Overspray (m <sub>o</sub> ) (g/min)	Mass of Air (g/min)**	m <sub>o</sub> /m <sub>i</sub>	Transfer Efficiency	Carton Number
		Before	After	Before	After							
1	242.45	3109.8	2538.3	234.8	692.5	141.4	113.3	28.2	285	2.0	0.801	1.8E+6
2	301.91	2977.7	2257.5	243	828.3	143.1	116.3	26.8	268	1.9	0.813	1.6E+6
3	570.87	2840.5	1556.7	244.5	1357.6	134.9	117.0	17.9	165	1.2	0.867	6.8E+5
4	781.6	2663.2	974.5	251.3	1756.5	129.6	115.5	14.1	131	1.0	0.891	4.1E+5
Blank	n/a	n/a	n/a	n/a	n/a	n/a	n/a	n/a	n/a	n/a	n/a	n/a
5	240.92	3383.8	2848.4	236.5	655.6	133.3	104.4	29.0	285	2.1	0.783	1.7E+6
6	304.97	3250.5	2565.3	251.6	805.8	134.8	109.0	25.8	268	2.0	0.809	1.6E+6
7	571.87	3120.5	1880.3	250.3	1322.5	130.1	112.5	17.6	165	1.3	0.865	6.6E+5
Blank	n/a	n/a	n/a	n/a	n/a	n/a	n/a	n/a	n/a	n/a	n/a	n/a
8	660.89	3460	2192	244.8	1329.5	115.1	98.5	16.6	165	1.4	0.855	6.4E+5
9	300.8	3283.5	2667.3	238.1	732.3	122.9	98.6	24.3	268	2.2	0.802	1.5E+6
10	243.2	3157	2649.6	239.8	636.5	125.2	97.9	27.3	285	2.3	0.782	1.7E+6
Blank	n/a	n/a	n/a	n/a	n/a	n/a	n/a	n/a	n/a	n/a	n/a	n/a

Table B.5: Dimensionless Concentration Worksheet

Run Number	Date	Mass of Liquid Overspray (m <sub>o</sub> ) (g/min)	Time (s)	Filter Weight (m)		Sample Mass (mg)	Sampling Flowrate (lpm)	Concentration (mg/m <sup>3</sup> )	Carlton Number	CUHD/m <sub>o</sub>
				Before	After					
1	12/13/96	28.16	242.45	14.419	15.684	1.265	1.90	165.20	1.6E+6	0.0768
2	12/13/96	26.81	301.91	14.241	15.572	1.331	1.90	139.59	1.8E+6	0.0682
3	12/13/96	17.94	570.87	14.362	14.783	0.421	1.90	23.35	6.8E+5	0.0170
4	12/13/96	14.09	781.6	13.889	13.880	-0.009	1.90	-0.36	4.1E+5	-0.0003
Blank	12/13/96	n/a	n/a	13.432	13.433	0.001	n/a	n/a	n/a	n/a
5	12/14/96	28.96	240.92	13.199	14.376	1.177	1.90	154.68	1.6E+6	0.0699
6	12/14/96	25.77	304.97	13.669	14.892	1.223	1.90	126.97	1.7E+6	0.0645
7	12/14/96	17.63	571.87	13.680	13.858	0.178	1.90	9.86	6.6E+5	0.0073
Blank	12/14/96	n/a	n/a	13.433	13.430	-0.003	n/a	n/a	n/a	n/a
8	12/15/96	16.64	660.89	13.577	13.840	0.263	1.91	12.51	1.5E+6	0.0098
9	12/15/96	24.34	300.8	13.351	14.450	1.099	1.91	114.89	6.4E+5	0.0618
10	12/15/96	27.31	243.2	13.299	14.375	1.076	1.91	139.13	1.7E+6	0.0667
Blank	12/15/96	n/a	n/a	13.430	13.431	0.001	n/a	n/a	n/a	n/a

## Appendix C: Statistical Analysis and Results

### C.1. Wind Tunnel Blockage Partial F Test

A test of coincidence was performed for the wind tunnel and paint booth data sets. This test uses a single multiple regression model that contains dummy variables to account for each group. An analysis using the SAS system was performed and the variable names used in the model are as follows:

1) Dummy Variable: ENC stands for enclosure and is either coded as p for paint booth or w for wind tunnel.

2) Dependent Variable: DC stands for dimensionless concentration,  $\frac{CHUD}{m_0}$

3) Independent Variable: CN stands for Carlton number,  $\frac{p_r H}{\mu_l U}$

The hypothesis is that the two regression lines were coincident (i.e. the slopes and intercepts were equal). The two models being compared in this test are therefore:

Full Model:  $DC = \beta_0 + \beta_1 CN + \beta_2 ENC + \beta_3 (CN)(ENC) + E$

Reduced Model:  $DC = \beta_0 + \beta_1 CN + E$

Test statistic:  $F = \frac{[\text{regression SS (CN, ENC, CN*ENC)} - \text{regression SS (CN)}]}{\text{MS residual (CN, ENC, CN*ENC)}}$

$$F = \frac{[0.01853125 - 0.01796297]/2}{[0.02125171/20]} = 0.2674$$

Comparing this F with  $F_{2, 20, 0.95} = 3.49$ , we accept the null hypothesis at a level of significance  $\alpha = 0.05$  and conclude that there is strong evidence that the two lines are coincident. Therefore, we can conclude that there is no significant difference between the wind tunnel and paint booth data sets. The SAS program output is shown in Figure C.1.



Figure C.1: SAS Output

Method I

General Linear Models Procedure

Dependent Variable: DC

Source	DF	Sum of Squares	Mean Square	F Value	Pr > F
Model	3	0.01853125	0.00617708	38.60	0.0001
Error	17	0.00272047	0.00016003		
Corrected Total	20	0.02125171			
R-Square		C.V.	Root MSE	DC Mean	
0.871988		24.86448	0.01265020	0.05087657	

Source	DF	Type I SS	Mean Square	F Value	Pr > F
CN	1	0.01796297	0.01796297	112.25	0.0001
ENC	1	0.00024853	0.00024853	1.55	0.2296
CN*ENC	1	0.00031974	0.00031974	2.00	0.1756

Source	DF	Type III SS	Mean Square	F Value	Pr > F
CN	1	0.01491359	0.01491359	93.19	0.0001
ENC	1	0.00051123	0.00051123	3.19	0.0917
CN*ENC	1	0.00031974	0.00031974	2.00	0.1756

Parameter	Estimate	T for H0: Parameter=0	Pr >  T	Std Error of Estimate
INTERCEPT	0.0005342564 B	0.08	0.9397	0.00696221
CN	0.0000000421 B	8.72	0.0001	0.00000000
ENC	-0.0256441624 B	-1.79	0.0917	0.01434759
	0.0000000000 B	.	.	.
CN*ENC	0.0000000144 B	1.41	0.1756	0.00000001
	0.0000000000 B	.	.	.

NOTE: The X'X matrix has been found to be singular and a generalized inverse was used to solve the normal equations.  
Estimates followed by the letter 'B' are biased, and are not unique estimators of the parameters.




***EFFECT OF POSITION AND MOTION ON PERSONAL EXPOSURE  
IN A HVLP SPRAY PAINTING OPERATION***

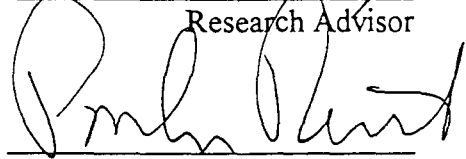
John L. McKernan

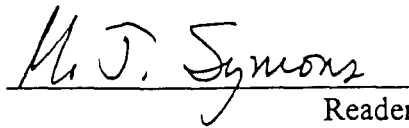
A technical report submitted to the Faculty of  
the University of North Carolina at Chapel Hill  
in partial fulfillment of the requirements for the degree of  
Master of Science in Public Health  
Department of Environmental Sciences and Engineering  
School of Public Health

Chapel Hill  
1997

Approved by:

  
\_\_\_\_\_  
Research Advisor

  
\_\_\_\_\_  
Reader

  
\_\_\_\_\_  
Reader



## Abstract

JOHN L. MC KERNAN. Effect of Position and Motion on Personal Exposure in a HVLP Spray Painting Operation. (Under the direction of MICHAEL R. FLYNN)

Worker exposure to particles is a problem in most spray painting processes. Previous studies, using a stationary mannequin and simple spray nozzle, showed that dimensional analysis could be used to correlate a dimensionless breathing zone concentration (which requires knowing the gun transfer efficiency) with a dimensionless nozzle pressure term (the Carlton number). This work expands on that study by using a real high volume-low pressure (HVLP) gun, and adding a representative spraying motion. A robot-mannequin, capable of holding and actuating the spray gun, and also performing a repeated side-to-side spraying motion was used. Vacuum pump oil was sprayed onto a flat plate in a wind tunnel to determine the relationship between nozzle pressure and breathing zone concentration. "Breathing zone" samples were collected using a cassette modified to mimic the IOM inlet.

Data collected in the absence of motion show that the dimensionless concentration in the 90° position is lower than the 180° position until a crossover point is reached at low values of the Carlton number ( $8 \times 10^5$ ). After this point, the dimensionless breathing zone concentration in the 180° position is lower than in the 90° orientation. For the case with motion, the importance of position to dimensionless breathing zone concentration was mitigated. Using task representative Carlton number values (alpha values) allows for simplification of the results. Alpha values for the 90° and 180° orientations without motion were 0.232 and 0.028. It was observed that the motion mitigated the positional effect in such a way as to make the alpha value for motion close to the average of the two no motion alpha values, 0.102. These results allow for the supposition of a formula to predict breathing zone concentrations or transfer efficiencies for conventional and HVLP spraying guns. The results also stress the association between contaminant generation, transport, and exposure. Models, such as the one used, are beneficial because they relate exposure to processes parameters that can be controlled to reduce it.

## Acknowledgments

I would like to start by thanking God for giving me the strength and ability to complete graduate school. Secondly I thank Betty Gatano for her *unending* patience and help, and Dr. Michael Flynn for his guidance. I thank Kevin H. Dunn for his knowledge and resourcefulness, Lauralynn Taylor for showing me how to work most of this darn lab equipment, Dr. David Leith, Maryanne Boundy, and all of the people who work in the Baity Lab. You have all been very helpful in so many ways that I cannot count them all. Lastly, I thank my family for believing in me, and giving their unwavering support.

The National Institute for Occupational Safety and Health Grant No. 5R01OH02858 supported this project and made my education at the University of North Carolina, Department of Environmental Sciences and Engineering possible.

## Table of Contents

Chapter	Page
<b>LIST OF TABLES.....</b>	<b>iv</b>
<b>LIST OF FIGURES.....</b>	<b>v</b>
<b>1.0 INTRODUCTION .....</b>	<b>1</b>
<b>2.0 THEORY .....</b>	<b>4</b>
2.1 OBJECTIVES OF STUDY .....	10
<b>3.0 METHODS .....</b>	<b>11</b>
3.1 LABORATORY SETUP .....	11
3.2 LABORATORY EXPERIMENTAL DESIGN.....	17
<b>4.0 RESULTS .....</b>	<b>18</b>
<b>5.0 DISCUSSION .....</b>	<b>24</b>
<b>6.0 CONCLUSIONS.....</b>	<b>27</b>
<b>7.0 APPENDIX A: CALIBRATION AND RAW EXPERIMENTAL DATA .....</b>	<b>29</b>
<b>8.0 APPENDIX B: ADDITIONAL MATERIALS.....</b>	<b>46</b>
<b>9.0 REFERENCES .....</b>	<b>75</b>

## List of Tables

TABLE A.2: PROCESS MEASUREMENTS .....	30
TABLE A.3: MEASURED FLOW RATES AND CALCULATED TRANSFER EFFICIENCIES .....	33
TABLE A.4: CALCULATION OF DIMENSIONLESS CONCENTRATION .....	36
TABLE B.1: CALCULATION OF TASK REPRESENTATIVE CARLTON NUMBER .....	47
TABLE B.2: ANCOVA ANALYSIS FOR 90° AND 180° ORIENTATIONS WITH MOTION .....	61



## List of Figures

FIGURE 1: FUNCTIONAL RELATIONSHIP BETWEEN DIMENSIONLESS GROUPS IDENTIFIED BY DIMENSIONAL ANALYSIS WITHOUT MOTION .....	8
FIGURE 2: MEASURED MEAN WORKER EXPOSURES FOR THE FIELD STUDY AND THEIR MODEL PREDICTIONS .....	9
FIGURE 3: FUNCTIONAL RELATIONSHIPS BETWEEN DIMENSIONLESS GROUPS USING THE HVLP NO MOTION DATA .....	20
FIGURE 4: FUNCTIONAL RELATIONSHIP BETWEEN THE DIMENSIONLESS GROUPS, USING COMPOSITE DATA .....	21
FIGURE 5: FUNCTIONAL RELATIONSHIPS BETWEEN DIMENSIONLESS GROUPS USING THE HVLP MOTION DATA .....	23
FIGURE A.1: AIR VOLUME AS A FUNCTION OF THE SQUARE ROOT OF THE PRESSURE DROP ACROSS ORIFICE .....	40
FIGURE A.2: CALIBRATION OF HOT WIRE ANEMOMETER .....	41
FIGURE A.3: CALIBRATION OF WIND TUNNEL USING HOT WIRE ANEMOMETER .....	42
FIGURE A.4: AIR VOLUMETRIC FLOWRATE FROM THE HVLP GUN AS A FUNCTION OF FAN PATTERN AND NOZZLE PRESSURE .....	43
FIGURE A.5: VISCOSITY OF VACUUM PUMP OIL AS A FUNCTION OF TEMPERATURE .....	44
FIGURE A.6: TRANSFER EFFICIENCY AS A FUNCTION OF $M_A/M_L$ .....	45
FIGURE B.1: SCHEMATIC OF COMPRESSOR AND SPRAY POT SYSTEMS .....	63
FIGURE B.4: ¼ J HIGH PRESSURE SPRAY NOZZLE .....	64

FIGURE B.5: HIGH VOLUME-LOW PRESSURE SPRAY GUN .....	65
FIGURE B.6: COMPLETE PRESSURIZED PAINT VESSEL.....	66
FIGURE B.7: LABORATORY EQUIPMENT SETUP .....	67
FIGURE B.8: MANNEQUIN IN 90° ORIENTATION .....	68
FIGURE B.9: MANNEQUIN IN 180° ORIENTATION .....	69

## 1.0 Introduction

Spray painting is the method of choice in industry to coat and finish many products, from furniture to automobiles. There are many different types of spray guns to choose from, each uses a different physical process such as electrostatic, air assisted airless, and low pressure air atomization to coat the workpiece. Although spray application gives a better finish than other methods, it has the disadvantage of creating a fine particulate “overspray” which reaches the workers’ breathing zone. Inhalation of this overspray is a major hazard because it contains pigments, solvents and binders. The inorganic compounds which make up the pigments commonly contain lead, chromium, cadmium. Many compounds of these elements induce respiratory, systemic, and possibly cancerous effects.<sup>(7)</sup> Solvents and binders such as polyisocyanates, n-hexane and toluene are also constituents of the overspray and have been associated with skin, eye and respiratory effects.<sup>(10)</sup>

Since there are a multitude of health effects related to overspray exposure, efforts are being made to control it. The favored approach is the use of engineering controls. Engineering controls commonly used in the spray painting process are local exhaust ventilation, and recently the use of new types of spray systems with more efficient application methods.

Designing controls for industrial operations is a difficult engineering undertaking. The American Conference of Governmental Industrial Hygienists

(ACGIH) has attempted to simplify the design process for local exhaust ventilation systems by providing engineers with VS plates.<sup>(1)</sup> Successful reduction of airborne contaminants by the use of these suggested designs is not guaranteed. Only after building the ventilation system can it be tested for proper contaminant control. The development and use of models may make this process of ventilation design more cost effective. Using a model, predictions about the concentration in the proposed system can be made before it is built, thus setting the stage for optimization.

The ability to reduce excess particles emanating from the spraying process is also an important engineering control. Industry and some states are very interested in reducing the overspray created by spraying systems. It saves industry money if they can improve the quality of finish while decreasing the amount of paint wasted in the overspray. States are more concerned with human safety issues, such as fires, exposure to the overspray, and complying with emissions standards for air quality. In this work, a new high volume low pressure (HVLP) spray gun was used. The HVLP spraying system has been shown to reduce exposures while increasing the quality of finish on the product.<sup>(9)</sup> The HVLP was used to test how well it would fit into a previously developed model by Carlton and Flynn.<sup>(2)</sup> There was also an interest in whether or not the gun, acting as an engineering control, increased transfer efficiencies while decreasing exposure to the contaminant as claimed.<sup>(9, 10)</sup>

It is advantageous to have an estimate of the reduction in worker exposure, before spending money to update or redesign the current engineering controls in a facility. In

the past, a proposed engineering control would have to be installed to evaluate its effectiveness. Since this procedure is expensive and sometimes impractical, methods to investigate the efficacy of a control before it is implemented are needed. This ability to predict exposure will allow for a more effective use of engineering controls. The Carlton-Flynn model may enable hygienists to predict breathing zone concentrations for spray painting operations. The model uses mathematical equations involving the dominant parameters of a spray painting task. The model has been evolving through continued exposure assessment research.

Previous studies using elementary models of flow around a worker with passive introduction of the contaminant and simple exposure assessment have been done by researchers such as Kim and George, et al.<sup>(12, 8)</sup> Kim also conducted breathing zone concentration evaluations for a simple spraying system, taking into account the source momentum. It was discovered that the added momentum negates the recirculation vortex documented by George<sup>(8)</sup>, and results in a reduction of breathing zone concentration when compared to the case with passive introduction of the contaminant.<sup>(13, 8)</sup>

The end result of this continuing research is to develop a working model which can evaluate possible exposures for a multitude of spraying operations. This working model can then facilitate estimates of worker exposures in any spray painting task. Industries stand to reduce paint particulate and solvent exposure to workers, saving money and preventing occupational disease.

## 2.0 Theory

In previous experiments by Kim <sup>(12, 13)</sup>, George <sup>(8)</sup> and Carlton <sup>(2, 3)</sup>, factors which contribute to exposure in spray painting tasks were determined. Of these, the dominant ones are ventilation, contaminant generation rate, and work practices. Carlton <sup>(2)</sup> most recently expanded on past work to develop and test an empirical-conceptual model. All of the relevant task defining parameters were included in the model and were combined to create two dimensionless terms, developed by dimensional analysis, to relate the spray painting task to worker breathing zone concentration.

The following parameters were significant in the Carlton-Flynn model; nozzle pressure at the cap of the spray gun in pounds per square inch gauge ( $p_n$ ), height of the mannequin in feet ( $H$ ), viscosity of the liquid to be sprayed in centipoise ( $\mu_l$ ), velocity of the wind tunnel in feet per minute ( $U$ ), concentration in the breathing zone of the mannequin in milligrams per cubic meter ( $C$ ), width (breadth) of the mannequin in feet ( $D$ ), and contaminant generation rate in grams per minute ( $m_0$ ).

There are three processes common to all liquid spray painting tasks. They are; droplet formation, droplet transfer, and droplet transport. These three processes define a conceptual model to predict a worker's exposure to paint overspray. <sup>(2)</sup> The dimensionless terms used in the model are a combined expression of the task defining

parameters and the dominant processes. Their groupings represent related mechanisms which lead to exposure. The expressions for the dimensionless terms are:

$$\text{Dimensionless Nozzle Pressure Term (Carlton Number): } \frac{p_n H}{\mu_1 U} = \frac{\text{droplet transport}}{\text{droplet transfer}}$$

$$\text{Dimensionless Breathing Zone Concentration Term: } \frac{CHUD}{m_o}$$

The dimensionless breathing zone concentration was defined by Carlton<sup>(2)</sup>.

Using dimensional analysis, the following dimensionless representation of the model was developed:

$$\frac{CHUD}{m_o} = \Phi \left( \frac{m_a}{m_i}, \frac{p_n H}{\mu_1 U}, \text{orientation} \right)$$

The model indicates the concentration group  $CHUD/m_o$  depends on worker orientation to the freestream and two other nondimensional groups; the air-to-liquid mass flow ratio  $m_a/m_i$  and the dimensionless pressure group  $p_n H/\mu_1 U$ . The empirical work indicated that  $CHUD/m_o$  is a strong function of the quantity  $p_n H/\mu_1 U$  and worker orientation. This can be seen in Figure 1.

The previous study<sup>(2)</sup> utilized a stationary mannequin holding a 1/4 J nozzle in two possible orientations (90° and 180°), a flat plate, and wind tunnel to develop the

model. The ¼ J spray nozzle was used because it had characteristics, such as droplet size distributions, and  $m_2/m_1$  values, similar to a commercial hand-held spray gun. Results from this research conducted by Carlton (1996) are shown graphically in Figure 1. The data suggest that for Carlton numbers greater than  $5 \times 10^6$ , the dimensionless concentration is higher in the  $90^\circ$  orientation. The data also suggest that there is a defining region of Carlton numbers where conventional high pressure spraying systems operate. This region is defined by Carlton numbers which most closely represent a real operation. Table B.1 in Appendix B contains a detailed description of the calculations used to represent a real operation. In Figure 1, the plateau regions in both orientations above Carlton number values of  $1.3 \times 10^7$  represent these real operation areas. Because the dimensionless concentrations at and above these Carlton number values do not change, we associate one value for the dimensionless concentration over the whole range of realistic operation for each orientation. These constant values for concentration are called the alpha ( $\alpha$ ) values. From the work displayed in Figure 1, these values are:

$$\alpha_{90} = 0.13$$

$$\alpha_{180} = 0.006$$

The HVLP operates in a range of Carlton numbers between  $3 \times 10^5$  and  $2.5 \times 10^6$ , lower than previously investigated.<sup>(2)</sup> A major hypothesis of this work is that the



HVLP will follow the defined trends in the 90 and 180° orientations shown in Figure 1.

Carlton (1996) completed field evaluations of his model, the results of which are in Figure 2.<sup>(2)</sup> Using volunteer workers, Carlton measured all of the necessary parameters needed for the model to see if the predicted concentrations matched their actual task exposures.

Figure 2 shows the model was fairly accurate, often within one standard error of the mean. Considering all of the data points, 71% of the measured task exposures are within a factor of three of the model prediction. This accuracy is satisfactory in light of the fact that the model is based solely on dimensional relationships. The measured field exposures tended to be less than those predicted by the model, but statistical analysis indicated that this was not significant. It was determined that the model was sufficient to make predictions of the average breathing zone concentration for workers performing spray painting tasks.

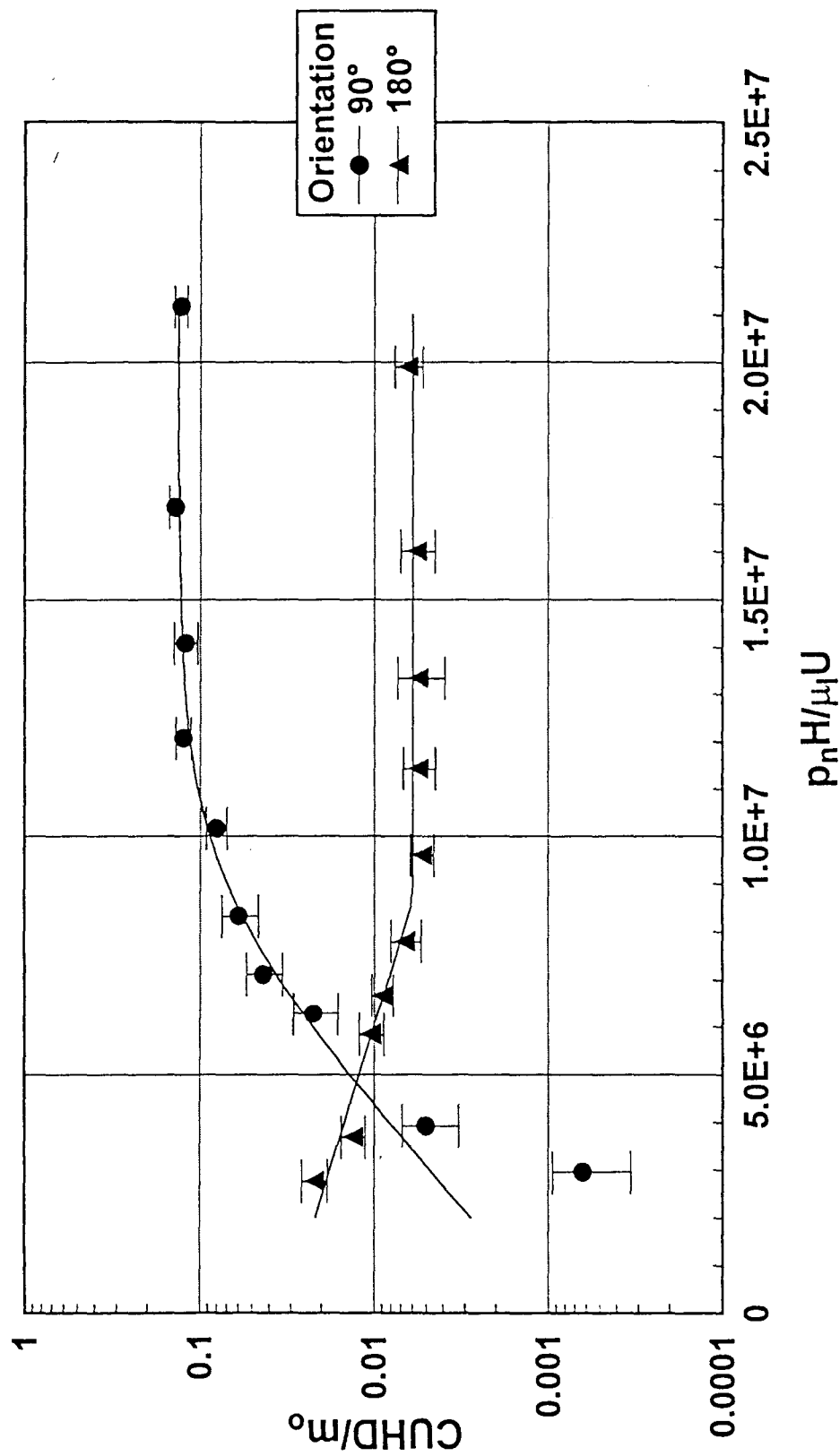


Figure 1: Functional relationship between the dimensionless groups identified by dimensional analysis without motion. (from Carlton, et al.)

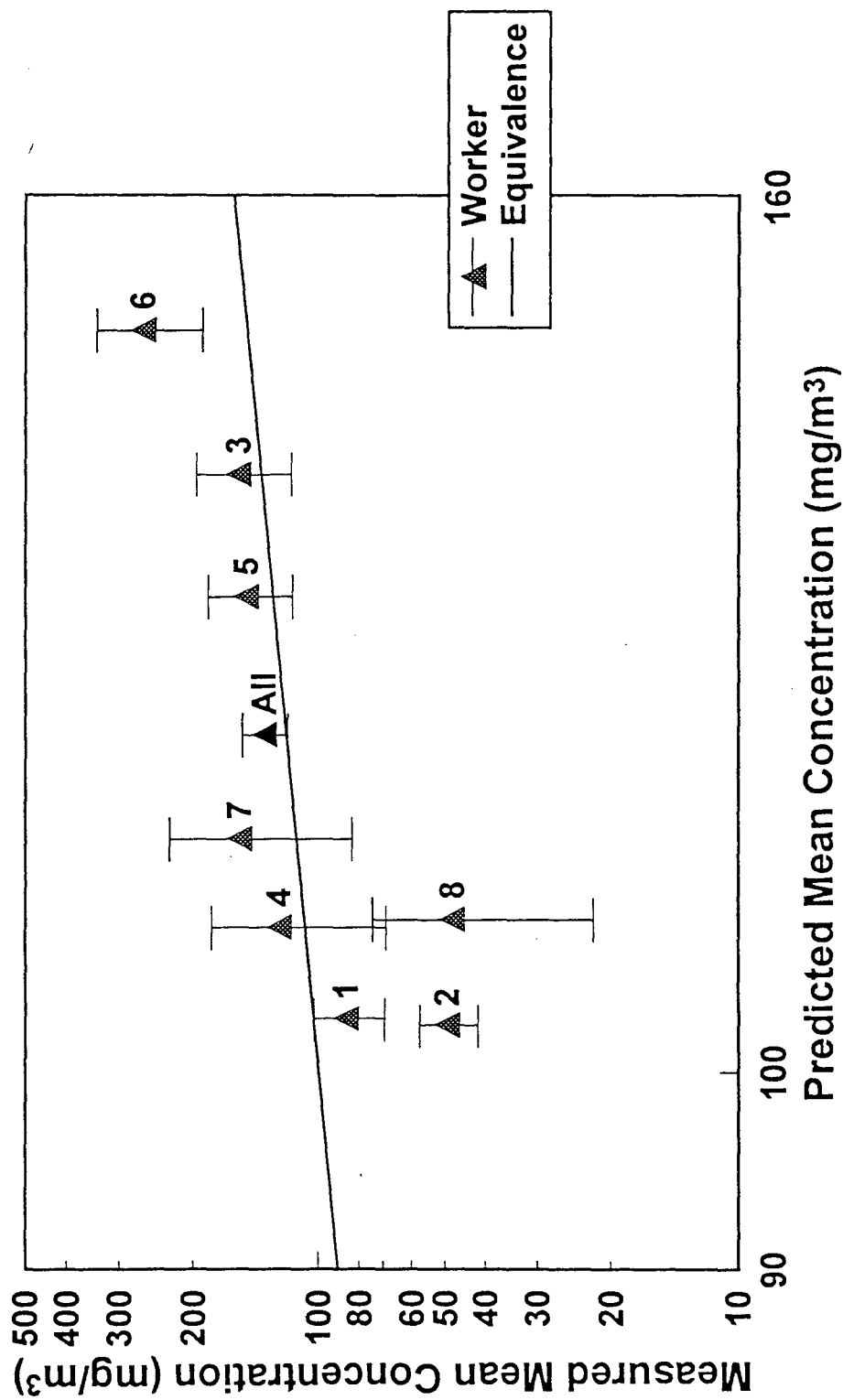


Figure 2: Measured mean worker exposures for the field study and their model predictions. Most of the predictions are within one standard error of the means.

The previous results indicate that spray painting is a variable exposure task and is difficult to characterize. Characterization is further complicated by the fact that each worker has different experiences that directly affect their individual work practices. This may explain some complications seen in the previous evaluation of the model, because no consideration was made for variations in work practices.

### *2.1 Objectives of Study*

The objective of this research is to determine the validity of the suggested empirical conceptual model. The addition of motion to the experimental trials and the use of an HVLP spray gun will help assess if the relationships shown in the Carlton-Flynn model are valid. The results of this experiment will ascertain if the model can be generalized to different spray operations.

This work expands on Carltons' by using the HVLP spraying system which operates at much lower pressures than a conventional system, like the 1/4 J. Using the HVLP as an engineering control has been highly recommended for industry. A comparison of the HVLP and conventional systems done by the National Institute for Occupational Safety and Health (NIOSH) showed that the HVLP system was approximately 30% more efficient than conventional systems. This efficiency was based on measured film thickness from the target workpiece. Overspray measured in the HVLP operation was  $\frac{1}{2}$  that in the conventional operation.<sup>(9)</sup> In using techniques similar to those outlined by Carlton (1996) in this experiment, it is hypothesized that

the new HVLP will follow the previous trends for the 90 and 180° positions as defined by the  $\frac{1}{4}$  J.

A second objective of this work is to determine if data from the mannequin with a representative spraying motion would fit the model. It is believed that moving the gun hand of the mannequin back and forth horizontally while spraying the workpiece will produce data that is more task-representative. There are limitations to this hypothesis. The mannequin will be spraying the workpiece in an arcing motion, with the gun close in the middle of the arc and far from the workpiece at the ends. Also, the fact that the gun trigger cannot be “fanned” like a real process limits the hypothesis of realistic representation by the moving mannequin. Both of the limiting factors mentioned may increase the measured breathing zone concentration.<sup>(6)</sup>

## 3.0 Methods

### 3.1 Laboratory Setup

The laboratory experiment required many pieces of equipment, such as:

1. a wind tunnel through which a uniform freestream could be varied
2. a mannequin to represent the worker and objects to represent the workpiece
3. a spraying system to deliver the simulated paint to the workpiece
4. an active sampling technique which would provide data for exposure concentrations

The wind tunnel used in this experiment was an 8 foot deep by 25 ft<sup>2</sup> tunnel in Baity Air Engineering Laboratory at UNC Chapel Hill. The wind tunnel is capable of producing uniform freestream velocities by the use of a flared inlet opening, resembling a bell, and a pegboard rear wall. It was possible to vary the freestream in the wind tunnel from 40 to 325 fpm using a Toshiba Tosvert-130H1, power source frequency inverter attached in-line to the system fan. The system fan was a New York Blower Co. general purpose 48" diameter fan. The wind tunnel was calibrated using an Alnor model 8565 nickel-wire thermoanemometer. The thermoanemometer was calibrated for use by implementing a ventilation system with an orifice meter in the ductwork. The orifice meter was previously calibrated in the duct work using a primary standard Dwyer pitot tube and manometers. A calibration curve was developed for this data set (Appendix A, Figure A.1). The thermoanemometer reading was calibrated with comparison to the pitot tube calculated velocity to correct to a 'true' velocity reading. The velocity read directly from the thermoanemometer was found to be approximately equal to the calculated 'true' velocity within the range of concern, so no correction factor was utilized when taking thermoanemometer readings in the wind tunnel. A calibration curve for the thermoanemometer velocity vs. 'true' velocity is in Appendix A, Figure A.2.

The calibration of the wind tunnel was done by averaging the velocity measurements, read from the thermoanemometer, for 16 points on a central vertical plane. This was done for 8 separate freestream velocities between 43 and 325 fpm.

Velocity measurements were correlated to static pressure readings taken with a large pitot tube upstream of the system fan. A wind tunnel calibration curve was made from this data set (Appendix A, Figure A.3).

The mannequin in this experiment was quite unique. It utilized electric motors and servo controls to actuate the trigger finger, and in later motion experiments, move its right arm in an arc about  $135^\circ$  wide. The mannequin was of the department store variety, but cut just above the knee to accommodate its use in the wind tunnel. It measured 4.25 feet high (H) and 1.17 feet at the chest (D). The HVLP gun was held in its right hand and actuated by use of the servo controlled index finger. There were two mannequin orientations in this experiment. It could face the rear of the wind tunnel, the  $180^\circ$  position, or it could face perpendicular to the freestream, in the  $90^\circ$  position. The mannequin in both cases sprayed the gun at a flat metal plate which represented the workpiece. The gun was held eight inches away from a 24 x 36 inch flat plate in both orientations of the no motion studies. When motion was implemented, the gun was held 8" away at the closest point in the arc motion of the arm, from a 36 x 36 inch plate in both orientations.

In place of spraying paint, we chose a non-volatile, non-toxic compound to apply to our workpiece. This compound was paraffin wax or vacuum pump oil (Inland 99, MSDS attached). It met all of the safety requirements of the university and research staff and was about the same consistency as the previously used corn oil.

Initially, corn oil was used because it was also considered a relatively safe compound and had about the same viscosity as enamel paints.

In using the new vacuum pump oil, it was important to find its viscosity at different temperatures to correct our data for temperature later. Because the experiment was done in the summer time, a temperature range from 68 to 98 degrees Fahrenheit was chosen. Viscosity measurements were done using a Haake falling ball viscometer in an adjustable temperature bath, and a stopwatch. A calibration curve for the measured viscosity ( $\mu_l$ ) of the oil at different temperatures in the predetermined range is in Appendix A, Figure A.5.

The compressed air system used was a Speedaire 5 horsepower air compressor pump model 5Z641, mounted on a large air reserve tank. The compressor delivered a set 110 psig through the outlet regulator, which was then reduced to 90 psig in a secondary pressure regulator. This pressure reduction is done to prevent “starving” of the spraying system which could cause pressure variations at the gun cap and pressurized paint feed tank. The pressurized paint feed tank was a DeVilbiss QMG T-5220 galvanized dual regulator tank. The two regulators on the pressurized feed tank were used to set the pressure inside of the feed tank and to set the air pressure going into the spray gun. The tank regulator was set to 10 psig for all experiments. The gun regulator had multiple settings which corresponded to different cap pressures from 10 psig down to 2 psig. A diagram and pictures of the spraying equipment used are in Appendix B.



The high volume low pressure (HVLP) gun was a DeVilbiss MSV-533-4-FF with a 33A air cap. It was specified to operate at a maximum spraying capacity of 18.75 cfm at 10 psig at the cap. The last piece of equipment in need of calibration was the HVLP spray painting gun. It was decided that for all experiments the gun would retain one fan pattern and liquid feed setting. These two parameters could be kept fixed because their adjustment settings were built into the gun. The fan pattern was shown to not significantly effect the volumetric flow rate through the cap of the gun. This was determined by replacing the 33A air cap on the gun with a factory modified one which measured air pressure in the horn and cap separately. Volumetric air flow rate was then measured using a Collins Inc. primary standard spirometer. The volumetric air flow rate was determined by attaching the gun cap to the intake side of the spirometer. The time it took for the air to raise the bell of the spirometer to a predetermined height was recorded. Using this recorded time, and knowing the air pressure, the volume going into the spirometer was calculated. Once the volume was attained, the mass of air coming from the gun ( $m_a$ ) could be calculated by using the known density of air at the room temperature. Spirometer readings were done for the five cap pressures that were used: 10, 8, 6, 4, 2 psig.

Personal sampling was done following NIOSH Method 0500 for total nuisance dust. This method calls for the use of 37 mm polyvinyl chloride (PVC) filter membranes with 5  $\mu$ m pore size and a sampling rate of 2 liters per minute.<sup>(17)</sup>

Sampling was done in the experiments using a modified 37mm cassette which mimics the IOM inlet. The modified cassette samplers were used partly because of the need to be able to compare data from previous experiments. Also, we assumed that the modified cassette sampler would give results which were more representative of the actual mannequin exposure. IOM samplers are able to collect particles more efficiently, partly due to the properties of the opening in the cassette.<sup>(15, 16, 5)</sup> A large limiting factor for our imitation IOM samplers were that they did not account for loss of the sampled material on the walls of the cassette, as the true IOM does.

The modified cassettes were fastened to the shirt collar of the mannequin while it was performing the spray tasks in the wind tunnel. The cassettes were affixed such that the filter membrane was held parallel to the body of the mannequin. This method counteracts the effect of gravity to settle out overspray particles to or from the filter surface. Prior to gathering data, a test was done to see whether the upstream or downstream side of the mannequin had more exposure in the 90° position. This test was not performed for the 180° position because it was assumed that the exposure would be the same on both sides. The test for the 90° position showed that the downstream side (right lapel) produced the higher exposures. Therefore, sampling was done from the mannequins right side throughout all of the experiments.

Sampling pumps were used to sample through the cassette system. Nalgene tubing was used to run from the cassette samplers to the personal sampling pumps.

The pumps were SKC Aircheck sampler model 224-PCXR8. The pumps were run for varying amounts of time, depending on loading of the filters. The NIOSH method 0500 recommends a mass collection on the filters between 0.1 and 2.0 mg.<sup>(17)</sup> This corresponded to sampling times of between 3 and 10 minutes for each of the experimental trials.

The sampling medium used were SKC 225-8-01 low-ash, 5 $\mu$ m pore size PVC filters. The filters were analyzed using a gravimetric technique. A Cahn 27 automatic electrobalance, was used for gravimetric analyzation.

### *3.2 Laboratory experimental design*

The design of the actual experiment was straightforward. There were two mannequin orientations and motion settings. The orientation was designated as the direction the gun sprayed relative to the freestream. This was either parallel with the freestream (180°) or perpendicular to the freestream (90°). Motion was either on or off. When in motion, the mannequin moved its arm in a 135° arc varying the spray gun distance to plate from 8 to 14 inches. Using a frequency counter, the motion was measured and found to be 8.25 cycles per minute (0.1375 Hz).

There were five different gun cap operating pressures that could be varied from 2 through 10 psig. The five cap pressures were converted to five Carlton numbers, since all other five variables were known. Thus, the experiment was run to determine the dimensionless concentration term for exposure evaluation.

Since there were five Carlton numbers, two positions and two motion settings, at least twenty experimental runs were needed. Truly, forty runs were performed to be sure the results were reproducible.

## 4.0 Results

Experimental data only partially supports the Carlton-Flynn exposure model. Because the HVLP spraying system and the 1/4 J nozzle operate over different ranges of Carlton numbers, they are not directly comparable. The HVLP gun data in Figure 3 shows, for the case without motion, that the crossover point for the position effect happens at very low Carlton numbers as compared to the 1/4 J (see Figure 1). It is also observable in Figure 4, that positional crossover happens at a Carlton number of  $8 \times 10^5$  and a dimensionless breathing zone concentration of 0.028 for the HVLP gun, compared to values of  $5 \times 10^6$  and 0.01 for the 1/4 J, respectively. Maximum values for the dimensionless breathing zone concentrations for the HVLP were 0.4 and 0.1 for the 1/4 J nozzle in the no motion test comparison. It is interesting to note that in the 180° position with no motion, the 1/4 J and the HVLP data fit well. The 90° data for the HVLP on the other hand, is quite independent of the 1/4 J data. This suggests that in the 90° orientation, the trend in the Carlton-Flynn model for high pressure conventional spraying systems with no motion does not fit the HVLP system data. This data, with standard deviations about the mean, is displayed in Figure 3. The best-fit lines from linear regression for the HVLP data without motion are:

$$90^\circ \text{ orientation: } \frac{\text{CHUD}}{m_o} = 3 \times 10^{-7} \left( \frac{p_n H}{u_l U} \right) - 0.1336 \quad r^2 = .93$$

$$180^\circ \text{ orientation: } \frac{\text{CHUD}}{m_o} = 3.23 \times 10^{-2} \exp \left( -1.94 \times 10^{-7} \frac{p_n H}{u_l U} \right) \quad r^2 = .95$$

Alpha values were also determined for the two orientations with no motion. They are as follows:

$$\alpha_{90, \text{ no motion}} = 0.232 \quad (1.3 \times 10^6 \leq \text{Carlton number} \leq 2.5 \times 10^6)$$

$$\alpha_{180, \text{ no motion}} = 0.0281 \quad (1.1 \times 10^6 \leq \text{Carlton number} \leq 2.5 \times 10^6)$$

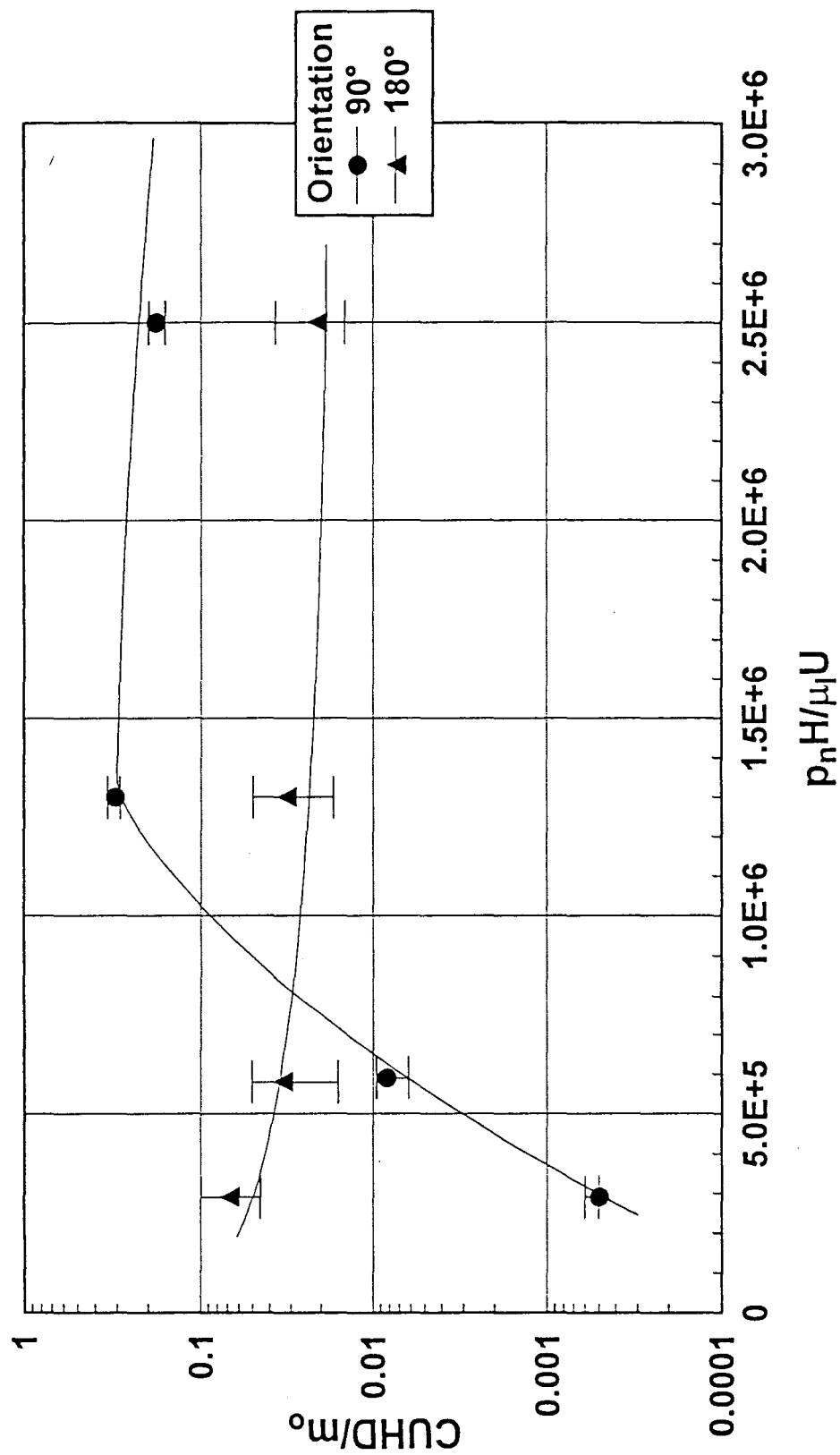


Figure 3: Functional relationship between the dimensionless groups using the HVLP data without motion.

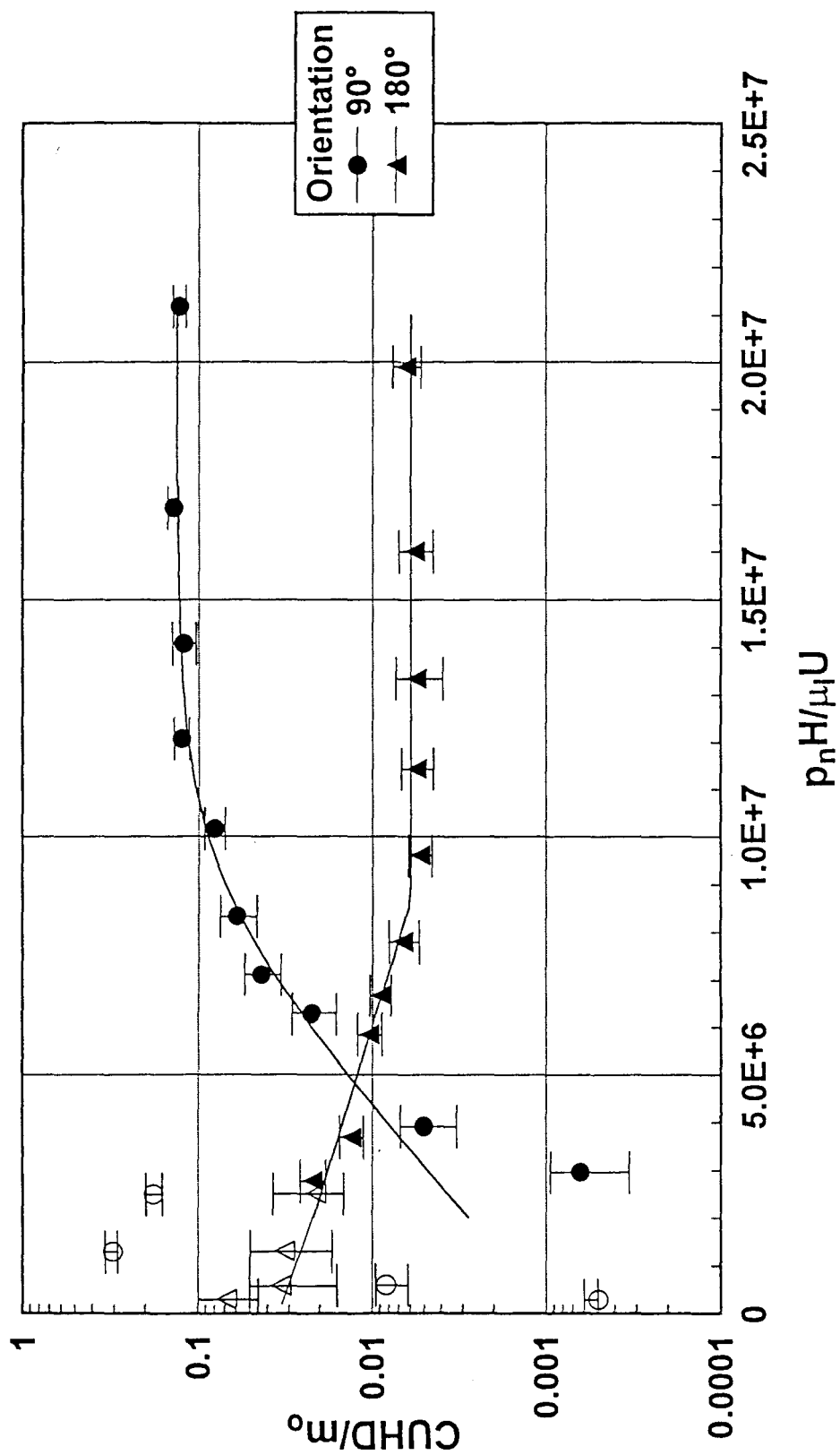


Figure 4: Functional relationship between the dimensionless groups. The graph is a composite of all the data without motion taken thus far using the current model.

This study also included a motion effect analysis on dimensionless concentration values. The motion experiment data, with standard deviations about the mean, are displayed in Figure 5. The figure shows that motion collapses the positional effect seen in the previous no motion case. This collapse brings both curves close to an average value of the no motion data in the Carlton number region between  $1.1 \times 10^6$  and  $2.5 \times 10^6$ . Since the data overlapped in the range for task representative Carlton numbers, a statistical test was performed. The test was used to discern if there was still an effect of position on dimensionless concentration with motion. See Appendix B for a description and outcome of the test performed. In summary, the test proved that the motion did indeed mitigate the positional effect to a degree that it can be said that both curves are not significantly different in the range of task representative Carlton numbers. Positional crossover happened at a Carlton number of  $8 \times 10^5$  and a dimensionless breathing zone concentration of 0.028 for the stationary HVLP gun, and at  $7 \times 10^5$  and 0.1 respectively for the moving HVLP setup. The maximum values for the dimensionless breathing zone concentrations for the stationary HVLP experiment were 0.4, and 0.2 for the moving HVLP experiment. Since there was no positional effect for motion, the data is expressed as an average concentration in the Carlton number region defined above. Therefore, there is only one alpha value expression for the motion experiment:

$$\alpha_{90-180, \text{ motion}} = 0.102 \quad (1.1 \times 10^6 \leq \text{Carlton number} \leq 2.5 \times 10^6)$$



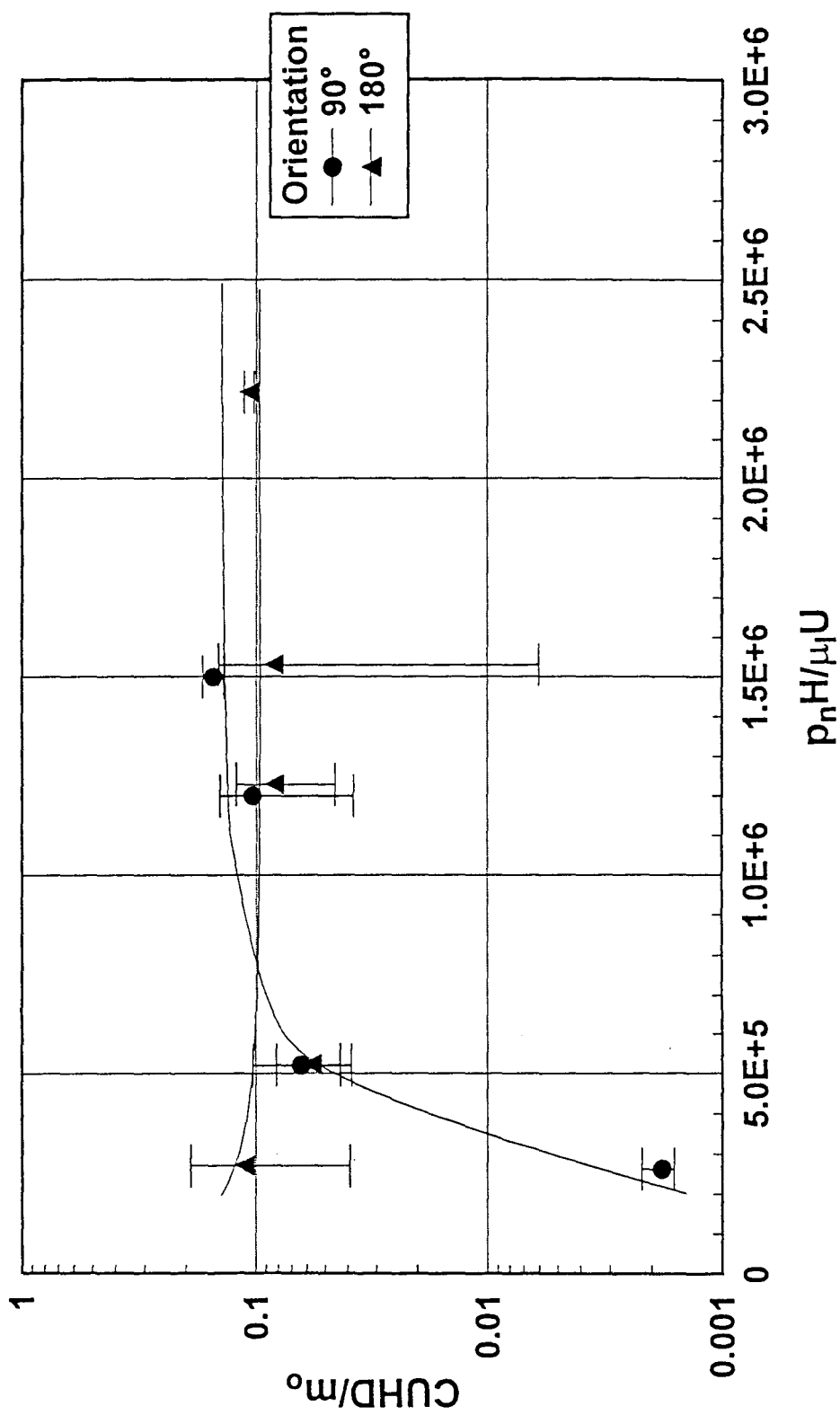


Figure 5: Functional relationship between the dimensionless groups using motion data from HVLP experimental trials.

## 5.0 Discussion

The model previously defined using the  $\frac{1}{4}$  J nozzle does not generalize completely to the HVLP spraying system. Figure 4, suggests that the trend seems to hold only in the  $180^\circ$  orientation no motion case. It is interesting that the trendlines for the two different spraying systems look similar, but occur over different ranges of Carlton numbers (See Figures 1 and 3). The HVLP data may be better understood by an explanation of how each system operates.

The  $\frac{1}{4}$  J uses a sonic airstream to atomize the sprayed liquid. This airstream is characterized as compressible flow. When the compressed (sonic) airstream exits the cap of the gun, it expands instantly to re-equilibrate itself with atmospheric pressure. This expansion is equivalent to an explosion, which violently atomizes the particles. This exploding airstream creates many small particles which do not impact on the workpiece and contribute significantly to breathing zone concentration.<sup>(19)</sup> The HVLP airstream is subsonic, but a higher volume of air and spray liquid is released compared to a high pressure system. This high volume of air under lower pressure blows the sprayed liquid apart and creates larger paint particles. The particles are then propelled toward the workpiece by the airstream where they are more likely to impact because of their size. This translates to the HVLP gun having a higher transfer efficiency.<sup>(19)</sup>

Differences in sampling technique may explain some of the variability between the ¼ J and the HVLP concentration measurements. The previous 1/4 J experiments used open-faced cassettes to collect samples to calculate breathing zone concentration. This experiment used an imitation IOM sampler to collect breathing zone concentrations. Loss factors due to the inlet and losses on the walls of the cassette were not adjusted for in this experiment.

Motion mitigated the position effect. Dimensionless breathing zone concentration tended toward the average value for the two positional trendlines in the no motion experiment. The distance to the plate varied, and the trigger on the gun was held back fully and not “fanned” as a true worker would have operated the gun. When the plate distance is not kept constant, excess overspray is generated adding to the breathing zone concentration. Not fanning the trigger lets the worker spray off of the edges of the target, also increasing the breathing zone concentration.<sup>(6)</sup>

Since results of the current experiments suggest that the position effect may be mitigated by motion, perhaps an average of the values obtained from the stationary estimates would be a reasonable estimate of the dimensionless concentration. If this approach is applied to the constant values from task representative Carlton number ranges for the 1/4 J data, one obtains:

$$\frac{(\alpha_{90} + \alpha_{180})}{2} = \frac{(0.13 + 0.006)}{2} = 0.068$$

While the HVLP with motion was 0.102. Thus, if one selected the same paint, booth velocity, worker characteristics, and liquid flow rate, the expected ratio of the HVLP dimensionless breathing zone concentration to that of a conventional gun should be:

$$\frac{(\alpha_{90-180, \text{motion}})}{0.068} = 1.5$$

By mathematical manipulation, the following expression results:

$$\frac{C_{\text{HVLP}}}{C_{\text{conv}}} = 1.5 \cdot \left( \frac{1 - \eta_{\text{HVLP}}}{1 - \eta_{\text{conv}}} \right)$$

Where C is the breathing zone concentration and  $\eta$  is the transfer efficiency. Thus, if an HVLP gun delivers a transfer efficiency of 80% and a conventional gun 60%, then the HVLP breathing zone concentration should be 75% of the conventional if the time to apply the paint is the same.

## 6.0 Conclusions

From previous experiments, it seems that a spraying system which operates below the high pressure system ( $1/4$  J) crossover point should have a lower breathing zone concentration in the  $90^\circ$  orientation. This experiment, utilizing an HVLP gun which operates well below the crossover point, illustrates that this assumption of less exposure in the  $90^\circ$  orientation is not true. Data for the  $180^\circ$  orientation with no motion follows the trendline from the previous experiment well, but HVLP data for the  $90^\circ$  orientation suggests that a mechanism not considered in the Carlton-Flynn model may be resulting in substantially higher dimensionless breathing zone concentration values than previously imagined. This experiment provides data that, in three out of four experimental cases, does not support the Carlton-Flynn model. Only in the case of no motion in the  $180^\circ$  orientation did the data from the HVLP system show agreement with the suggested model. There is a definite increase in dimensionless breathing zone concentration using the HVLP in the  $90^\circ$  orientation in comparison to the  $1/4$  J with no motion. In the trials with motion, neither orientation agreed with the  $1/4$  J assumptions.

The trials without motion using the HVLP system showed that the dimensionless breathing zone concentration is constant above Carlton number values representative of a real spray painting task for the two orientations without motion. The positional effect appeared to be mitigated by the motion of the mannequin.

Motion tests resulted in a dimensionless breathing zone concentrations that, above Carlton numbers representative of a real spraying task, is approximately the *average* value of the two no motion task representative regions. It must be noted that the variability with motion was much higher than the no motion studies. This variability suggests a mixing or “stirring” effect in the wind tunnel when the mannequin is moving.

It should be noticed that now it is possible to use the results of this and the previous experiments to estimate worker breathing zone concentration by using the predefined alpha values (the task representative Carlton number) for the ¼ J and HVLP systems. The relation between the breathing zone concentration, spraying systems, and transfer efficiency can be expressed in the formula:

$$\frac{C_{HVLP}}{C_{conv}} = 1.5 \cdot \left( \frac{1 - \eta_{HVLP}}{1 - \eta_{conv}} \right)$$

Where C is the breathing zone concentration and  $\eta$  is the transfer efficiency. The relation allows for estimation of the breathing zone concentration when using either system. Expanding on the results obtained in this experiment, by gathering data from a conventional hand-held spraying system and an HVLP system is a topic suggestible for further studies. The comparison of the two systems with more data will give a better understanding of the relationship above, and determine if it is applicable.

## **7.0 Appendix A:**

### **Calibration and Raw Experimental Data**

Table A.2 Process Measurements

Run Number	Static Pressure (in wg)	Freestream Velocity (fpm)	Liquid Temp (F)	Viscosity	Relative Humidity %	Air Temp (F)	Gauge Pressure (psig)	Cap Pressure (psig)	Cap & Horn Pressure (psig)	Orientation	Motion
1	0.16	150.3	81	56.94	62	81	16	1.5	2.5	90°	NO
2	0.12	126.8	81	56.94	62	81	27	2.5	4.5	90°	NO
3	0.08	99.0	81	56.94	62	81	38	4.25	7.5	90°	NO
4	0.048	71.1	81	56.94	62	81	46	6	10.5	90°	NO
5	0.048	71.1	81	56.94	62	81	53	6.5	11.5	90°	NO
6	0.16	150.3	79	60.53	79	76	16	1.5	2.5	180°	NO
7	0.12	126.8	79	60.53	79	76	27	2.5	4.5	180°	NO
8	0.08	99.0	79	60.53	79	76	36	4.25	7.5	180°	NO
9	0.048	71.1	79	60.53	79	76	46	6	10.5	180°	NO
10	0.048	71.1	79	60.53	79	76	53	6.5	11.5	180°	NO
11	0.055	77.8	78	62.41	64	79	53	6.5	11.5	180°	NO
12	0.048	71.1	78	62.41	64	79	46	6	10.5	180°	NO
13	0.08	99.0	78	62.41	64	79	38	4.25	7.5	180°	NO
14	0.12	126.8	78	62.41	64	79	27	2.5	4.5	180°	NO
15	0.16	150.3	78	62.41	64	79	16	1.5	2.5	180°	NO
16	0.16	150.3	78	62.41	64	79	16	1.5	2.5	90°	NO
17	0.12	126.8	78	62.41	64	79	27	2.5	4.5	90°	NO
18	0.08	99.0	78	62.41	64	79	38	4.25	7.5	90°	NO
19	0.048	71.1	78	62.41	64	79	46	6	10.5	90°	NO
20	0.048	71.1	78	62.41	64	79	53	6.5	11.5	90°	NO
21	0.16	150.3	77	64.35	68	77	53	6.5	11.5	90°	NO
22	0.05	73.0	77	64.35	68	77	53	6.5	11.5	90°	NO
23	0.05	73.0	77	64.35	68	77	46	6	10.5	90°	NO
24	0.08	99.0	77	64.35	68	77	38	4.25	7.5	90°	NO
25	0.123	128.7	77	64.35	68	77	27	2.5	4.5	90°	NO
26	0.16	150.3	77	64.35	68	77	16	1.5	2.5	90°	NO
27	0.16	150.3	79	60.53	58	82	16	1.5	2.5	180°	NO
28	0.12	126.8	79	60.53	58	82	27	2.5	4.5	180°	NO
29	0.08	99.0	79	60.53	58	82	38	4.25	7.5	180°	NO
30	0.05	73.0	79	60.53	58	82	46	6	10.5	180°	NO



Table A.2 Process Measurements

Run Number	Static Pressure (in wg)	Freestream Velocity (fpm)	Liquid Temp (F)	Viscosity	Relative Humidity %	Air Temp (F)	Gauge Pressure (psig)	Cap Pressure (psig)	Cap & Horn Pressure (psig)	Orientation	Motion
31	0.05	73.0	79	60.53	58	82	53	6.5	11.5	180°	NO
32	0.16	150.3	80	58.71	58	80	16	1.5	2.5	90°	NO
33	0.12	126.8	80	58.71	58	80	27	2.5	4.5	90°	NO
34	0.12	126.8	80	58.71	58	80	27	2.5	4.5	180°	NO
35	0.08	99.0	80	58.71	58	80	38	4.25	7.5	180°	NO
36	0.08	99.0	80	58.71	58	80	38	4.25	7.5	180°	NO

Table A.2 Process Measurements

Run Number	Static Pressure (in wg)	Freestream Velocity (fpm)	Liquid Temp (F)	Viscosity	Relative Humidity %	Air Temp (F)	Gauge Pressure (psig)	Cap Pressure (psig)	Cap & Horn Pressure (psig)	Orientation	Motion
101	0.16	150.3	75	68.41	47	75	16	1.5	2.5	180°	YES
102	0.12	126.8	75	68.41	47	75	27	2.5	4.5	180°	YES
103	0.08	99.0	75	68.41	47	75	38	4.25	7.5	180°	YES
104	0.05	73.0	75	68.41	47	75	46	6	10.5	180°	YES
105	0.05	73.0	75	68.41	47	75	53	6.5	11.5	180°	YES
106	0.08	99.0	75	68.41	47	75	38	4.25	7.5	90°	YES
107	0.12	126.8	75	68.41	47	75	27	2.5	4.5	90°	YES
108	0.16	150.3	75	68.41	47	75	16	1.5	2.5	90°	YES
109	0.1	113.6	76	66.35	51	76	53	6.5	11.5	90°	YES
110	0.08	99.0	76	66.35	51	76	38	4.25	7.5	90°	YES
111	0.12	126.8	76	66.35	51	76	27	2.5	4.5	90°	YES
112	0.16	150.3	76	66.35	51	76	16	1.5	2.5	90°	YES
113	0.1	113.6	77	64.35	56	77	53	6.5	11.5	180°	YES
114	0.1	113.6	77	64.35	56	77	53	6.5	11.5	180°	YES
115	0.08	99.0	77	64.35	56	77	38	4.25	7.5	180°	YES
116	0.12	126.8	77	64.35	56	77	27	2.5	4.5	180°	YES
117	0.16	150.3	77	64.35	56	77	16	1.5	2.5	180°	YES
118	0.16	150.3	77	64.35	56	77	16	1.5	2.5	180°	YES
119	0.12	126.8	77	64.35	56	77	27	2.5	4.5	180°	YES
120	0.08	99.0	77	64.35	56	77	38	4.25	7.5	180°	YES
121	0.1	113.6	75	68.41	70	75	53	6.5	11.5	180°	YES
122	0.1	113.6	75	68.41	70	75	53	6.5	11.5	180°	YES
123	0.12	126.8	75	68.41	70	75	27	2.5	4.5	180°	YES
124	0.16	150.3	75	68.41	70	75	16	1.5	2.5	90°	YES
125	0.12	126.8	75	68.41	70	75	27	2.5	4.5	90°	YES
126	0.08	99.0	75	68.41	70	75	38	4.25	7.5	90°	YES
127	0.1	113.6	75	68.41	70	75	53	6.5	11.5	90°	YES

Table A.3 Measured Flowrates and Calculated Transfer Efficiencies

Run Number	Run Time (s)	Bucket Weight (g)		Trough Weight (g)		Mass of Liquid Sprayed (g/min)	Mass of Liquid Transferred (g/min)	Mass of Liquid Overspray (m <sub>o</sub> ) (g/min)	Mass of Air (g/min)**	m <sub>a</sub> /m <sub>i</sub>	Transfer Efficiency	t <sub>2</sub> (sec)
		Before	After	Before	After							
1	611.78	3472.6	1984.9	240	1538.7	145.9	127.4	18.5	131	0.9	0.873	5.5E-6
2	610.58	3281.6	1796.4	241.3	1509.4	145.9	124.6	21.3	165	1.1	0.854	3.3E-6
3	302.64	3167.7	2543.8	241.7	741	123.7	99.0	24.7	216	1.8	0.800	1.9E-6
4	303.25	3316.5	2678.9	239.4	733	126.2	97.7	28.5	268	2.1	0.774	1.4E-6
5	304.41	3048.4	2376.8	235.7	750.3	132.4	101.4	30.9	285	2.2	0.766	1.3E-6
6	602.65	3428.5	2203.1	208.5	1277.2	122.0	106.4	15.6	131	1.1	0.872	5.8E-6
7	303.92	3223.9	2596.3	255.5	780.1	123.9	103.6	20.3	165	1.3	0.836	3.5E-6
8	303.12	3139.6	2510.1	235.3	737.9	124.6	99.5	25.1	216	1.7	0.798	2.1E-6
9	303	3411	2760.4	240.6	743.1	128.8	99.5	29.3	268	2.1	0.772	1.5E-6
10	303.89	3251.1	2571.2	251.7	761.8	134.2	100.7	33.5	285	2.1	0.750	1.3E-6
11	305.27	3399.9	2709.5	223	738	135.7	101.2	34.5	285	2.1	0.746	1.4E-6
12	301.4	3211.1	2650.4	236.1	655.3	111.6	83.5	28.2	268	2.4	0.748	1.5E-6
13	303.76	3062.8	2517.3	241.9	668.1	107.7	84.2	23.6	216	2.0	0.781	2.1E-6
14	303.85	3587.6	2976.3	241.6	748	120.7	100.0	20.7	165	1.4	0.828	3.6E-6
15	602.35	3484.3	2312.4	239.9	1260.8	116.7	101.7	15.0	131	1.1	0.871	6.0E-6
16	603.15	3304.6	2108.6	243.8	1289.2	119.0	104.0	15.0	131	1.1	0.874	6.0E-6
17	304.11	3615.7	3052.3	244.2	717.7	111.2	93.4	17.7	165	1.5	0.840	3.6E-6
18	184.03	3525.1	3189.9	244.2	508.2	109.3	86.1	23.2	216	2.0	0.788	2.1E-6
19	183.83	3448	3094.5	249.8	524.4	115.4	89.6	25.8	268	2.3	0.777	1.5E-6
20	183.5	3376.1	3020.9	242.2	502.2	116.1	85.0	31.1	285	2.5	0.732	1.4E-6
21	188.31	3296.6	2934.2	215.3	476.9	115.5	83.4	32.1	285	2.5	0.722	1.4E-6
22	187.5	3174.2	2810.7	236.6	507.9	116.3	86.8	29.5	285	2.5	0.746	1.4E-6
23	188.44	3349.2	3008	244.2	505.4	108.6	83.2	25.5	268	2.5	0.766	1.6E-6
24	182.87	3269	2944.8	244.2	501.7	106.4	84.5	21.9	216	2.0	0.794	2.2E-6
25	303.63	3204.2	2690.6	242	671.9	101.5	85.0	16.5	165	1.6	0.837	3.7E-6
26	603.45	3113.8	2145.3	247.7	1088.3	96.3	83.6	12.7	131	1.4	0.868	6.2E-6
27	602.9	3866.4	2788.5	225.1	1152.7	107.3	92.3	15.0	131	1.2	0.861	5.8E-6

\*\* Mass of air from cap only

Table A.3 Measured Flowrates and Calculated Transfer Efficiencies

Run Number	Run Time (s)	Bucket Weight (g)		Trough Weight (g)		Mass of Liquid Sprayed (g/min)	Mass of Liquid Transferred (g/min)	Mass of Liquid Overspray ( $m_o$ ) (g/min)	Mass of Air (g/min)**	$m_a/m_i$	Transfer Efficiency	$t_2$ (sec)
		Before	After	Before	After							
28	303.36	3697.6	3136.1	243.3	702.9	111.1	90.9	20.2	165	1.5	0.819	3.5E-6
29	182.34	3595.6	3241.7	242.2	517.5	116.5	90.6	25.9	216	1.9	0.778	2.1E-6
30	189.91	3511	3133.2	243	525.4	119.4	89.2	30.1	268	2.2	0.747	1.5E-6
31	193.04	3414	3009.2	244.5	542.4	125.8	92.6	33.2	285	2.3	0.736	1.3E-6
32	602.94	3698.3	2572.3	207.6	1170.6	112.1	95.8	16.2	131	1.2	0.855	5.7E-6
33	302.27	3497.1	2887.6	242.5	753.1	121.0	101.4	19.6	165	1.4	0.838	3.4E-6
34	182.31	3390.7	2985.9	249.3	589.5	133.2	112.0	21.3	165	1.2	0.840	3.4E-6
35	198.84	3330.2	2903	245.1	585.6	128.9	102.7	26.2	216	1.7	0.797	2.0E-6
36	182.1	3242.3	2823.4	246.1	585.2	138.0	111.7	26.3	216	1.6	0.810	2.0E-6

\*\* Mass of air from cap only

Table A.3 Measured Flowrates and Calculated Transfer Efficiencies

Run Number	Run Time (s)	Bucket Weight (g)		Trough Weight (g)		Mass of Liquid Sprayed (g/min)	Mass of Liquid Transferred (g/min)	Mass of Liquid Overspray (m <sub>o</sub> ) (g/min)	Mass of Air (g/min)**	m <sub>s</sub> /m <sub>i</sub>	Transfer Efficiency	$\tau_2$ (sec)
		Before	After	Before	After							
101	603.67	3626	2578	212.9	1097.2	104.2	87.9	16.3	131	1.3	0.844	6.6E-6
102	303	3924	3380.8	213.4	639.1	107.6	84.3	23.3	165	1.5	0.784	4.0E-6
103	182.64	3779.5	3447.7	240.6	485.9	109.0	80.6	28.4	216	2.0	0.739	2.3E-6
104	182.04	3693.4	3375.4	239.9	471.6	104.8	76.4	28.4	268	2.6	0.729	1.6E-6
105	183.81	3617.9	3305.9	227.2	431.9	101.8	66.8	35.0	285	2.8	0.656	1.5E-6
106	182.8	3423.5	3104.8	242.5	470.6	104.6	74.9	29.7	216	2.1	0.716	2.3E-6
107	302.73	3338.5	2819.7	236.8	658.7	102.8	83.6	19.2	165	1.6	0.813	4.0E-6
108	603.08	3240.2	2213.9	237.8	1121.7	102.1	87.9	14.2	131	1.3	0.861	6.6E-6
109	182.11	3528.5	3182.7	235.9	501.2	113.9	87.4	26.5	285	2.5	0.767	1.5E-6
110	222	3442.2	3036.1	241.2	555.8	109.8	85.0	24.7	216	2.0	0.775	2.3E-6
111	304.56	3354.6	2821.6	233.8	666.6	105.0	85.3	19.7	165	1.6	0.812	3.8E-6
112	602.04	3243	2265.8	242.1	1072.9	97.4	82.8	14.6	131	1.3	0.850	6.4E-6
113	181.5	3349.7	2999.6	211.1	451.1	115.7	79.3	36.4	285	2.5	0.686	1.4E-6
114	199.58	3651.8	3255.9	234.1	508.5	119.0	82.5	36.5	285	2.4	0.693	1.4E-6
115	182.3	3520	3160.8	243.9	510.3	118.2	87.7	30.5	216	1.8	0.742	2.2E-6
116	300.3	3433.9	2863.1	236.8	693.3	114.0	91.2	22.8	165	1.4	0.800	3.7E-6
117	604.4	3311.2	2302.9	244.9	1102.7	100.1	85.2	14.9	131	1.3	0.851	6.2E-6
118	618.75	3619.8	2586.1	242.2	1121.5	100.2	85.3	15.0	131	1.3	0.851	6.2E-6
119	303.31	3464.9	2927.1	242.3	666.8	106.4	84.0	22.4	165	1.6	0.789	3.7E-6
120	181.73	3350	3010.4	243.7	496.6	112.1	83.5	28.6	216	1.9	0.745	2.2E-6
121	182.84	3772.9	3432.1	211.1	445.1	111.8	76.8	35.0	285	2.5	0.687	1.5E-6
122	188.63	3639.9	3285.2	237.4	481.8	112.8	77.7	35.1	285	2.5	0.689	1.5E-6
123	304.29	3515.7	3002.7	233.1	635.9	101.2	79.4	21.7	165	1.6	0.785	4.0E-6
124	604.92	3399.3	2426.5	238.7	1069.9	96.5	82.4	14.0	131	1.4	0.854	6.6E-6
125	303.87	3551.4	3045.5	241.5	650.6	99.9	80.8	19.1	165	1.7	0.809	4.0E-6
126	183.85	3458.3	3138.9	237.3	485.3	104.2	80.9	23.3	216	2.1	0.776	2.3E-6
127	184.73	3392.8	3036.5	231.4	484.9	115.7	82.3	33.4	285	2.5	0.711	1.5E-6

\*\* Mass of air from cap only

Table A.4 Calculation of Dimensionless Concentration

Run Information  
 Mannequin Size: Height = 51 inches; Breadth = 14 inches  
 Gun Type: HVL P Devilbiss Spray Gun: MSV-533-4-FF  
 Gun Setting: Liquid Setting: 2 turns  
 Air Fan Pattern: 2 turns  
 Fluid Used: Inland #99 Vacuum Pump Oil  
 Experimenters: John McKernan and Betty Galano  
 Plate Size: Motion: 36" by 36"  
 No Motion: 24" by 36"  
 Distance to Plate: 8 inches

Position of Mannequin: 180°;  
 90°;

Run Number	Date	Mass of Liquid Overspray (mg)	Time (s)	Filter Weight (mg)		Sample Mass (mg)	Sampling flowrate (l/min)	Concentration (mg/m <sup>3</sup> )	Carton Number	CUHD/m <sub>0</sub>
				Before	After					
1	8/8/96	18.54	611.78	13.991	13.991	0.000	2.00	0.00	3.1E+5	0.0000
2	8/8/96	21.33	610.58	14.217	14.445	0.228	2.00	11.20	6.1E+5	0.0094
3	8/8/96	24.70	302.64	14.658	20.710	6.052	2.00	599.92	1.4E+6	0.3385
4	8/8/96	28.49	303.25	14.277	19.800	5.523	2.00	548.38	2.6E+6	0.1919
5	8/8/96	30.95	304.41	14.845	20.270	5.425	2.00	534.64	2.8E+6	0.1729
6	8/9/96	15.60	602.65	15.955	17.421	1.466	2.00	72.98	2.9E+5	0.0990
7	8/9/96	20.33	303.92	15.750	16.334	0.584	2.00	57.85	5.7E+5	0.0506
8	8/9/96	25.12	303.12	15.254	16.166	0.912	2.00	90.26	1.3E+6	0.0501
9	8/9/96	29.33	303	15.340	16.442	1.102	2.00	109.11	2.5E+6	0.0372
10	8/9/96	33.53	303.89	15.556	16.715	1.159	2.00	114.42	2.7E+6	0.0342
BLANK	8/9/96									
11	8/10/96	34.47	305.27	15.591	16.058	0.467	2.00	45.89	2.4E+6	0.0146
12	8/10/96	28.17	301.4	15.437	15.935	0.498	2.00	49.57	2.4E+6	0.0176
13	8/10/96	23.56	303.76	15.275	15.566	0.291	2.00	28.74	1.2E+6	0.0170
14	8/10/96	20.71	303.85	15.585	16.115	0.530	2.00	52.33	5.6E+5	0.0451
15	8/10/96	15.04	602.35	15.238	15.883	0.645	2.00	32.12	2.8E+5	0.0452
BLANK	8/10/96									
16	8/10/96	14.98	603.15	15.269	15.278	0.009	2.00	0.45	2.8E+5	0.0006
17	8/10/96	17.74	304.11	14.900	14.962	0.062	2.00	6.12	5.6E+5	0.0062
18	8/10/96	23.21	184.03	14.655	17.732	3.077	2.00	501.60	1.2E+6	0.3012
19	8/10/96	25.75	183.83	14.731	17.717	2.986	2.00	487.30	2.4E+6	0.1894
20	8/10/96	31.13	183.5	14.465	17.514	3.049	2.00	498.47	2.6E+6	0.1603
BLANK	8/10/96									
21	8/14/96	32.12	188.31	14.154	16.896	2.742	2.00	436.83	1.2E+6	0.2879
22	8/14/96	29.50	187.5	14.270	17.374	3.104	2.00	496.64	2.4E+6	0.1731
23	8/14/96	25.47	188.44	14.565	17.656	3.091	2.00	492.09	2.3E+6	0.1987
24	8/14/96	21.88	182.87	13.169	16.105	2.936	2.00	481.65	1.2E+6	0.3068
25	8/14/96	18.54	303.63	13.132	13.051	-0.081	2.00	-8.00	5.3E+5	-0.0088
26	8/14/96	12.72	603.45	14.650	14.583	-0.067	2.00	-3.33	2.7E+5	-0.0055

Table A.4 Calculation of Dimensionless Concentration

## Run Information

Mannequin Size: Height = 51 Inches; Breadth = 14 Inches  
 Gun Type: HVLP Devilbiss Spray Gun: MSV-533-4-FF  
 Gun Setting: Liquid Setting: 2 turns  
 Air Fan Pattern: 2 turns  
 Fluid Used: Inland #99 Vacuum Pump Oil  
 Experimenters: John McKernan and Betty Galano  
 Plate Size: Motion: 36" by 36"  
 No Motion: 24" by 36"  
 Distance to Plate: 8 inches

Position of Mannequin: 180°:  
 90°:

Run Number	Date	Mass of Liquid Overspray (m <sub>a</sub> ) (g/min)	Time (s)	Filter Weight (mg)		Sample Mass (mg)	Sampling flowrate (l/min)	Concentration (mg/m <sup>3</sup> )	Carlton Number	CUHD/m <sub>a</sub>
				Before	After					
27	8/16/96	14.96	602.9	14.159	15.039	0.880	2.00	43.79	2.9E+5	0.0620
28	8/16/96	20.15	303.36	13.607	13.788	0.181	2.00	17.90	5.7E+5	0.0159
29	8/16/96	25.86	182.34	13.067	13.261	0.194	2.00	31.92	1.3E+6	0.0172
30	8/16/96	30.14	189.91	12.953	13.099	0.146	2.00	23.06	2.4E+6	0.0079
31	8/16/96	33.23	193.04	13.105	13.426	0.321	2.00	49.89	2.6E+6	0.0154
BLANK	8/16/96									
32	8/20/96	16.22	602.94	17.343	17.350	0.007	2.00	0.35	3.0E+5	0.0005
33	8/20/96	19.63	302.27	16.777	16.882	0.105	2.00	10.42	5.9E+5	0.0095
34	8/20/96	21.26	182.31	16.798	16.966	0.168	2.00	27.65	5.9E+5	0.0232
35	8/20/96	26.16	198.84	16.506	16.922	0.416	2.00	62.76	1.3E+6	0.0334
36	8/20/96	26.29	182.1	16.355	16.843	0.488	2.00	80.40	1.3E+6	0.0426
BLANK	8/20/96			16.140	16.176	0.036				

### Table A.4 Calculation of Dimensionless Concentration

### Run Information

**Mannequin Size: Height = 51 inches; Breadth = 14 inches**

Gun Type: HVL P Devilb's Spray Gun: MSV-533-4-FF

Gun Setting: Liquid Setting: 2 turns

**Air Fan Pattern: 2 turns**

**Fluid Used:** Inland #99 Vacuum Pump Oil

**Experimenters:** John McKernan and Betty Gatano

**Plate Size:** Motion: 36" by 36"

**No Motion: 24" by 36"**

Distance to Plate: 8 inches

Position of Mannequin: 180°: 90°:

[illegible]



Table A.4 Calculation of Dimensionless Concentration

## Run Information

Mannequin Size: Height = 51 inches; Breadth = 14 inches

Gun Type: HVL P Devilbis Spray Gun: MSV-533-4-FF

Gun Setting: Liquid Setting: 2 turns

Air Fan Pattern: 2 turns

Fluid Used: Inland #99 Vacuum Pump Oil

Experimenters: John McKernan and Betty Gatano

Plate Size: Motion: 36" by 36"

No Motion: 24" by 36"

Distance to Plate: 8 inches

Position of Mannequin: 180°:  
90°:

Run Number	Date	Mass of Liquid Overspray (m <sub>o</sub> ) (g/min)	Time (s)	Filter Weight (mg)		Sample Mass (mg)	Sampling flowrate (l/min)	Concentration (mg/m <sup>3</sup> )	Carton Number	CUHD/m <sub>o</sub>
				Before	After					
124	10/2/96	14.04	604.92	15.018	15.039	0.021	2.00	1.04	2.6E+5	0.0016
125	10/2/96	19.11	303.87	14.789	15.335	0.546	2.00	53.90	5.1E+5	0.0504
126	10/2/96	23.30	183.85	14.047	15.392	1.345	2.00	219.47	1.1E+6	0.1313
127	10/2/96	33.39	~ 184.73	14.103	15.876	1.773	2.00	287.93	1.5E+6	0.1380

Figure A.1 Air Flow Volume As Function of Square Root of Pressure Drop Across Orifice

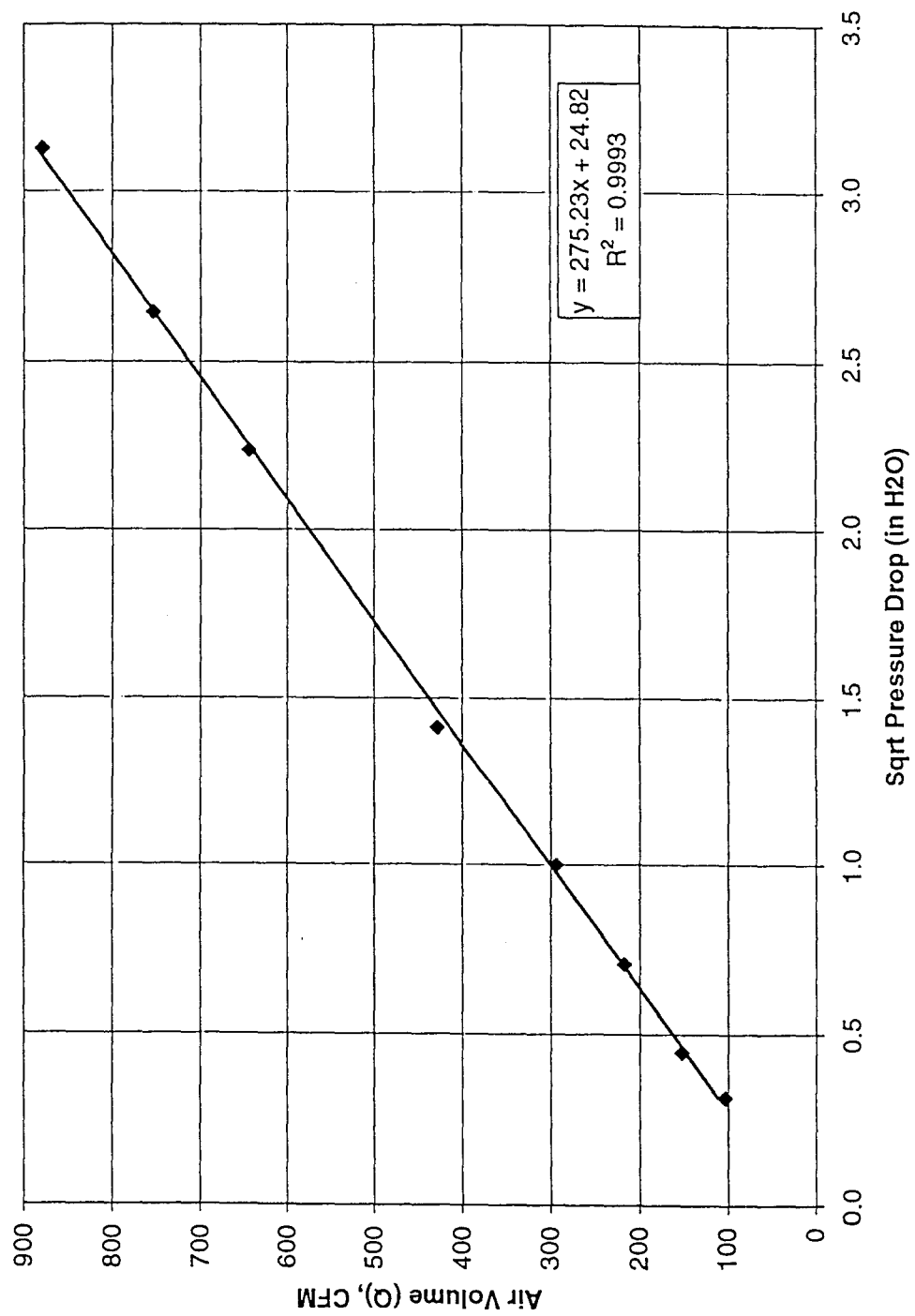


Figure A.2 Calibration of Hot-Wire Anemometer

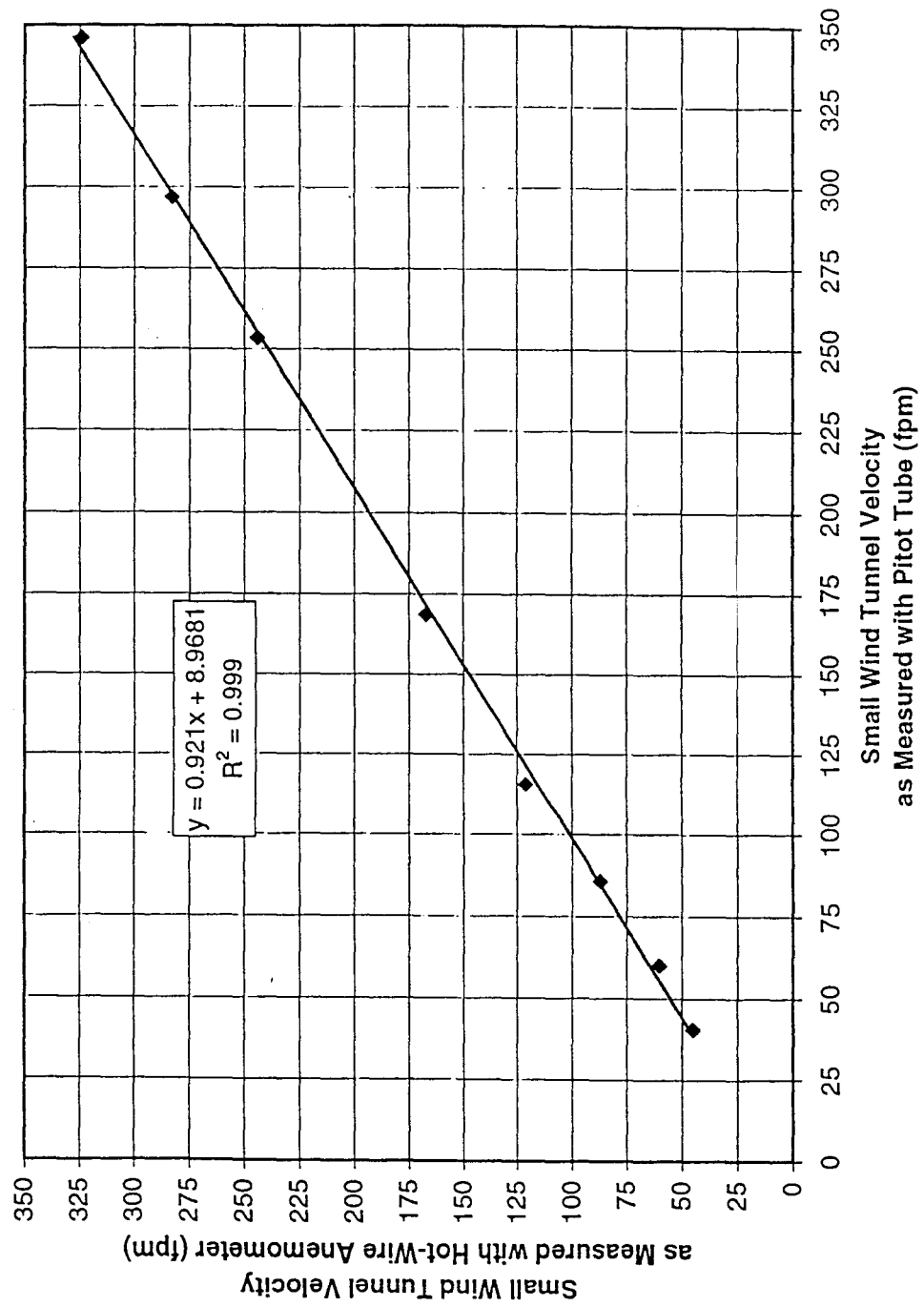


Figure A.3 Calibration of Wind Tunnel Using Hot Wire Anemometer

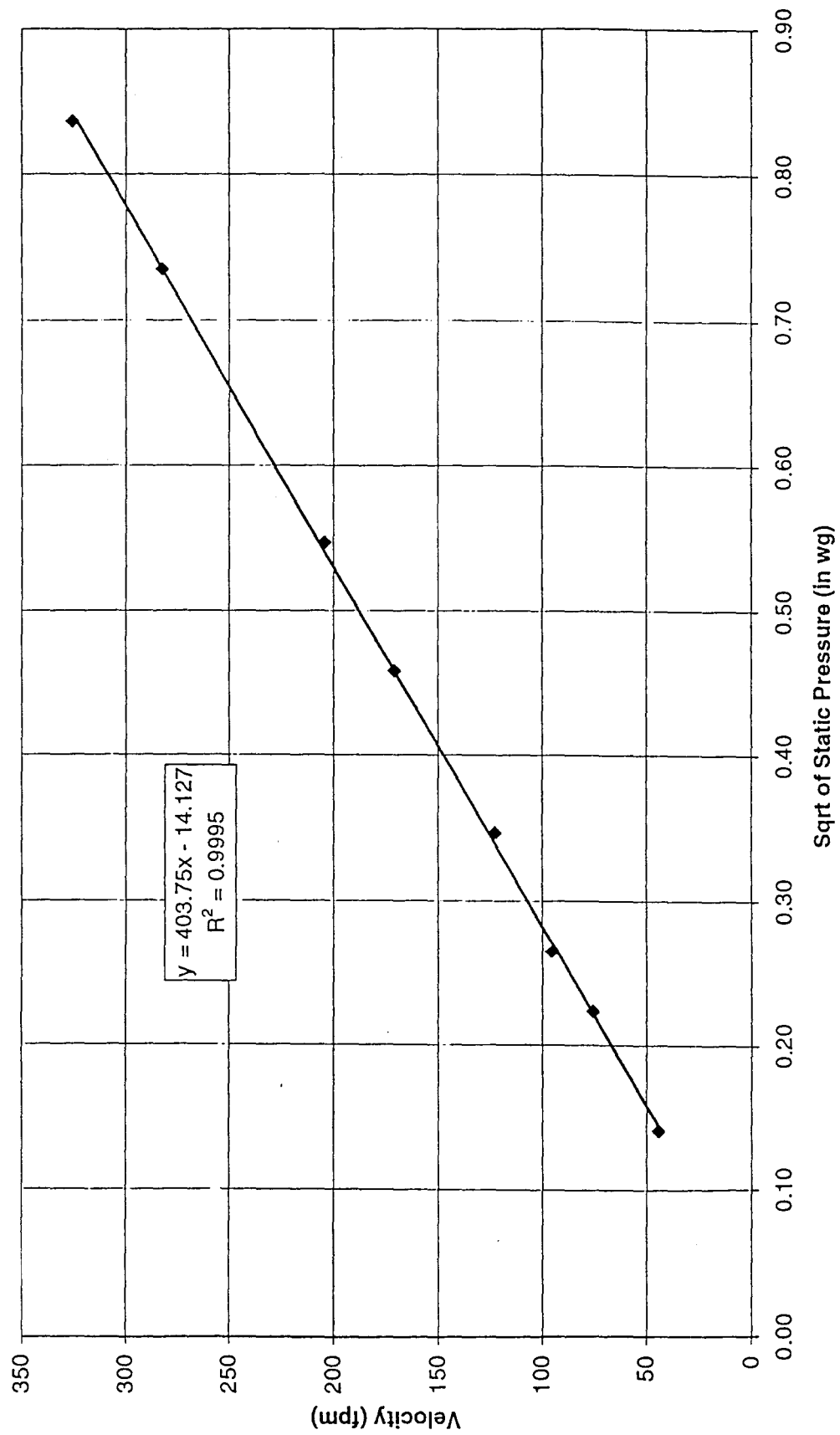


Figure A.4 Air Volumetric Flowrate from the HVLP Gun as a Function of Fan Pattern and Nozzle Pressure

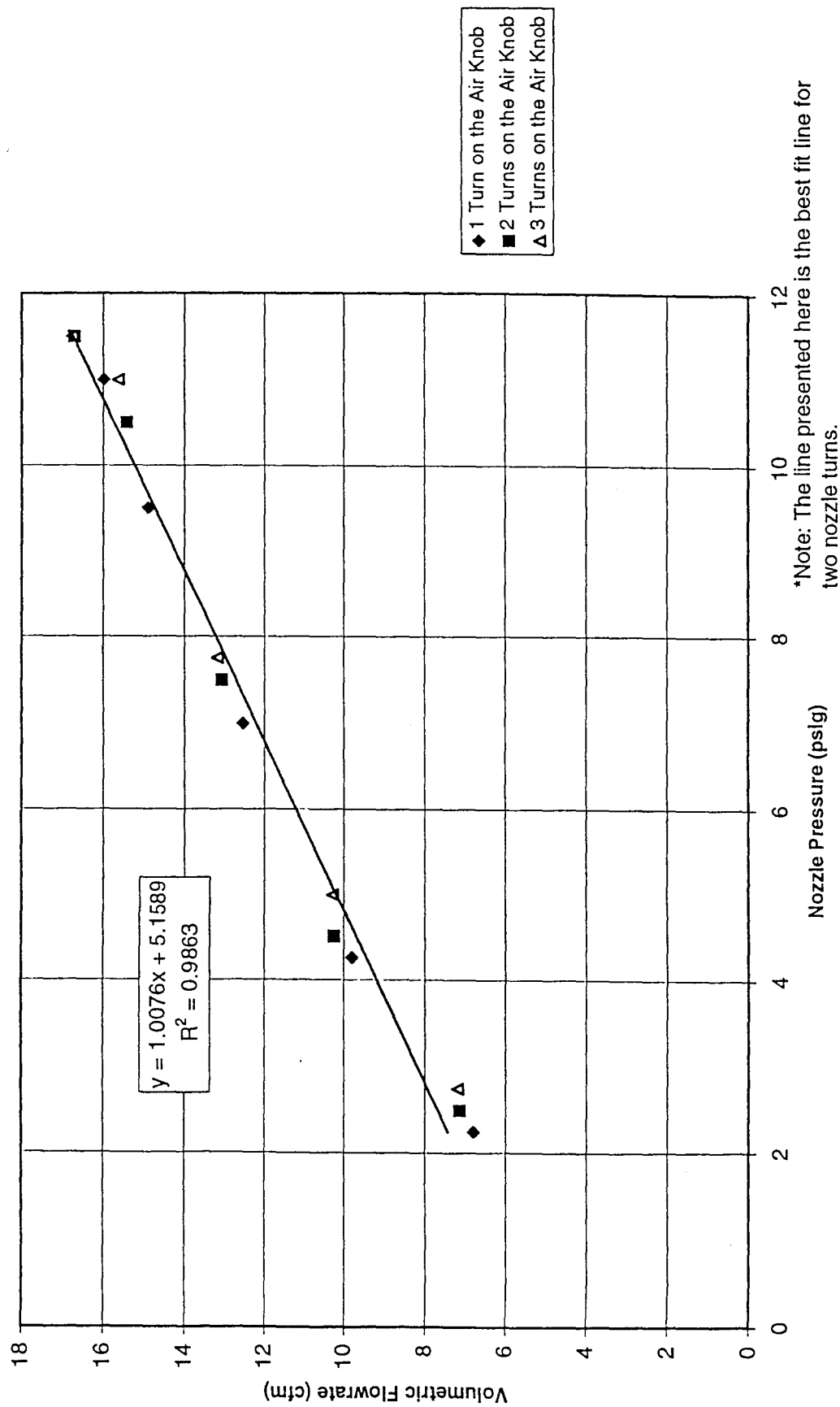


Figure A.5 Viscosity of Vacuum Pump Oil as a Function of Temperature

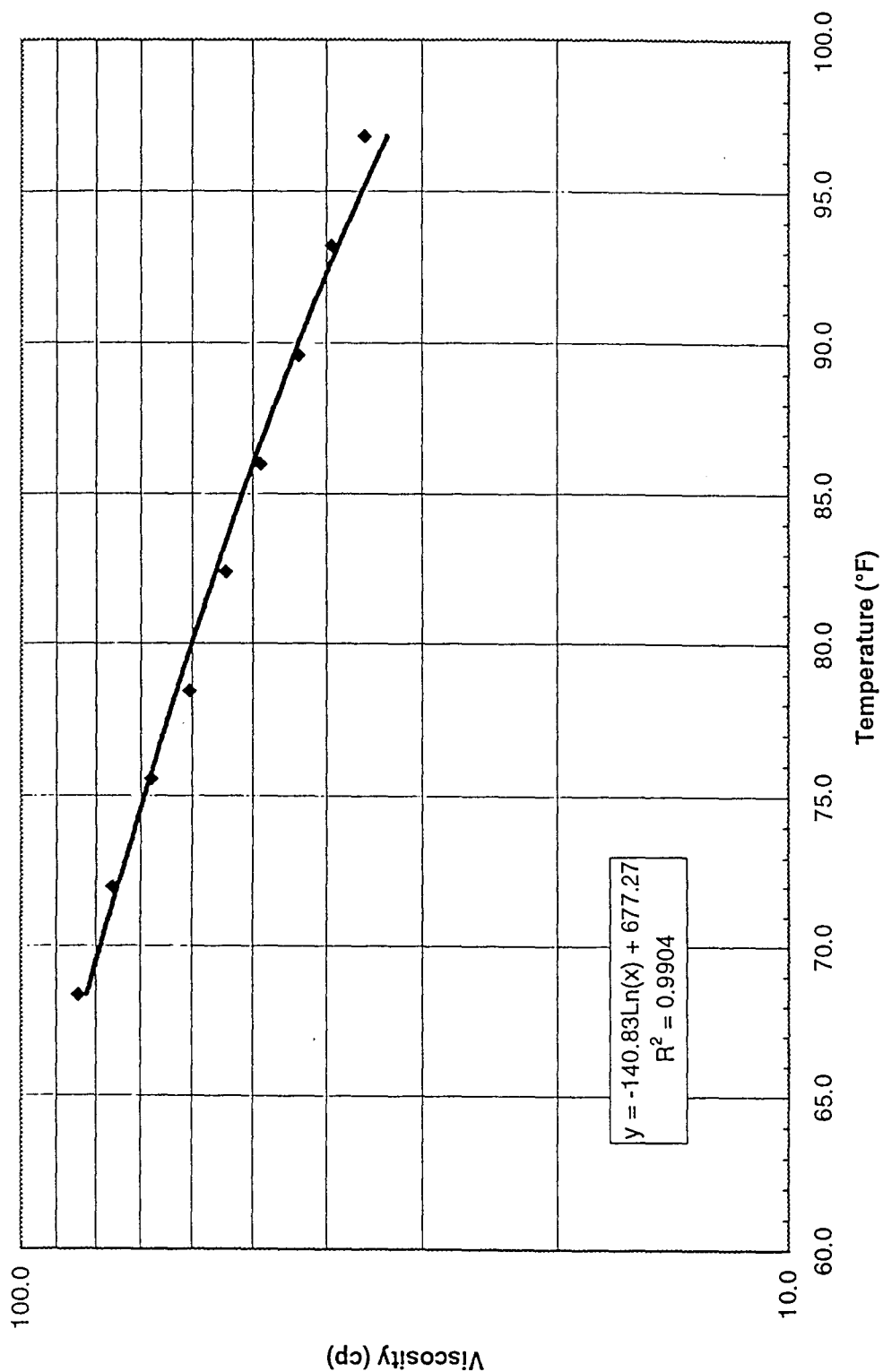
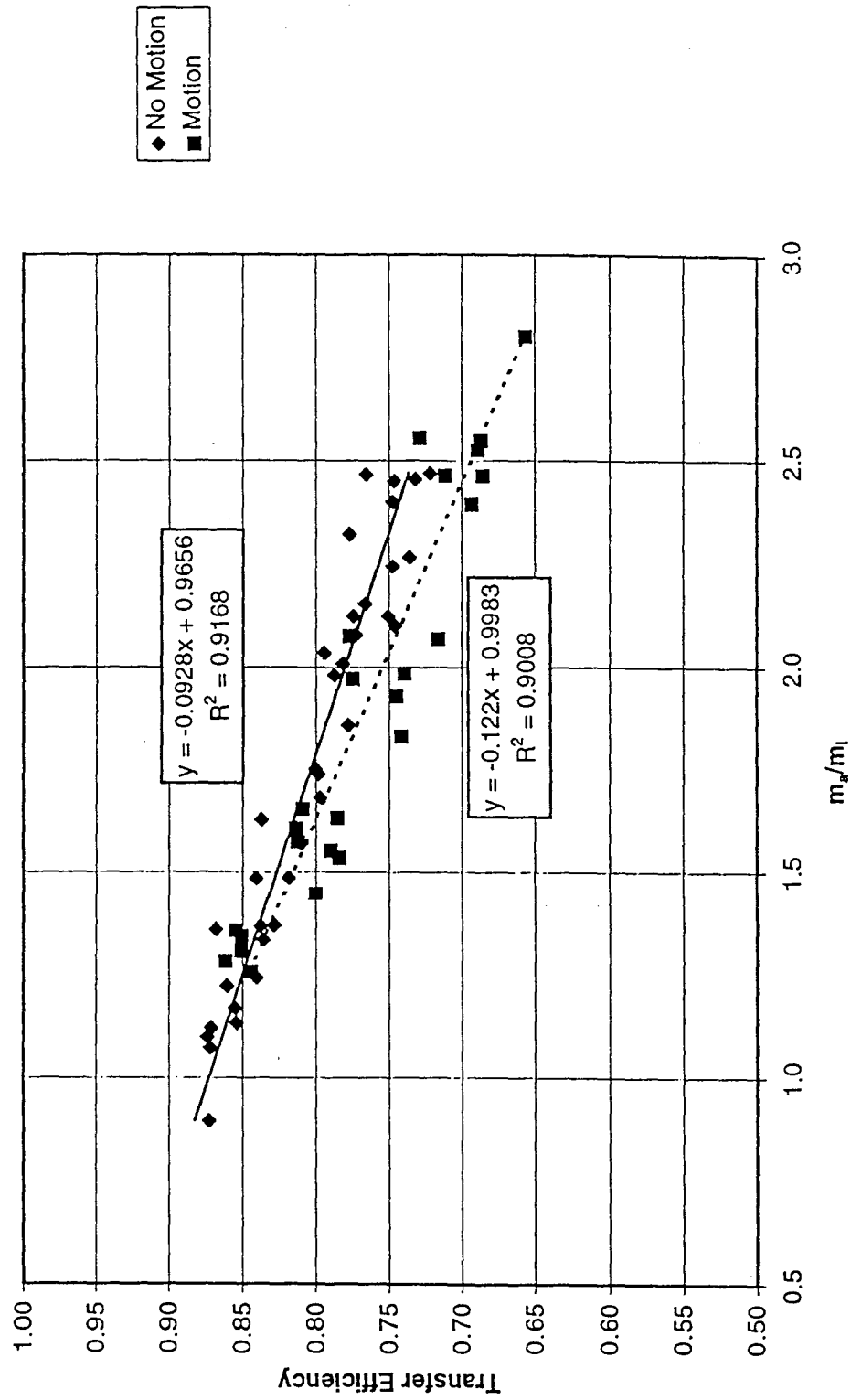


Figure A.6 Transfer Efficiency as a Function of  $m_a/m_i$ 

## **8.0 Appendix B:**

### **Additional Materials**



## Appendix B: Additional Materials

### B.1. Calculating Task-Representative Carlton Numbers

Before analyzing the data for the experiments, it was considered important to determine the range of dimensionless pressure terms which would most likely correspond to real applications in the field. This was considered because the ultimate purpose of the current model is its use in predicting personal breathing zone concentrations (exposures) in the field. Breathing zone concentrations can be predicted for particular spraying tasks using the current model, when only the Carlton number is known. Therefore, Table B.1 was created to determine the high and low range of Carlton numbers ( $p_a H / \mu U$ ) which could be expected in normal HVLP applications.

Table B.1. Calculation of Task Representative Carlton Numbers:

U	$p_a$	H	$\mu$	Unit $p_a H / \mu U$ Upper	Unit $p_a H / \mu U$ Lower
75	4	5	40	0.021667	0.002667
90	6	5.5	45	0.011852	0.006286
105	8	6	50		
125	10	6.5	60		

Multiplier for calculating dimensionless pressure term =  $4.18E+8$

Dimensionless $p_a H / \mu U$ Upper	Dimensionless $p_a H / \mu U$ Lower
$9.0 \times 10^6$	$1.1 \times 10^6$
$4.9 \times 10^6$	$2.6 \times 10^5$

It can be seen in the table for common HVLP use, the Carlton numbers vary from  $1.1 \times 10^6$  at the lowest values and  $9.0 \times 10^6$  at the highest values. The lowest value from this table is referred to as the task representative Carlton number. The dimensionless concentration above the task representative Carlton number in each of the orientation equations are set as constants to aid in the estimation of exposure.

## B.2. Overspray Generation Rate

The overspray generation rate,  $m_o$ , is a measure of the total mass of overspray entrained in the freestream available for exposure in a given time. The  $m_o$  term was calculated using the measured transfer efficiency ( $t_e$ ) at the nozzle pressure used, the mass of the liquid sprayed, and the time over which spraying occurred ( $t_s$ ) in the formula below:

$$m_o = (1 - t_e) \times \left( \frac{\text{mass of liquid sprayed}}{t_s} \right)$$

The mass of the liquid sprayed from the gun minus the mass of the liquid transferred to the workpiece, in g/min, also gives the overspray generation rate. The transfer efficiency ( $t_e$ ) is equal to the amount of the liquid transferred to the workpiece divided by the amount of the liquid sprayed from the gun ( $m_l$ ). This term is dimensionless and can be used as another possible predictor of exposure, in place of the dimensionless

breathing zone concentration term. This was the focus of Gatanos' work done jointly in this study.

### **B.3. Dimensionless Nozzle Pressure Term**

The dimensionless nozzle pressure term, or Carlton number, was found by multiplying the measured nozzle pressure ( $p_n$ ) of the gun at the cap in psig, by the height ( $H$ ) of the mannequin in ft, and dividing this by the product of the freestream velocity ( $U$ ) measured in the tunnel in fpm, multiplied by the viscosity of the oil ( $\mu_1$ ) in cp.

$$\frac{p_n H}{\mu_1 U} = \frac{\text{droplet transport}}{\text{droplet transfer}}$$

And also, as you can see, the Carlton number incorporates the relative contributions of the droplet transfer and transport processes in producing an exposure. This is what makes the dimensionless nozzle pressure so important to this model for spray painting. Once values for the Carlton number were obtained, a unit conversion factor of  $4.1759 \times 10^8$  (cp · fpm/psig · ft) was applied. After some manipulation it can be seen that the units cancel.

## B.4. Calculating Concentrations

### *B.4.1. Average Breathing Zone Concentration*

Concentration is determined by considering that the worker's average breathing zone concentration (C) is a function of the variables identified in the conceptual model. Representing the dependence as an equation:

$$C = \phi \left( m_o, p_n, \mu_1, \frac{m_a}{m_1}, U, H, D, \text{orientation} \right)$$

Numerical calculation of the average breathing zone concentration was more straightforward. Total contaminant concentration for each run was calculated using the filter weight change after sampling in mg ( $m_s$ ), and dividing by the product of the volume sampled through the filter in liters per minute ( $v_s$ ), and the run time for the sample in seconds ( $t_s$ ):

$$C = \frac{m_s}{v_s t_s}$$

Once this value was obtained, it was transformed to the units  $\text{mg}/\text{m}^3$  by the use of a conversion factor of  $6.0 \times 10^4 \text{ (L/min} \cdot \text{s)}/\text{m}^3$ .

#### ***B.4.2. Dimensionless Breathing Zone Concentration***

The dimensionless breathing zone concentration was defined by the Carlton model. Dimensional analysis done by Carlton provides the following dimensionless representation of the model:

$$\frac{CUHD}{m_o} = \Phi \left( \frac{m_a}{m_l}, \frac{p_n H}{\mu_l U}, \text{orientation} \right)$$

The model indicates the concentration group  $CUHD/m_o$  depends on worker orientation to the freestream and two other nondimensional groups; the air-to-liquid mass flow ratio  $m_a/m_l$  and the dimensionless pressure group  $p_n H/\mu_l U$ . The model strongly suggests that  $CUHD/m_o$  is a function of the quantity  $p_n H/\mu_l U$  and worker orientation. This makes the comparison of the two nondimensional groups of pressure and concentration more significant. To make the values dimensionless, it is necessary in calculating the data to use a factor to relate volume units. For the data,  $3.048 \times 10^{-7} \text{ ft}^3/\text{m}^3$  was used.

### B.5. Statistical Analysis

Statistical analysis was performed on the data obtained in this experiment for two reasons:

- To express the relationships between dimensionless breathing zone concentrations and dimensionless pressure terms.
- To determine the statistical significance of the data.

The first set to be analyzed was the no motion 90 and 180 degree position data. This data, with standard deviations about the mean, is displayed in Figure 3. First looking at the 90° position data, linear regression with a best fit equation was determined:

$$\frac{CHUD}{m_o} = 3 \times 10^{-7} \left( \frac{p_n H}{\mu_1 U} \right) - 0.1336 \quad r^2 = .93$$

The formula was applied to data below the constant concentration achieved at Carlton numbers  $> 1.3 \times 10^6$ . The constant concentration for Carlton numbers  $> 1.3 \times 10^6$  was = 0.232.

The following set to be analyzed was the no motion 180° position data. This data, with standard deviations about the mean, is also displayed in Figure 3.

Regression analysis with a best fit equation was determined for the 180° position. The equation used in past research by Carlton gave a better fit than the new data analysis could provide. Therefore, the formula for the best fit line was:

$$\frac{CHUD}{m_o} = 3.23 \times 10^{-2} \exp\left(-1.94 \times 10^{-7} \frac{p_n H}{\mu_1 U}\right) \quad r^2 = .95$$

This formula gives a best fit throughout the range of data. Despite this goodness of fit, values greater than the task representative Carlton number were once again expressed as a constant concentration. For Carlton numbers  $> 1.1 \times 10^6$ , the constant concentration was given as 0.0281.

The motion data was last to be considered. Both orientations with motion produced very similar results. One statistical tests were performed on the data for both orientations to determine significance. An analysis of covariance was used to test if the position of the worker effected dimensionless breathing zone concentration in the range representative of a spray painting task. The ANCOVA analysis was done using the SAS program and is included in Table B.2. Analysis provided support to the hypothesis that the 90° and 180° orientation data were not significantly different in the motion experiment. Since there was no positional effect, no formulae were used to explain the relation between dimensionless concentration and dimensionless pressure terms for the individual orientations. Instead, an average of all the data points in the task representative Carlton number range (Carlton numbers  $> 1.1 \times 10^6$ ) was taken.

This produced an average dimensionless breathing zone concentration for motion in either position of 0.102. The motion data, with standard deviations about the mean, is displayed in Figure 5.

## **B.6. Sources of Error**

### ***B.6.1. Gravimetric Analysis:***

The gravimetric analysis using the Cahn 27 automatic electrobalance had a  $\pm 0.005\%$  error associated with it due to the accuracy of the electrical range of the scale. The scale precision allows measurement of changes in weight of  $0.1 \mu\text{g}$  in a sample.

### ***B.6.2. Breathing Zone Concentration (C or BZC):***

The NIOSH 0500 method (particulates not otherwise regulated, total) was used to determine airborne particulate concentration in this experiment. The accuracy of the method was given as  $\pm 11.04\%$  over a  $20 \text{ mg/m}^3$  range. Overall precision of the analysis was limited to  $56 \mu\text{g/m}^3$ . A bias of  $0.01\%$  was also associated with the use of the method.

### ***B.6.3. Measuring Distances, Height and Width (H, D):***

Accuracy of measure with retractable measuring tapes and rulers were to  $1/16$  of one inch ( $0.15875 \text{ cm}$ ).



#### ***B.6.4. Flow Rate ( $U$ ):***

The Alnor thermoanemometer was accurate at measuring air velocities within  $\pm 3\%$  in the range of operation for these experiments. The equipment was limited to an accuracy of  $\pm 2$  fpm in optimal circumstances. The resolution of the equipment was within 1 fpm from the value displayed.

#### ***B.6.5. Gun Pressure ( $p_n$ ):***

Pressure readings for the gun cap pressures were within 1 psig of the actual value. This reading error is associated with the resolution of the gauge.

#### ***B.6.6. Overspray Generation Rate ( $m_0$ ):***

Error for mass measurement of  $m_0$  associated with the use of a Mettler PM34-K was associated with the resolution of the scale (readability) which is 1g / 0.1g. Weighing range of the scale is 0 to 32,000g, and repeatability of the scale is  $\leq 0.3$ g per 0.1g. Linearity for this scale is given as less than or equal to  $\pm 0.5$ g per  $\pm 0.2$ g. Time was also a source of error for this calculation. Time measurements, because of human error, were assumed to be within  $\pm 1.6\%$ .

#### ***B.6.7. Viscosity ( $\mu$ ):***

The falling ball viscometer had a 'tolerance range' for error. This tolerance range involved only human time measurement error which is  $\pm 1.6\%$  throughout the experiment.

#### ***B.6.8. Mass of Air ( $m_a$ ):***

Pressure readings for the gun cap pressures were within 1 psig of the actual value. This reading error is associated with the resolution of the gauge. Density of the air was calculated using the barometric pressure on the day these calibrations were performed.

#### ***B.6.9. Mass of Liquid ( $m_l$ ):***

Error for mass measurement of  $m_l$  associated with the use of a Mettler PM34-K was associated with the resolution of the scale (readability) which is 1g / 0.1g. Weighing range of the scale is 0 to 32,000g, and repeatability of the scale is  $\leq 0.3$ g per 0.1g. Linearity for this scale is given as less than or equal to  $\pm 0.5$ g per  $\pm 0.2$ g. For a more detailed error analysis, see Carlton <sup>(1)</sup>.

### **B.7. Sample Calculations (Run Number 1)**

#### ***B.7.1. Freestream Velocity ( $U$ )***

$$\begin{aligned}\text{Hot Wire Anemometer (fpm)} &= 403.75 \sqrt{SP} - 14.127 \\ &= 403.75 \sqrt{0.05} - 14.127 \\ &= 76.154 \text{ fpm}\end{aligned}$$

$$\begin{aligned}\text{Freestream Velocity (fpm)} &= 1.0848 (\text{Hot Wire Anemometer}) - 9.5625 \\ &= 1.0848 (76.154) - 9.5625 \\ &= 73.05 \text{ fpm}\end{aligned}$$

**B. 7.2. Viscosity ( $\mu$ )**

$$\begin{aligned}
 \text{Viscosity (cp)} &= 678.95 \exp (-0.0306 * T(^{\circ}\text{F})) \\
 &= 678.95 \exp (-0.0306 * 81) \\
 &= 68.412 \text{ cp}
 \end{aligned}$$

**B. 7.3. Liquid Mass Sprayed ( $m_l$ )**

$$\begin{aligned}
 m_l (\text{g/min}) &= \frac{\text{Container Mass (Grams Before)} - \text{Container Mass (Grams After)}}{\text{Run Time (Seconds)} \cdot \frac{\text{Minutes}}{60 \text{ Seconds}}} \\
 &= \frac{3400.9 - 2986.8}{183.97 \cdot \frac{1}{60}} \\
 &= 135 \text{ g/min}
 \end{aligned}$$

**B. 7.4. Liquid Mass Transferred**

$$\begin{aligned}
 \text{Mass Transferred (g/min)} &= \\
 &= \frac{\text{Trough Mass (Grams Before)} - \text{Trough Mass (Grams After)}}{\text{Run Time (Seconds)} \cdot \frac{\text{Minutes}}{60 \text{ Seconds}}} \\
 &= \frac{551.9 - 223.8}{183.97 \cdot \frac{1}{60}} \\
 &= 107 \text{ g/min}
 \end{aligned}$$

**B. 7.5. Mass of Liquid Overspray**

$$\begin{aligned}
 \text{Mass of Liquid Overspray (g/min)} &= m_l (\text{g/min}) - \text{Liquid Mass Transferred (g/min)} \\
 &= 135.1 - 107 \\
 &= 28.1 \text{ g/min}
 \end{aligned}$$

***B. 7.6. Mass of Air ( $m_a$ )***

$$\text{Volumetric Flow Rate (ft}^3/\text{min)} = 1.0076 (p_n \text{ (psig)} - \text{Cap Pressure (psig)}) + 5.1589$$

$$\text{g/min} = \text{ft}^3/\text{min} \times (0.075 \text{ lb/ft}^3) \times (4.3359 \times 10^2 \text{ g/lb})$$

$$= 34 (\text{Volumetric Flow Rate}) (0.5)$$

$$= 34 (16.75) (0.5)$$

$$= 284.7 \text{ g/min}$$

***B.7.7. Dimensionless Pressure Term (Carlton number)***

$$\begin{aligned}
 \text{Carlton number} &= \frac{4.14 \times 10^8 \cdot (p_n (\text{psig}) - \text{Cap Pressure (psig)}) \cdot H (\text{ft})}{\mu_1 (\text{cp}) \cdot U (\text{fpm})} \\
 &= \frac{4.14 \times 10^8 \cdot (6.5) \cdot (4.25)}{(68.41) \cdot (73)} \\
 &= 2.29 \times 10^6
 \end{aligned}$$

***B.7.8.8 Concentration (C)***

$$\begin{aligned}
 C (\text{mg/m}^3) &= 60000 \frac{\text{Sample Filter Mass (mg)}}{\text{Sampling Rate (l / min)} \cdot (\text{Sampling Time (s)})} \\
 &= 60000 \frac{0.146}{2 \cdot (189.91)} \\
 &= 23.06 \text{ mg/m}^3
 \end{aligned}$$

***B.7.8.9. Dimensionless Concentration***

$$\begin{aligned}
 \frac{\text{CUHD}}{m_o} &= 2.8317 \times 10^{-5} \frac{C (\text{mg / m}^3) \cdot H (\text{ft}) \cdot U (\text{fpm}) \cdot D (\text{ft})}{m_o (\text{g / min})} \\
 &= 2.8317 \times 10^{-5} \left( \frac{4.25 \cdot 1.17 \cdot 73 \cdot 217.86}{28} \right) \\
 &= 0.07998
 \end{aligned}$$

***B.7.8.10. Mass of Air to Mass of Liquid Ratio ( $m_a/m_l$ )***

$$\begin{aligned} m_a/m_l &= \frac{284.7}{135.1} \\ &= 2.1 \end{aligned}$$

***B.7.8.11. Sample Filter Mass***

$$\text{Filter Mass (mg)} = \text{Filter After (mg)} - \text{Filter Before (mg)}$$

$$= 14.741 - 13.405$$

$$= 1.336 \text{ mg}$$

Table B.2: ANCOVA analysis of the motion data

## Class Level Information

Class	Levels	Values
ORIENT	2	90 180

Number of observations in data set = 14

General Linear Models Procedure

Dependent Variable: CON

Source	DF	Sum of Squares	Mean Square	F Value	Pr > F
Model	2	0.00561686	0.00280843	1.29	0.3137
Error	11	0.02393719	0.00217611		
Corrected Total	13	0.02955406			

R-Square	C.V.	Root MSE	CON Mean
0.190054	45.81752	0.04664878	0.10181429

Source	DF	Type I SS	Mean Square	F Value	Pr > F
ORIENT	1	0.00384209	0.00384209	1.77	0.2108
CNUM	1	0.00177478	0.00177478	0.82	0.3858

Source	DF	Type III SS	Mean Square	F Value	Pr > F
ORIENT	1	0.00528479	0.00528479	2.43	0.1474
CNUM	1	0.00177478	0.00177478	0.82	0.3858

Parameter	Estimate	T for H0: Parameter=0	Pr >  T	Std Error of Estimate
INTERCEPT	0.0282812759 B	0.41	0.6919	0.06951256
ORIENT 90	0.0431861897 B	1.56	0.1474	0.02771223
180	0.0000000000 B			
CNUM	0.0000000384	0.90	0.3858	0.00000004

NOTE: The X'X matrix has been found to be singular and a generalized inverse was used to solve the normal equations. Estimates followed by the letter 'B' are biased, and are not unique estimators of the parameters.

Least Squares Means				
ORIENT	CON	Std Err	Pr >  T	Pr >  T  H0:
	LSMEAN	LSMEAN	H0:LSMEAN=0	LSMEAN1=LSMEAN2
90	0.12957684	0.02174421	0.0001	0.1474
180	0.08639065	0.01591827	0.0002	

OBS	_NAME_	ORIENT	LSMEAN	STDERR	NUMBER	COV1	COV2
1	CON	90	0.12958	0.021744	1	0.00047281	-0.0002088
2	CON	180	0.08639	0.015918	2	-0.0002088	0.00025339

## General Linear Models Procedure

## Class Level Information

Class Levels Values  
 ORIENT 2 90 180

Number of observations in data set = 14

## General Linear Models Procedure

Dependent Variable: CON

Source	DF	Sum of Squares	Mean Square	F Value	Pr > F
Model	1	0.00384209	0.00384209	1.79	0.2054
Error	12	0.02571197	0.00214266		
Corrected Total	13	0.02955406			
R-Square	C.V.	Root MSE	CON Mean		
0.130002	45.46407	0.04628892	0.10181429		

Source	DF	Type I SS	Mean Square	F Value	Pr > F
ORIENT	1	0.00384209	0.00384209	1.79	0.2054
IND1	0	0.00000000			

Source	DF	Type III SS	Mean Square	F Value	Pr > F
ORIENT	0	0			
IND1	0	0			

Parameter	Estimate	T for H0: Parameter=0	Pr >  T	Std Error of Estimate	
INTERCEPT	0.0894666667 B	5.80	0.0001	0.01542964	
ORIENT 90	0.0345733333 B	1.34	0.2054	0.02581873	
180	0.0000000000 B				
IND1	0.0000000000 B				

NOTE: The X'X matrix has been found to be singular and a generalized inverse was used to solve the normal equations. Estimates followed by the letter 'B' are biased, and are not unique estimators of the parameters.



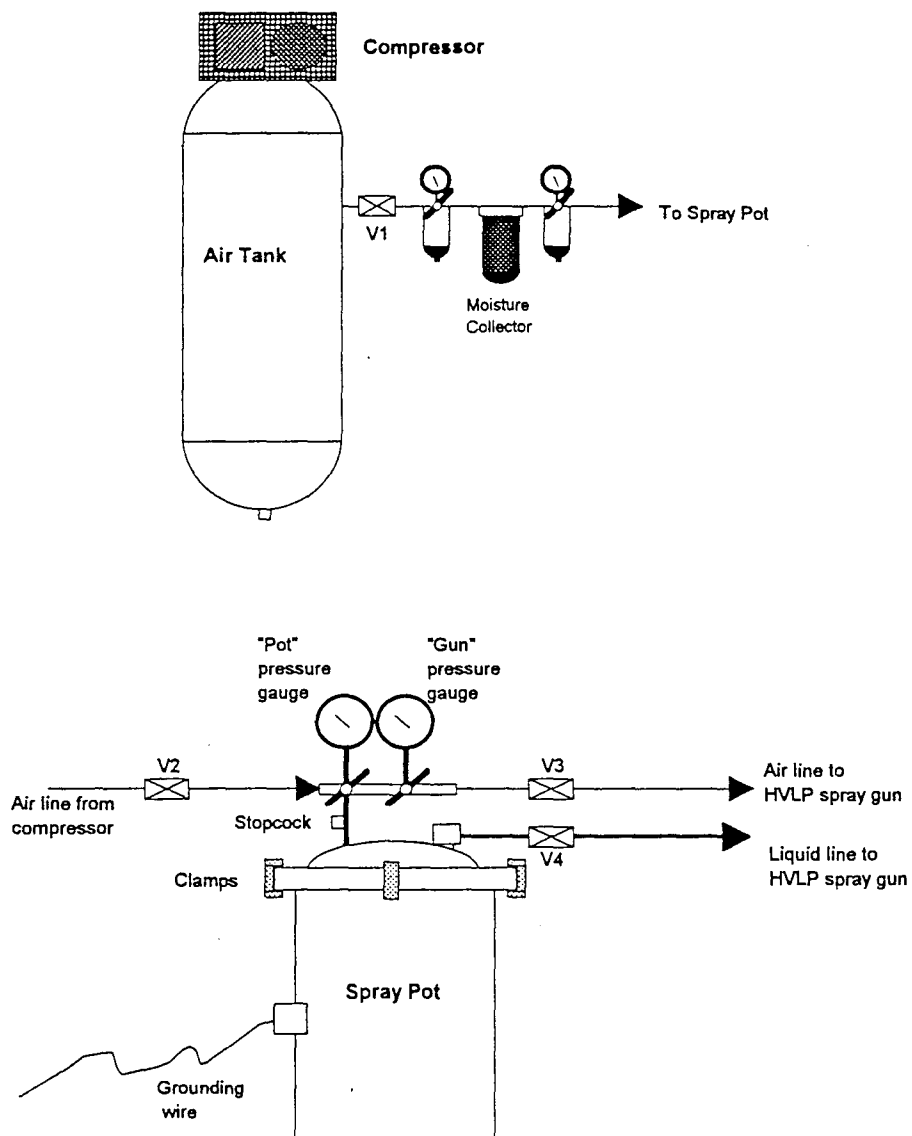


Figure B.3. Schematic of Compressor and Spray Pot Systems

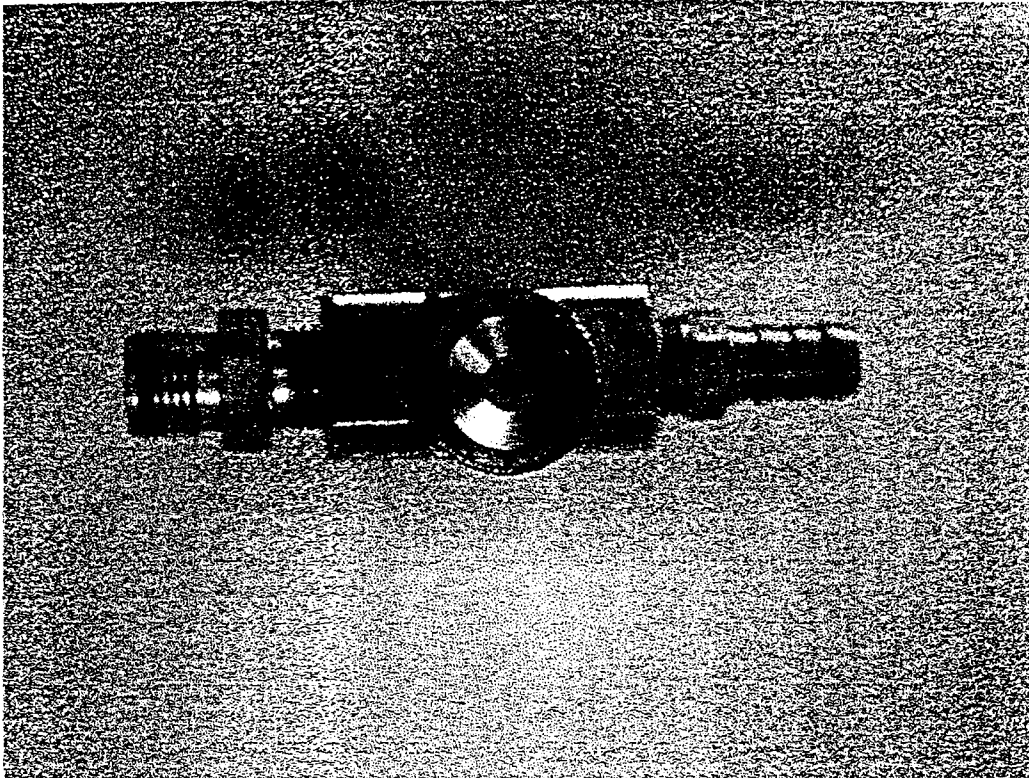


Figure B.4: 1/4 J High Pressure Spray Nozzle



Figure B.5: High Volume-Low Pressure Spray Gun

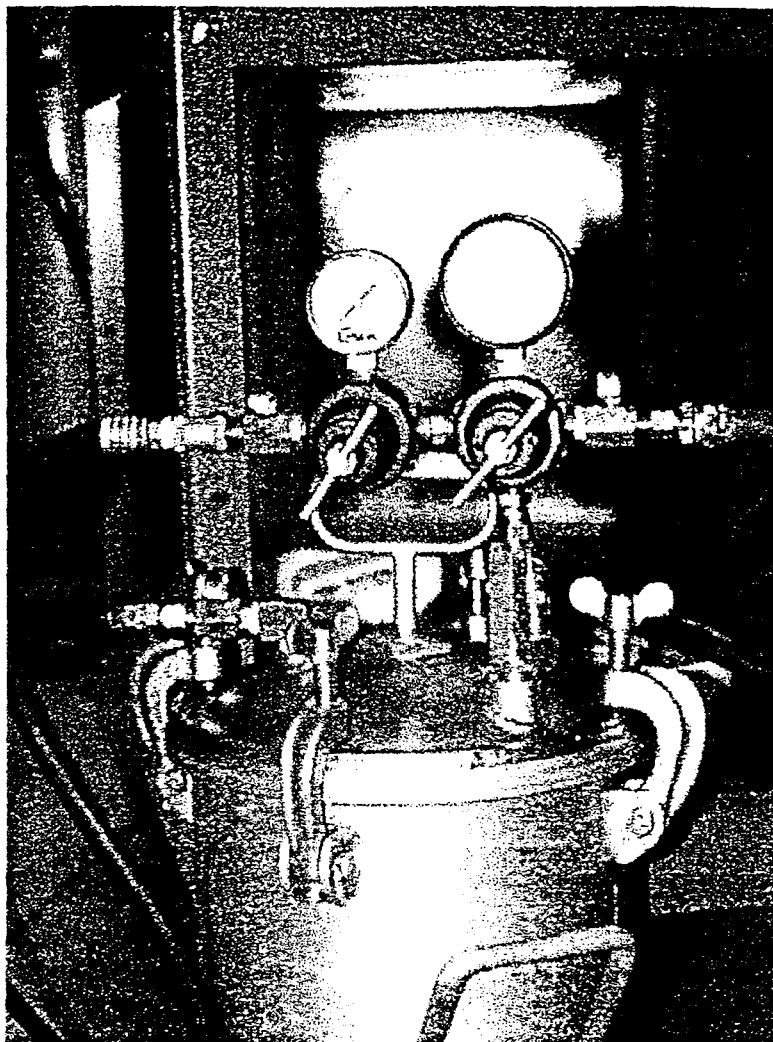


Figure B.6: Complete Pressurized Paint Vessel



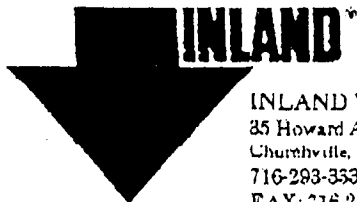
Figure B.7: Laboratory Equipment Setup



Figure B.8: Mannequin in 90° Orientation



Figure B.9: Mannequin in 180° Orientation



INLAND VACUUM INDUSTRIES  
35 Howard Avenue • P.O. Box 373  
Churchville, NY 14428-0373  
716-293-3530 • 800-902-8099  
FAX: 716-293-3093

## INLAND 99

### SPECIFICATIONS

VAPOR PRESSURE @ 25 C	$2 \times 10^{-4}$ torr
VISCOSITY @ 40 C	28 cSt (134SUS)
@ 100 C	4.5 cSt (41SUS)
BOILING POINT @ .01 torr	112 C (234 F)
POUR POINT	-15 C (5 F)
FLASH POINT	199 C (390 F)
FIRE POINT	221 C (430 F)
DENSITY	0.86 g/ml



## MATERIAL SAFETY DATA SHEET

MANUFACTURER: Inland Vacuum Industries      EMERGENCY TELEPHONE  
35 Howard Ave      DAYS: 716-293-3330  
Churchville NY 14428      EVENINGS: 800-644-4829 X6186

PREPARED BY: Marc C. Tarplee      DATE: 01-23-95

\*\*\*\*\*

## SECTION ONE: GENERAL INFORMATION

\*\*\*\*\*

PRODUCT CODE: 462014

PRODUCT NAME: Inland 99- Liquid Ring Pump Seal Fluid

## NFPA RATING

FLAMMABILITY	1
HEALTH HAZARD	0
REACTIVITY	0
SPECIAL HAZARD	NONE

CAS NUMBER: 64742-65-0

CHEMICAL FORMULA:  $(CH_2)_n$  20  $\leq n \leq$  40

GENERIC NAME: Solvent refined neutral paraffinic oil

\*\*\*\*\*

## SECTION TWO: REGULATED INGREDIENTS

(29 CFR 1910.1200)

\*\*\*\*\*

REGULATED MATERIALS AT CONCENTRATION  
OF 1 % (WT) OR GREATER

NO HAZARDOUS INGREDIENTS. MATERIAL IS  
100 % NEUTRAL PARAFFINIC OIL. MATERIAL  
HAS BEEN SUBJECT TO SEVERE SOLVENT REFINING

\*\*\*\*\*

## SECTION THREE: HEALTH HAZARDS

\*\*\*\*\*

POSSIBLE ENTRY ROUTES: Ingestion, inhalation of oil mists

TARGET ORGANS:

## EFFECTS OF OVEREXPOSURE

ACUTE EFFECTS: Exposure to oils mists may cause nausea and eye irritation. Detailed studies have not been made, but material is not expected to be dermatitic or a sensitizer.

CHRONIC EFFECTS: Unknown.

FIRST AID PROCEDURES: Skin - wash with soap and water. Eyes - flush with water. Contact a physician! Ingestion: Contact a physician! Small amounts in mouth may be washed out.

REFERENCES:

\*\*\*\*\*

## SECTION FOUR: FIRE AND EXPLOSION DATA

\*\*\*\*\*

FLASH POINT: > 213 C      METHOD USED: Cleveland Open Cup

EXPLOSIVE LIMITS    LOWER: Unknown

UPPER: Unknown

EXTINGUISHING MEDIA: Water fog, chemical foam or carbon dioxide.

SPECIAL FIREFIGHTING PROCEDURES: Wear breathing gear when fighting fires in enclosed spaces; incomplete combustion of this material produces carbon monoxide!

UNUSUAL FIRE AND/OR EXPLOSION HAZARDS: None

\*\*\*\*\*  
SECTION FIVE: PHYSICAL PROPERTIES  
\*\*\*\*\*

PHYSICAL STATE: Liquid

VAPOR PRESSURE: &lt; .001 Torr @ 25C BOILING POINT: &gt; 200 C

EVAPORATION RATE (ether = 1): Nil

VAPOR DENSITY: approximately 14 WT % VOLATILES: Nil

SPECIFIC GRAVITY: 0.86 VISCOSITY: 28 cst @ 40 C

SOLUBILITY IN WATER: Nil

APPEARANCE: Pale yellow, viscous liquid with faint petroleum odor.

\*\*\*\*\*  
SECTION SIX: REACTIVITY  
\*\*\*\*\*

STABILITY: Material is stable

CONDITIONS TO AVOID: Continuous exposure to temperatures &gt; 200 C

INCOMPATIBILITY (MATERIALS TO AVOID): Strong oxidizers

HAZARDOUS DECOMPOSITION PRODUCTS: Incomplete combustion may produce carbon monoxide.

\*\*\*\*\*  
SECTION SEVEN: RELEASE PROCEDURES  
\*\*\*\*\*

PROCEDURE TO BE FOLLOWED IN EVENT OF RELEASE: Small spills may be wiped up with a rag. Large spills should be picked up immediately with an absorbent.

PROCEDURES FOR PROPER WASTE DISPOSAL: Proper waste disposal procedures are dependent on the product's end-use. Check applicable Federal, State and Local covering treatment, storage and disposal of your process effluents.

\*\*\*\*\*

#### SECTION EIGHT:SPECIAL PROTECTION

\*\*\*\*\*

RESPIRATORY PROTECTION: See notes on ventilation below.

PROTECTIVE GLOVES: Yes - made of oil-impermeable rubber

SAFETY GLASSES/GOGGLES: Yes - glasses should have side shields

OTHER PROTECTIVE EQUIPMENT: None should be required under normal use.

VENTILATION US Gov't 8 hr TWA limit for exposure to oil mists is 5 mg  
per cubic meter

LOCAL EXHAUST: As required to meet limit shown above

MECHANICAL EXHAUST: As required to meet limit shown above

OTHER REQUIREMENTS:

\*\*\*\*\*

#### SECTION NINE:SPECIAL PRECAUTIONS

\*\*\*\*\*

SPECIAL HANDLING PRECUATIONS: None

SPECIAL STORAGE PRECAUTIONS: None

ADDITIONAL INFORMATION. NFPA Class III B material

## 9.0 References

- 1 American Conference of Governmental Industrial Hygienists: Industrial Ventilation, A Manual of Recommended Practice. ACGIH. 22nd Ed. Cincinnati, OH (1995).
- 2 Carlton, Gary N.: A Model to Estimate a Worker's Exposure to Spray Paint Mists. Ph.D. Thesis, UNC Chapel Hill, Chapel Hill, NC (1996).
- 3 Carlton, Gary N.: Modeling a Worker's Exposure During Spray Painting Tasks; a research proposal. UNC Chapel Hill, Chapel Hill, NC (1995).
- 4 Cedoz, R.; Treuschel, J.: HVLP, the Wonder Gun. **Industrial Finishing, Coatings Mfg. and Appl.** (1993).
- 5 Demange, M.; Gendre, J.C.; Herve-Bazin, B.; Carton, B.; Peltier, A.: Aerosol Evaluation Difficulties Due to Particle Deposition on Filter Holder Inner Walls. **Ann. Occup. Hyg.** 34 (4) (1990).
- 6 DeVilbiss: The ABC's of Spray Finishing; A Working Guide to the Selection and Use of Spray Finishing Equipment. ITW DeVilbiss, Maumee, OH (1995).
- 7 Doull, J.; Klaassen, C.D.; Amdur, M.O.: Casarett and Doull's Toxicology. Macmillan Pub. Co. 2nd. Ed. New York, NY (1975).
- 8 George, D.; Flynn, M.; Goodman, R.: The Impact of Boundary Layer Separation on Local Exhaust Design and Worker Exposure. **Appl. Occup. Environ. Hyg.** 5 (8) (1990).

- 9 Heitbrink, W.A.; Wallace, M.E.; Verb, R.H.; Fischbach, T.J.: A Comparison of Conventional and High Volume-Low Pressure Spray Painting Guns. **Am. Ind. Hyg. Assoc. J.** 57 (3) (1996).
- 10 Heitbrink, W.A.; Wallace, M.E.; Bryant, C.J.; Ruch, W.E.: Control of Paint Overspray in Autobody Repair Shops. **Am. Ind. Hyg. Assoc. J.** 56 (10) (1996).
- 11 Heitbrink, W.A.: In Depth Survey Report: Control Technology for Autobody Repair and Painting Shops at Team Chevrolet. DHHS (NIOSH) Report No. CT-179-18a. NIOSH, Cincinnati, Ohio (1993).
- 12 Kim, T.; Flynn, M.R.: Modeling a Worker's Exposure From a Hand Held Source in a Uniform Freestream. **Am. Ind. Hyg. Assoc. J.** 56 (11) (1991).
- 13 Kim, T.; Flynn, M.R.: The Effect of Contaminant Source Momentum on a Worker's Breathing Zone Concentration in a Uniform Freestream. **Am. Ind. Hyg. Assoc. J.** 53 (12) (1992).
- 14 Kwok, K.C.: A Fundamental Study of Air Spray Painting. Ph.D. Thesis U. of Minnesota, MN (1991).
- 15 Mark, D.; Vincent, J. H.: A New Personal Sampler for Airborne Total Dust in Workplaces. **Ann. Occup. Hyg.** 30 (1) (1986).
- 16 Mark, D.; Vincent, J. H.: Entry Characteristics of Practical Workplace Aerosol Samplers in Relation to the ISO Recommendations. **Ann. Occup. Hyg.** 34 (3) (1990).
- 17 National Institute for Occupational Safety and Health: Particulates Not Otherwise Regulated, Total: Method 0500. In: NIOSH Manual of Analytical Methods, 4th Ed. P.M. Eller, Ed. NIOSH, Cincinnati, OH (1994).

18 O'Brien, D.M.; Hurley, D.E.: An Evaluation of Control Technology for Spray Painting. **Am. Ind. Hyg. Assoc. J.** 43 (9) (1982).

19 Triplett, T.: The HVLP Way to Spray. **Industrial Paint and Powder.** 72 (2).

20 Willeke, K.; Baron, P.: Sampling and Interpretation Errors in Aerosol Monitoring. **Am. Ind. Hyg. Assoc. J.** 51 (3) (1990).

